Advanced Drug Delivery Reviews 125 (2018) 48–77

Contents lists available at ScienceDirect

Advanced Drug Delivery Reviews

journal homepage: www.elsevier.com/locate/addr

Nanoplasmonic sensors for detecting circulating cancer biomarkers☆

Abdul Rahim Ferhan [a], Joshua A. Jackman [a], Jae Hyeon Park [a], Nam-Joon Cho [a,*], Dong-Hwan Kim [b,*]

[a] School of Materials Science and Engineering, Nanyang Technological University, Singapore, 639798, Singapore
[b] School of Chemical Engineering, Sungkyunkwan University, 16419, Republic of Korea

ARTICLE INFO

Article history:
Received 1 August 2017
Received in revised form 29 September 2017
Accepted 8 December 2017
Available online 14 December 2017

Keywords:
Circulating tumor cells
microRNA
Circulating tumor DNA
Exosomes
Nanoplasmonics
SERS
LSPR

ABSTRACT

The detection of cancer biomarkers represents an important aspect of cancer diagnosis and prognosis. Recently, the concept of liquid biopsy has been introduced whereby diagnosis and prognosis are performed by means of analyzing biological fluids obtained from patients to detect and quantify circulating cancer biomarkers. Unlike conventional biopsy whereby primary tumor cells are analyzed, liquid biopsy enables the detection of a wide variety of circulating cancer biomarkers, including microRNA (miRNA), circulating tumor DNA (ctDNA), proteins, exosomes and circulating tumor cells (CTCs). Among the various techniques that have been developed to detect circulating cancer biomarkers, nanoplasmonic sensors represent a promising measurement approach due to high sensitivity and specificity as well as ease of instrumentation and operation. In this review, we discuss the relevance and applicability of three different categories of nanoplasmonic sensing techniques, namely surface plasmon resonance (SPR), localized surface plasmon resonance (LSPR) and surface-enhanced Raman scattering (SERS), for the detection of different classes of circulating cancer biomarkers.

Contents

1. Introduction . . . 48
2. Measurement strategies . . . 50
 2.1. Surface plasmon resonance (SPR) . . . 50
 2.2. Localized surface plasmon resonance (LSPR) . . . 52
 2.3. Surface-enhanced Raman scattering (SERS) . . . 54
3. Detection targets . . . 55
 3.1. miRNA . . . 55
 3.2. ctDNA . . . 59
 3.3. Proteins . . . 62
 3.4. Exosomes . . . 63
 3.5. CTCs . . . 65
4. Conclusions & future outlook . . . 69
Acknowledgements . . . 69
References . . . 69

1. Introduction

The detection of cancer biomarkers represents an important aspect of cancer diagnosis and prognosis [1–3]. Traditionally, cancer detection is performed by means of conventional tissue biopsy, which involves the removal of small portion of cells from the primary tumor growth site via a surgical procedure followed by the examination of tumor specimens [4,5]. This poses a significant degree of complication- and injury-related risk to the patient [6,7], making it almost impractical to perform repeated biopsies to track disease progression and treatment responses. In addition, there is always a likelihood of clone formation within the tumor [8–11], which may complicate diagnosis and lead to misleading conclusions especially with respect to the cancer identity. Finally, since tumors are often spatially concentrated in remote parts of the body, such as in the ovaries, pancreas and brain, the surgical procedures often need to be performed with great level of dexterity and precision by highly trained healthcare professionals [12,13]. This may contribute

☆ This review is part of the *Advanced Drug Delivery Reviews* theme issue on "Nanotechnology enabling the use of circulating tumor cells (CTCs) as reliable cancer biomarkers".

* Corresponding authors.
E-mail addresses: njcho@ntu.edu.sg (N.-J. Cho), dhkim1@skku.edu (D.-H. Kim).

https://doi.org/10.1016/j.addr.2017.12.004
0169-409X/

to relatively high costs associated with tissue biopsy procedures, making it less affordable to the masses [14,15]. In order to circumvent these issues, the concept of liquid biopsy has been recently introduced [16,17]. Liquid biopsy involves the extraction of biological fluid samples (e.g. blood, urine, saliva etc.) from the patient and the analysis of circulating cancer biomarkers contained within the samples. Unlike conventional tissue biopsy, liquid biopsy is minimally invasive, relatively simple, and can be performed repeatedly at a fraction of the cost involved in tissue biopsies. Most notably, some circulating cancer biomarkers are already present at the very early stages of disease progression [18–20], enabling quicker intervention through more effective cancer treatments. Liquid biopsies also facilitate real-time tracking of the disease progression and treatment responses, as well as real-time assessment of any clonal evolution [21,22]. Based on these advantages, liquid biopsy has great potential to improve the management of cancer patients, provided there is a firm understanding of the plethora of circulating cancer biomarkers.

Circulating cancer biomarkers can be largely divided into five main categories namely, circulating tumor cells (CTCs) [23–25], exosomes [26–28], proteins [29–31], circulating tumor DNAs (ctDNAs) [17,32–34] and micro RNAs (miRNAs) [35–37]. CTCs are directly shed off from primary tumor sites and/or metastatic sites into the bloodstream and can provide information on the cancer identity and staging through their physical properties such as cell counts, microstructures and clustering propensities [24,38]. For example, variations in CTC counts have been directly correlated to changes in the amount of cancer or tumor load [39,40], and the presence of CTC clusters point towards a 20–50 times higher propensity of metastasis [41,42]. While CTCs are essentially whole cells, circulating exosomes are small membrane-bound cell fragments between 30 and 100 nm in diameter [43]. They are released either from the cell when multivesicular bodies fuse with the plasma membrane or directly from the plasma membrane [27,44]. They represent a new class of circulating cancer biomarkers and their specific roles, especially within the context of metastasis, are still currently being elucidated. So far, there has been evidence to suggest that they have specialized functions and play a major role in intercellular signaling and coagulation [45,46]. Indeed, high levels of exosomes have been detected in the presence of cancer [47], although the exact reason for such an occurrence is yet to be deduced. Unlike exosomes, the relationship between protein cancer biomarkers and cancer progression is well defined. Generally, higher expressions of protein cancer biomarkers suggest a more advanced stage of the disease [31,48]. Interestingly, information on cancer type and disease progression can likewise be inferred from much simpler and smaller biomolecules, specifically nucleic acids. For example, circulating tumor DNAs (ctDNA), which can be released from primary tumors and CTCs, provide cancer identification through cancer-specific genetic aberrations [49,50]. While the specificity of the genetic aberrations is particularly advantageous for the purpose of therapeutic selection in the clinical setting, ctDNA is usually present in very low amounts in the bloodstream; it was discovered in only 50–70% in patients with localized cancers. This poses a significant challenge for its detection especially in the early stages of cancer [51,52]. Most recently, another class of nucleic acids has been identified as promising circulating cancer biomarkers. Micro RNAs (miRNAs) are short-stranded nucleic acids (around 20–25 base-pairs) released from primary tumor tissues into the bloodstream, and can be found in a wide variety of biological fluids. It was revealed that they can regulate target gene expression in recipient cells [53–55]. Similar to the case of exosomes, the exact role of miRNAs in carcinogenesis is currently still unclear. In a specific case of breast cancer, it was suggested that miRNAs play a significant role in the initial trigger and subsequent development of the disease by regulating the expression of breast cancer target proto-oncogenes or tumor suppressor genes (TSG) at the post-transcriptional level [56,57].

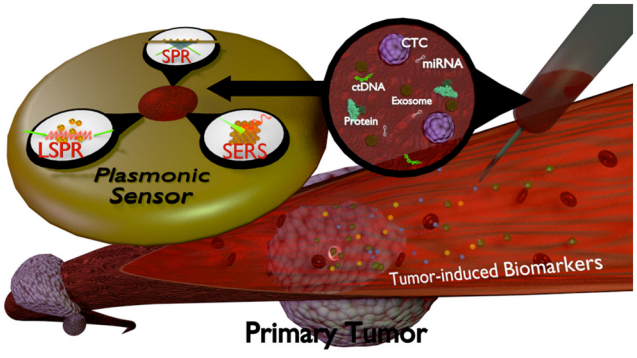

Scheme 1. A simplified illustration of the different types of circulating cancer biomarkers present in the bloodstream, which can be extracted and quantified using the different plasmonic measurement strategies discussed herein.

Several strategies have been developed to isolate, enhance and detect these circulating cancer biomarkers [24,58–61]. For example, CTCs can be isolated based physical properties such as size [62–64], shape and deformability [62,65,66] as well as based on specific adhesion molecules presented on their surfaces [67–70]. CTC isolation techniques include CTC microchips [71], filtrations systems [72–74], and bead-based capture [75]. Along this line, the first and only FDA approved technique for CTC isolation and quantification is the CellSearch™ technology, which is commercially available and has since been widely applied both in the research and clinical settings [76,77]. The platform employs EpCAM antibodies attached to magnetic beads to isolate tumor cells. Among the circulating biomarkers, measurements techniques of protein tumor markers are perhaps most well established. At present, the measurement of protein tumor markers in serum via enzyme-linked immunosorbent assays (ELISA) is the standard protocol in monitoring disease progression in a clinical setting [78]. Conversely, ELISA represents the current gold standard for which other techniques have to compare. The advantage of ELISA is that it is easy to operate and relatively inexpensive. However, it is difficult to achieve multiplex measurements, which may hamper rapid analysis of multiple samples. Besides protein quantification, ELISA has also been applied to measure the purity of exosomes. However, for concentration determination of exosomes, optical methods such as nanoparticle tracking analysis (NTA) [79], dynamic light scattering (DLS) [80] and flow cytometry, specifically fluorescence-activated cell sorting (FACS) [81] can be used. With respect to the detection of ctDNA and miRNA, techniques with high specificity and selectivity need to be employed since they are small, highly sequence-specific and present in the fluid samples at extremely low concentrations. Current techniques used for the detection and quantification of ctDNA and miRNA include commercially available sequencing systems such as safe sequencing system (Safe-SeqS), tagged amplicon sequencing (TamSeq), and digital polymerase chain reaction (PCR) [82]. These techniques are capable of detecting single-nucleotide mutations as well as perform whole-genome sequencing to establish copy-number changes.

The current techniques clearly suffer from several limitations such as the need for a complicated, multi-step protocol, difficulty to achieve multiplex detection and the difficulty to attain device miniaturization; techniques such as NTA, DLS, FACS and respective sequencing systems are generally laboratory-based, some of which require complex instrumentation. In order to address this issue, nanoplasmonic sensing techniques have been developed [83,84]. In brief, nanoplasmonic sensing techniques are optical-based techniques that rely on local refractive index changes within a small sensing volume to produce a signal readout, usually in the form of an optical spectral shift [85]. Nanoplasmonic sensing techniques are generally label free, do not require complex instrumentation and can be easily designed to allow multiplex detection using small sample volumes. Since nanoplasmonic sensors essentially operate as optical sensors, the measured parameter is the dry mass of target molecules. As a result, nanoplasmonic sensors are less likely to suffer from solution-based interferences (i.e. effects from bound or

coupled solvents are eliminated). Owing to these features, the nanoplasmonic sensing technique has been successfully applied in the field of biointerfacial science to study various interactions involving lipid bilayers [86–91], lipid vesicles [92–97] and proteins [98–102], among others [103,104]. There is a wide variety of plasmonic sensing strategies that can be adopted for biomolecular detection, which can be broadly categorized into three types, namely the surface plasmon resonance (SPR) [105,106], localized surface plasmon resonance (LSPR) [107,108], and surface enhanced Raman scattering (SERS) [109–111] techniques (See Scheme 1). Within the specific context of cancer biomarker detection, the suitability of each technique for the detection of a particular class of cancer biomarker depends on several factors such as the degree of matching between the sensing depth of the technique and the size of the target molecule, as well as the detection approach. For example, SPR-based sensors have sensing depths of around 100–200 nm [112], making it suitable for direct measurements involving CTCs, proteins and exosomes, but not nucleic acids, since they are significantly smaller and would only occupy a small portion of the sensing depth. In contrast, the LSPR-based sensors are much more surface sensitive, with sensing depths of around 5–20 nm [113], making it suitable for direct detection of nucleic acids. In this review, we describe the principles and measurement operations of the three types of nanoplasmonic sensing strategies before we discuss the relevance and applicability of each of these strategies for the detection of the five different classes of circulating cancer biomarkers (i.e. detection targets). Besides providing an overview of the current state of the art in nanoplasmonic sensor design for the detection of circulating cancer biomarkers, this review serves to highlight existing challenges that need to be overcome before nanoplasmonic sensors can successfully be translated to a clinical setting.

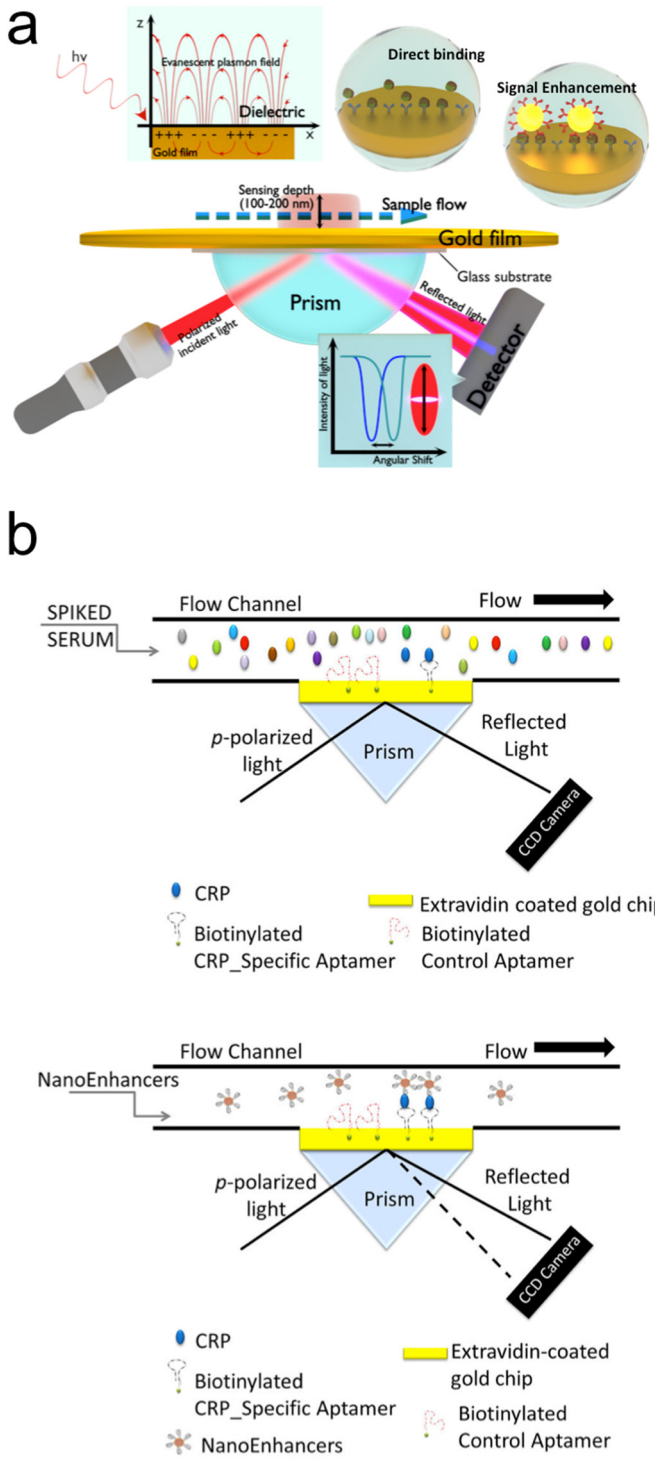

2. Measurement strategies

There are three main measurement strategies in nanoplasmonic sensing, namely surface plasmon resonance (SPR), localized surface plasmon resonance (LSPR), and surface enhanced Raman scattering (SERS). In this chapter, we discuss the measurement principles, general design of the sensing platform, measurement operation as well as the different detection formats adopted in each strategy.

2.1. Surface plasmon resonance (SPR)

Surface plasmon resonance (SPR) refers to the collective oscillation of conduction band electrons (i.e. surface plasmons) at the interface between a conductor and a dielectric upon interaction with plane-polarized light [106,112,114]. This will generate a surface plasmon wave that will propagate along the conductor-dielectric interface, but evanescently confined in the perpendicular direction within a distance of around 100–200 nm [115,116] (Scheme 2). In most cases, gold represents the ideal conductor material since it possesses a high density of conduction band electrons [117]. When the interface is illuminated with a focused beam of monochromatic, plane-polarized light from an angle sufficient to cause total internal reflection, maximum light absorption occurs when the electromagnetic wave frequency of the incident light matches the surface plasmon wave frequency [118,119]. This will result in a loss of intensity in the reflected light and is manifested as a dip in the SPR spectrum, which is typically presented as a function of incident angle along the abscissa and reflection intensity along the ordinate. In the event of biomolecular adsorption at the interface,

Scheme 2. (a) An illustration of a conventional surface plasmon resonance (SPR) detection setup in the Kretschman configuration. A laser beam is made to pass through a glass prism before it undergoes total internal reflection on the bottom side of the sensing surface. The totally internally reflected light is then captured by a detector, and the signal is then converted to a SPR spectrum. In the presence of an adsorbate, the refractive index at the interface as well as the surface plasmon wave frequency will change. Consequently, the amount of bound molecules can be measured either by tracking the change in reflected intensity at a fixed incident angle or by maintaining the reflectivity and tracking the shift in the incident angle, otherwise referred to as the angular shift. The inset in the background depicts the generation of a surface plasmon wave that will propagate along the conductor-dielectric interface, but evanescently confined in the perpendicular direction within a distance, upon interaction with an incident plane-polarized light. (b) An example of a gold-coated prism pre-functionalized with aptamers specific to CRP and control aptamers followed by the direct detection of CRP (fg/ml) spiked in human serum (top) and sandwich based assay using CRP-Specific_aptamer-coated QDs for SPRi signal amplification (bottom). Direct detection of CRP (fg/ml) does not generate a quantifiable sensor response as depicted with no change in the angle of reflectivity, however, with sandwich assay the NanoEnhancers induce a change in the reflectivity. Adapted from Scientific Reports 4 (2014) 5129.

the refractive index and the surface plasmon wave frequency will change. Consequently, the amount of bound molecules can be measured either by tracking the change in reflected intensity at a fixed incident angle or by maintaining the reflectivity and tracking the shift in the incident angle, otherwise referred to as the angular shift. The latter approach is more widely adopted since keeping the intensity constant will generally retain the overall shape of the SPR curve [120]. In other words, features such as the full width at half maximum (FWHM) will not change significantly, leading to the preservation of sensing resolution and simplifying signal interpretation.

Traditionally, SPR-based sensors operate in a prism coupled configuration [121], although various other configurations are currently available employing diffraction gratings [122,123], optical fibers [124,125] and other types of optical waveguides [126,127]. In the prism coupled configuration, the laser beam passes through a glass prism before it undergoes total internal reflection. There are generally two variants to this arrangement, namely the Otto [115,128] and Kretschmann [118] configurations. In the Otto configuration, a thin metal film (e.g. gold) is placed at a distance near enough for the totally internally reflected light in the prism to interact with the plasmons on the gold surface

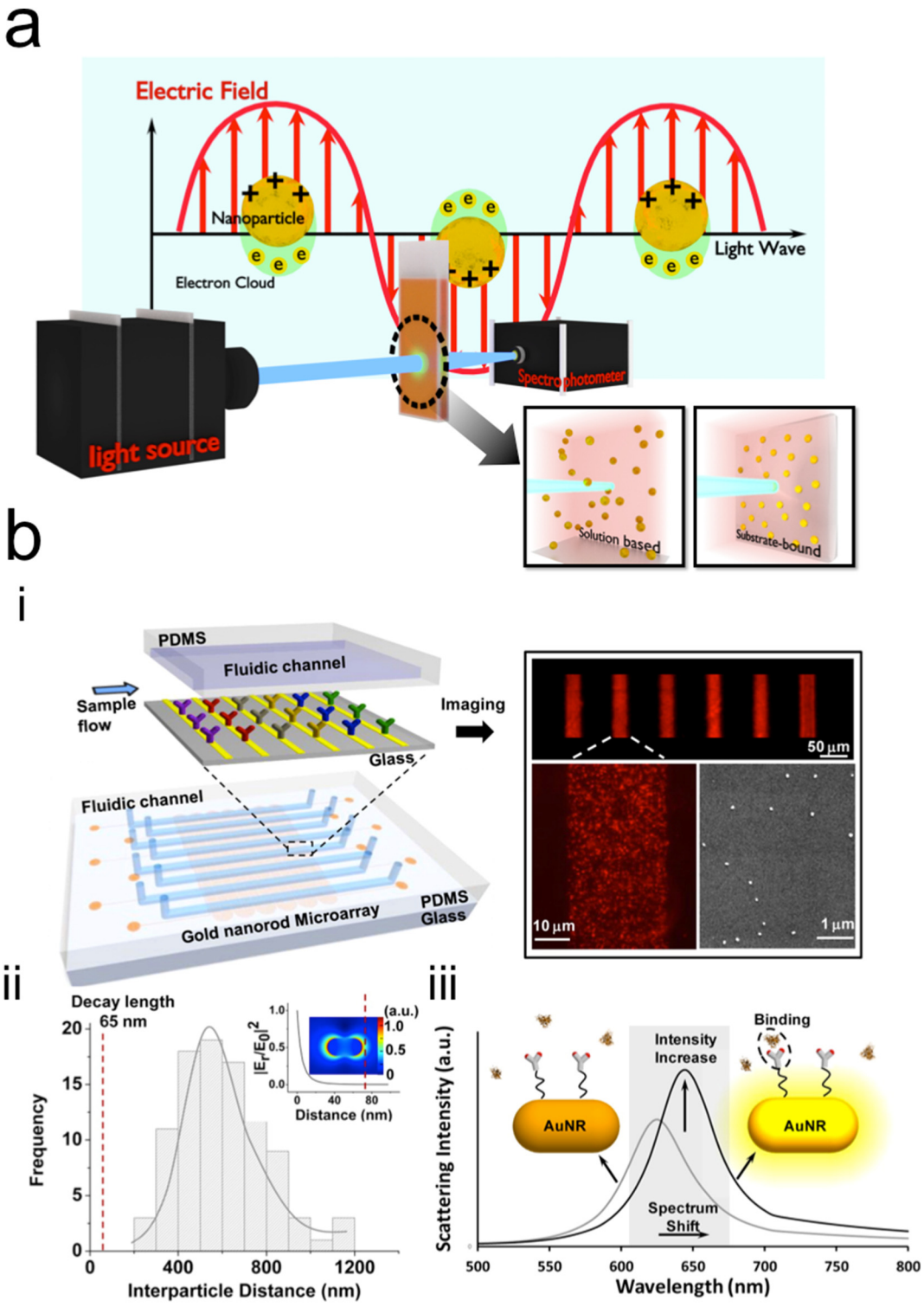

and the sample material is filled in the small gap. While this configuration is generally suitable for measurements involving solid samples (or materials with relatively high refractive indices), it is less suitable for liquid samples (or materials with relatively low refractive indices) since the small gap reduces the efficiency of photon-plasmon coupling at the metal surface, which will decrease the overall detection performance [129]. By contrast, in the Kretschmann configuration, the thin metal film is directly coated onto the glass prism to a thickness of around 50 nm, and the samples are directly detected on the film, on the opposite side of the total internally reflecting surface. This arrangement allows maximum plasmon generation efficiency, making it suitable for measurements in both solid and liquid states [130,131]. Regardless of the configuration, the totally internally reflected light is then captured by a detector, and the signal is then converted to a SPR spectrum.

For the purpose of biomolecular detection, there are two major formats that can be adopted. In the first approach, a thin film of gold that is typically utilized as the plasmon generating surface is functionalized with specific biorecognition elements (e.g. complementary nucleic acid strands, aptamers, antibodies) with the aid of thiol chemistry [114,132], and passivated either via bovine serum albumin (BSA) blocking [133] or by means of a polymeric coating [134–138]. This maximizes the amount of target biomolecule captured on the surface and minimizes interference arising from the non-specific adsorption of other molecules when liquid sample is introduced to the detection platform. During measurement, the angular shift on the SPR spectrum, which directly reveals to the amount of bound target, is monitored over time. Along this line, it is important to note that since SPR is evanescently confined in the perpendicular direction within 100–200 nm from the gold surface, the SPR response is sensitive to any refractive index change that occurs within this distance, which constitutes its effective sensing depth [116]. Conversely, this means that SPR-based biosensing platforms employing the approach described above are most suited to measure the binding of biomolecules with dimensions in the ten to hundred nanometer length scales such as proteins and exosomes. While it is also feasible to employ the approach to measure the binding of larger targets (i.e. micron range) such as circulating tumor markers, it is less suitable for the detection of smaller biomolecules (i.e. measuring <10–25 nm) such as short-chain peptides and nucleic acids. Measurements involving such small biomolecules will result in minute angular shifts since they only occupy a small fraction of the sensing depth. At the same time, the measurements are also more prone to interferences arising from the bulk environment [104,139–141]. In order to circumvent this limitation, another approach has been developed involving an additional signal enhancement step [142]. This is achieved by attaching gold nanoparticles, which have been pre-functionalized with a secondary biorecognition element, to the targets that have already been captured on the metal film, resulting in a sandwich-type configuration [143–148]. By doing so, the effective increase in refractive index is enhanced, leading to greater shifts in the SPR response.

A major advantage of SPR over other optical detection techniques arises from the fact that light does not penetrate the sample. As such, the sensing performance is not affected by the turbidity of the sample, allowing detection from both colored and clear samples [149,150]. In other words, as long as an appropriate surface passivation strategy is adopted, it is feasible to employ SPR-based biosensors to detect the presence of target biomolecules even at low concentrations directly from complex biological fluids, including whole blood [151–155]. This is difficult to achieve via optical techniques relying on light absorbance and scattering. In addition, since SPR essentially measures variations in the surface concentration of target biomolecule in a direct fashion based on refractive index changes, the time course of target binding events can be tracked with good precision, allowing detailed analysis on the binding and interaction kinetics.

2.2. Localized surface plasmon resonance (LSPR)

While the interaction of electromagnetic waves with a planar substrate induces SPR, the interaction with discrete metallic nanoparticles with dimensions smaller than the incident wavelength leads to localized surface plasmon resonance (LSPR) [84,85]. In LSPR, photons in the incident light interact with the nanoparticles to cause a non-propagating collective oscillation of free electrons in the conduction band of the metal (Scheme 3). This resonant excitation results in a significant enhancement of the electromagnetic field close to the nanoparticle surface (i.e. local electromagnetic field). At the same time, the absorption and scattering of light by the nanoparticles (i.e. light extinction) occurs with maximum intensity at the plasmon resonance frequency [85,156]. Since the oscillation of free electrons is spatially restricted to the immediate vicinity of the nanoparticle surface, any change to the local dielectric environment will affect the polarizability of the nanoparticle, which in turn will vary the plasmon resonance frequency and alter the optical extinction spectrum [156,157]. In particular, there will be a noticeable shift in the wavelength at which maximum light extinction occurs, also referred to as the LSPR peak wavelength. This represents the fundamental principle that enables the detection of a molecular adsorption or binding event at the nanoparticle surface, which paves the way for LSPR sensing to be widely adopted for biomolecular detection. As the enhanced electromagnetic field distribution is concentrated near the nanoparticle surface with a very short decay length on the order of 10–30 nm [113,158–160], LSPR sensing represents a highly surface sensitive technique facilitating the direct detection of even small biomolecules such as nucleic acids.

Generally, the sensing platform consists of nanoparticles that are either freely suspended in solution [102,161,162] or deposited onto a solid support [163–168]. Alternatively, metallic nanostructure arrays can be directly fabricated on the solid support with the aid of well-established micro- and nanofabrication lithographic techniques [169–173]. While LSPR can be induced in a wide variety of metals, gold nanostructures are most popularly employed as optical transducers in LSPR sensors due to their chemical inertness, ease of surface functionalization via thiol chemistry and the fact that their plasmon resonance frequency falls within the visible wavelength range, facilitating detection using a

Scheme 3. (a) A simplified schematic of a localized surface plasmon resonance (LSPR) sensor setup in transmission mode. The background illustration shows a non-propagating collective oscillation of free electrons in the conduction band of the metallic LSPR transducer upon interaction with light. This resonant excitation results in a significant enhancement of the electromagnetic field close to the nanoparticle surface (i.e. local electromagnetic field) and maximum light absorption at a peak wavelength. In a typical measurement setup (as shown in the foreground) the incident light illuminates an ensemble of LSPR transducers (i.e. noble metal nanoparticles) and the transmitted light is then collected at the detector, which translates the signal into an absorbance spectra. In the presence of an adsorbate on the LSPR transducer surface, the wavelength at which maximum light absorption occurs will be shifted to a higher value (i.e. peak shift). The peak shift linearly correlates to the amount of adsorbate. (b) (i) An example of a LSPR microarray chip. The nanorod microarray fabrication was performed using a one-step microfluidic patterning technique assisted by electrostatic attractive interactions between the nanorods and the substrate surface within microfluidic channels (Materials and Methods and Supporting Information Section 2). Subsequently, these nanorod microarrays were integrated in a microfluidic chip with eight parallel microfluidic detection channels consisting of inlet and outlet ports for reagent loading and washing. Specific antibodies were conjugated to the patterned AuNR microarrays using thiolated cross-linker and EDC/NHC chemistry. The current chip design integrates 480 AuNR microarray sensor spots. The prepared LSPR microarray chip was then imaged under dark-field microscopy and scanning electron microscopy (SEM). (ii) Histograms of the particle-to-particle distance of the AuNRs on the LSPR microarray chip characterized using SEM images. The resulted interparticle distance was measured to be >200 nm, much larger than the decay length of the localized electric field on the AuNR surface as shown in the inserted EM simulation. (iii) The principle of the LSPR microarray method. Analyte molecules are introduced to an antibody-functionalized AuNR LSPR biosensor. Binding of the analyte molecules to the receptors induces a redshift and scattering intensity change of the longitudinal SPR (exaggerated in the illustration). This intensity change is imaged via the characteristic frequency (gray area) using EMCCD coupled dark-field microscopy.
Adapted from ACS Nano, 9 (2015) 4173–4181.

standard UV–vis spectrophotometer and in some cases, the unaided eye [174,175]. In a typical measurement setup involving an ensemble of nanostructures, light passes through the sensing platform and the ensemble-average optical extinction (i.e. absorbance + scattering) spectra is obtained from transmitted light collected by the UV–vis spectrophotometer [176–180]. Scattering spectra from single nanostructures on a solid support can also be measured by coupling a dark-field microscope to an imaging monochromator and a charged coupled device (CCD) camera or spectrophotometer [181–184]. The characteristics of these two types of LSPR spectra would vary depending on the shape, size and orientation of the nanostructures [185–191]. Conversely, the response sensitivity, which depends on the position of LSPR peak wavelength, can therefore be tuned by adjusting these physical parameters [159,192–194]. In order to selectively capture a target biomolecule of interest, the nanostructures are usually modified to present a bioreceptor that can specifically bind to the target (e.g. complementary nucleic acid strands, aptamers, antibodies), while the exposed surfaces are passivated to prevent non-specific adsorption of other interfering materials [195–197]. Along this line, it is critical to ensure that the target would remain within the enhanced electromagnetic field decay length having taken into consideration the vertical distance occupied as a result of bioreceptor functionalization and passivation, otherwise no detectable signal will be obtained [198].

During a biosensing operation, the sample is introduced to the detection platform after a baseline measurement is obtained in a blank solution, which is usually an appropriate buffer. In general, the refractive index of the biomolecular target of interest is greater than the surrounding aqueous medium (i.e. buffer) and its binding to the corresponding bioreceptor on the nanoparticle surface will perturb the local dielectric environment such that the LSPR peak will shift to a higher wavelength (i.e. red shift) [85,107]. The amount of target on the nanoparticle surface can then be directly correlated to the peak shift, allowing quantification of the target concentration in the sample. This approach is sometimes referred to as refractive index-based LSPR biosensing and represents the simplest detection scheme in LSPR biosensing, which can be executed using nanostructures in solution [199,200] as well as on a solid support [165,166], applicable to both ensemble average [166,201] and single nanoparticle measurements [202–205]. While its main advantage lies in its simplicity, the refractive index-based LSPR sensors usually produce peak shifts that are small, in the order of <10 nm, making it difficult to quantify biomolecules at very low concentrations [206,207]. Several strategies have been devised to amplify the peak shift response and enhance the detection capability. For example, after the target has been captured, the signal can be further amplified by attachment of a relatively large secondary bioreceptor [208]. Since refractive index-based LSPR responses are proportional to the optical mass of the adsorbing molecule, the attachment of a relatively large biomolecule to the nanoparticle surface will induce a more pronounced LSPR peak shift, as long as it remains within the enhanced electromagnetic field decay length.

A more exaggerated improvement in the peak shift can be obtained based on plasmonic coupling by the addition of a secondary bioreceptor-functionalized nanoparticle [209–211]. Plasmonic coupling occurs when nanoparticles approach each other to a distance close enough for their plasmon modes to interact [212–214]. This results in further enhancement of the electromagnetic field, the degree of which depends on the inter-particle distance with smaller gap distances producing higher enhancements [214–216]. Plasmonic coupling has been most widely exploited in solution for LSPR-based colorimetric sensing [217–219]. In this approach, the introduction of target molecules trigger the clustering of receptor-functionalized nanoparticles leading to significant changes in the optical extinction profile, which entails extensive peak broadening and a huge peak shift in the order of 50–100 nm. Such changes translate to a distinct color change of the nanoparticle solution (e.g. red to blue) that can be clearly discerned by the naked eye. While traditional methods of colorimetric sensing rely on uncontrolled nanoparticle aggregation that usually produces a sharp change in color above a certain target concentration, more refined approaches have been recently developed to facilitate quantitative detection especially at low concentrations [220,221]. For example, instead of forming large aggregates, nanoparticles can be designed to only dimerize (i.e. pair up) upon the introduction of the target molecule [222]. This eliminates peak broadening and improves the sensing resolution, which ultimately lowers the limit of detection by several orders of magnitude.

Dimerization can also be realized on a solid support, most effectively for the detection of nucleic acids (e.g. miRNA, ctDNA) [223,224]. In this approach, nanoparticle pairs connected via a non-rigid linker molecule (e.g. nucleic acid hairpin probe) are prefabricated on the solid support. The interaction of the target with the linker molecule will modulate the distance between the nanoparticles allowing them to switch between monomer and dimer configurations. For example, when a target nucleic acid strand binds to a nucleic acid hairpin probe connecting the nanoparticle pairs, the probe translates from a closed-loop to an extended configuration, in effect separating the nanoparticle dimers. In most cases, such measurements are performed at the single particle level using a darkfield microscope set-up, which effectively allows distinct color changes of the scattered light to be directly visualized through the microscope eyepiece or captured by the CCD camera. At the same time, large peak shifts in the scattering spectra in the order of 50–100 nm will be registered when the nanoparticles switch configurations.

Although measurements based on single nanoparticles using a darkfield microscope potentially allow highly sensitive detection down to single molecule [225,226], they require extensive instrumentation and a trained operator. Meticulous optimization of the setup before sample measurement is also needed and the interpretation of the output signal is not straightforward primarily due to variations in the optical properties of individual nanoparticles arising from slight differences in size, shape and surface morphology [204,227–231]. That being said, while darkfield-based measurements are appropriate for fundamental studies into biomolecular interactions that focus on isolated biomolecules [232,233], they are less suitable for practical applications. On the other hand, most ensemble-average measurements require much simpler instrumentation that can be miniaturized consisting of a light source and a spectrophotometer, making them more promising for biomarker detection applications [108]. Sensing platforms on a solid support are generally more robust than their solution-based counterparts since they are more stable during storage and are not prone to unintended aggregation over time. Furthermore, nanoparticles on a solid support can also be coated by a thin layer of dielectric material (e.g. silicon oxide, titanium oxide and aluminium oxide) [234–238], allowing greater flexibility in terms of surface functionalization and passivation. Optical fibers can also serve as solid supports, facilitating sensing device miniaturization and integration with microfluidics [239]. Nonetheless, solution-based colorimetric sensors are potentially the most convenient since they rely on detection via the unaided eye and can operate even without any form of instrumentation. However, proper standards need to be established in order to accurately interpret the responses.

In all the detection schemes described above, the target detection event occurs directly on the surface of the LSPR optical transducers (i.e. surface of nanoparticles). While most works describing LSPR biosensing typically employ one of these detection schemes, there is also a growing sub-field of LSPR biosensing that involves linking LSPR transducers to enzyme-linked immunosorbent assays (ELISA); an approach sometimes referred to as plasmonic ELISA [240–243]. In plasmonic ELISA, protein detection follows the conventional ELISA procedure, which begins with the binding of the target protein to capture antibody pre-coated onto a microtiter plate, followed by the subsequent attachment of a primary antibody and an enzyme-labelled secondary antibody. However instead of linking the biocatalytic cycle of the enzyme to the generation of fluorescence, it is linked to the growth of gold nanoparticles. The primary advantage of plasmonic ELISA stems from the fact

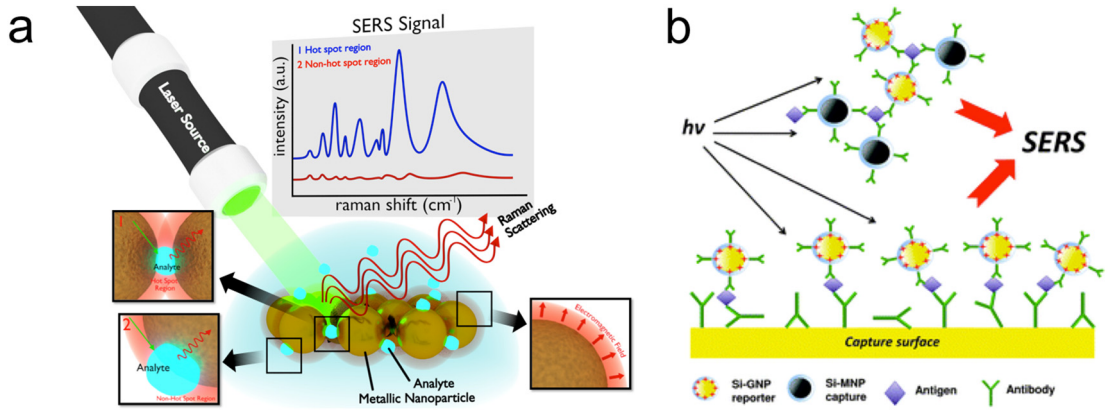

Scheme 4. (a) A simplified illustration of surface enhanced Raman scattering (SERS) arising the interaction of a laser beam with molecules directly adsorbed on the surfaces of nanoparticle clusters (or hot-spots). The Raman scattered light (i.e. Stokes scattering) is collected by a spectrophotometer, which translates the signal into a unique SERS spectrum. (b) Essential features of SERS immunoassays conducted in solution and using a solid surface substrate for antigen capture.
Adapted from Physical Chemistry Chemical Physics, 15 (2013) 20415–20433.

that the growth of gold nanoparticles can be visualized without a fluorescence excitation source. Color development based on LSPR is also highly stable, consistent, and not prone to photobleaching effects [243]. This has allowed the naked eye detection of several disease biomarkers down to the attomolar level.

2.3. Surface-enhanced Raman scattering (SERS)

The generation of LSPR is also partially responsible for surface-enhanced Raman scattering (SERS) [85]. In SERS, inelastic Raman scattering signals originating from molecules that adsorb onto metallic nanostructures are enhanced by several orders of magnitude primarily through the amplification of the local electromagnetic field that occurs when monochromatic light (i.e. from a laser source) interacts with the metal. This is known as the electromagnetic contribution to SERS [244], which plays a major role in Raman signal amplification with theoretical estimates suggesting that the maximum SERS enhancement factor arising from this contribution is in the order of 10^{11} [245–247]. Although there is a second contribution to SERS identified as the chemical contribution [248–251], which arises from the formation of a charge-transfer state between the molecule and the metal surface, it is believed to play a minor role in Raman signal amplification [252]. The SERS enhancement factor arising from this contribution is only estimated to be in the range of 10^1 to 10^3 [250–252]. Based on these two contributions, the overall SERS enhancement is maximized when the molecule is in direct contact with the metal surface, or within its immediate vicinity (around 10 nm [110]) due to the short decay length of the amplified local electromagnetic field.

An appreciable SERS enhancement can be achieved by employing metals that can produce the highest degree of electromagnetic field enhancement via LSPR, such as gold and silver [253,254]. On a related note, since the electromagnetic field enhancement is also strongly dependent on the nanostructure geometry and arrangement [254,255], the substrate design requires several key features in order to effectively realize SERS. As earlier mentioned in the previous sub-section, the clustering of nanoparticles result in plasmonic coupling which will lead to further enhancements of the electromagnetic field. Following this principle, SERS is most effectively achieved at the nanoscale gap junctions between adjacent nanostructures, also known as "hot-spots" [256–258]. There exist various methods to obtain a high spatial density of SERS hot-spots ranging from random aggregation of nanoparticles in solution [259–261] to micro- and nanofabrication of well-defined multimer arrays on a solid support [262–265]. In addition, the enhanced electromagnetic field distribution around a single non-isotropic nanostructure is non-uniform with the enhancement effect concentrated at high-index facets (i.e. tips and edges) [266–268]. As such, the use of nanostructures with sharp tips and edges such as nanopyramids and nanostars are preferred over conventional spherical nanoparticles.

In a typical SERS measurement, the SERS substrate, either in solution or on a planar solid support (e.g. glass, silicon oxide etc.), is illuminated by a laser beam and the scattered light from the surface-adsorbed molecule is filtered to isolate the Raman scattered light (i.e. Stokes) from the Rayleigh and anti-Stokes scattered light (Scheme 4). Raman scattered photons are captured by the detector of a Raman spectrophotometer and the signal is then decoded to present the SERS spectrum of the molecule. The SERS spectrum consists of several narrow-band peaks, each of varying intensities at different Raman shifts, which reflect the frequency or energy change between the Raman scattered photons and the incident beam corresponding to different vibrational energy levels of the molecule. The identity of a particular molecule can therefore be ascertained either from the signature peak pattern or from a single peak at a certain Raman shift value [269]. At the same time, the amount of molecule adsorbed on the SERS substrate can be inferred from the peak intensities. Generally, greater SERS enhancement will result in sharper peaks and increase the detection sensitivity [252,270,271]. Aside from proper materials selection and nanostructure design, another important determinant of SERS enhancement related to the measurement instrumentation is the laser excitation wavelength since SERS enhancements ultimately arise from a resonant response of the substrate [272–275]. In other words, the degree of SERS enhancement observed from a particular substrate varies greatly with the excitation wavelength. In fact, a given substrate typically exhibit good enhancements only within a narrow excitation wavelength range [276]. For most gold and silver-based SERS substrates, they are usually designed to operate optimally at a wavelength that falls within the visible to near infrared range (i.e. 400–1000 nm).

In general, there are two major formats that can be employed for SERS-based biodetection applications, namely the label-free detection format [277–279] and the indirect detection format utilizing SERS tags [280–284]. In the label-free approach, the target biomolecule of interest will directly bind to the surface of the SERS substrate upon sample introduction. Along this line, it is worthy to note that unlike SPR- and LSPR-based sensing, bio-receptor functionalization is not a pre-requisite in label-free SERS-based biosensing since the direct interaction between the target biomolecule and the surface will reveal vibrational spectroscopic information in the form of a fingerprint SERS spectrum unique to the biomolecule [285,286]. While this represents the simplest approach in SERS-based biosensing, the possibility of interference from other adsorbing molecules in the sample can reduce the detection efficiency [287]. Firstly, the competitive adsorption of other biomolecules to the surface will reduce the amount of available space for direct contact between the target biomolecule and the SERS substrate thereby

reducing the amount of target detected. Secondly, SERS signals from co-adsorbed molecules will also contribute to the SERS spectrum and may potentially complicate data analysis, especially when SERS footprints from other molecules overwhelm those from the target. Taken together, the label-free detection format is therefore less suitable for detection from complex biomatrices such as blood and serum. On the other hand, the indirect detection format utilizing SERS tags possess a higher degree of specificity and are generally more robust in terms of signal output [283,288]. SERS tags are essentially SERS signal transducers comprising of the substrate (i.e. gold or silver nanoparticles), a layer of reporter molecules possessing a strong Raman fingerprint directly adsorbed onto the substrate and an outer coating layer of a dielectric material (e.g. silica) to encase the reporter molecules and enhance biocompatibility and stability. Most importantly, the outer layer allows functionalization with bioreceptor molecules and further passivation to achieve specificity towards the target molecule. During detection, the SERS tags will bind to the target via the bioreceptor molecules on the outer coating before the tag is illuminated with the laser beam. Unlike the direct detection format, the signal detected will originate from the reporter molecule instead of the target molecule. It is worthy to note that target molecules will not contribute to the signal at all since it is well separated from the SERS substrate. Besides achieving a high level of specificity towards the target, the utilization of SERS tags is particularly advantageous since a strong signal is obtained solely from the reporter molecule with little to no interference, facilitating quantitative analysis with improved detection performance [289].

The direct detection format is typically employed for in vitro detection of circulating biomarkers. In such cases, biological fluid samples (e.g. from blood, urine, saliva) are either purified first or directly introduced to the detection platform. Most often, this is achieved by flowing the samples over SERS substrates that are deposited or fabricated on a planar solid support, although there exist several approaches that describe the mixing of samples with SERS substrates that are suspended in solution, usually involving other solution-based target isolation techniques (e.g. via magnetic or electrochemical separation etc.) [290–293]. The direct detection format is, however, not suitable for detection in vivo since the introduction of bare SERS substrates into the physiological environment will less likely result in effective target adsorption due to biocompatibility issues. In contrast, detection using SERS tags are suitable for both in vitro as well as in vivo settings [111,282,294,295]. For in vitro detection involving a solid support, the target will usually be first captured on the support that has been pre-functionalized with the target recognition element. After eliminating other interfering materials, SERS tags are introduced to bind with the targets on the solid support, resulting in a sandwich type configuration, before the SERS signals are acquired. For solution-based in vitro detection, the biological fluid sample is mixed with the SERS tag solution. The target-bound SERS tags are then isolated and quantified. Clearly, this is facilitated by the ability to functionalize the outer coating of the SERS tags with the target recognition element. Similarly, the ability to include additional functionalities to SERS tags can be exploited to improve biocompatibility [296–298], which paves way for its use in vivo. There are generally two mechanisms for in vivo cancer detection using SERS tags namely, passive and active targeting [299,300]. In the passive targeting mechanism, the SERS tags are not functionalized by any target recognition element and accumulate preferentially at tumor sites based on an enhanced permeability and retention effect [282]. In the active targeting mechanism, the SERS tags are functionalized with target recognition elements such as antibodies and peptides in order to recognize specific tumor antigens that are present on tumor cells at the primary growth site as well as on circulating tumor cells.

Besides its direct utilization for biomarker detection, SERS can also be employed in conjunction with ELISA [301,302]. In SERS-ELISA, the detection protocol is similar to conventional ELISA up to the enzyme introduction step. However, instead of linking the biocatalytic cycle of the enzyme to the generation of fluorescence, it is linked to the aggregation of SERS tags. The main advantages of SERS-ELISA over conventional ELISA stem from the fact that SERS scattering is not affected by quenchers such as oxygen and is less susceptible to photobleaching effects [303]. This facilitates detection from a variety of sample matrices. It also permits extended signal averaging, which will effectively lower detection limits. Finally, SERS can also be combined with fluorescence imaging [304–306] to achieve dual mode sensing. In a typical arrangement, nanoparticle clusters encoded with a Raman dye are mixed with an organic fluorescent dye and the mixture is contained within a biofunctionalized polymeric nanoparticle. The ability to detect the target binding event through both SERS and fluorescence modes leads to greater sensitivity and specificity, owing to the sensitive and specific nature of the SERS signals, as well improved multiplexing capability, owing to a wide range fluorescent dye with non-overlapping emission spectra.

3. Detection targets

3.1. miRNA

Micro RNA (miRNA) are small molecules of very short length of around 20–25 nucleic acid base-pairs (i.e. around 6–8 nm in length) [307–309]. They are non-coding RNAs and regulate gene expression through mRNA degradation or translation inhibition [310,311]. In general, the correlation between miRNA and a specific type cancer is based on the up-regulation/down-regulation of miRNA or miRNA expression patterns [310,312–315].

The detection of miRNA using SPR-based sensing platforms typically require a signal amplification step since the capture of miRNA without any amplification will only result in an infinitesimal SPR shift due to the small size of miRNA (6–8 nm) [307–309] compared to the sensing depth of SPR (i.e. 100–200 nm) [116,128]. In fact, even in conventional complementary DNA microarrays, the detection of miRNA is difficult due to its short length and a chemical or enzymatic modification to the captured miRNA is usually required to obtain an appreciable readout [316–318]. Fortunately, these post-modification approaches can be adopted in SPR-based systems and miRNA can be conveniently labelled with larger biomolecules or nanoparticles for signal amplification, resulting in the effective construction of nanosandwiches and a significant enhancement of the SPR signal [319–321]. One of the earliest demonstrations of SPR-based miRNA detection was conducted on a microarray format, for the detection of 3 synthetic miRNAs (i.e. miR-16, miR-122b and miR-23b) [322]. The detection and identification of miRNAs follow a three-step scheme beginning with the binding of target miRNAs to single-stranded locked nucleic acid (LNA) probes, followed by the addition of poly(A) tails via the poly(A) polymerase surface reaction and finally the hybridization of the poly(A) tails with T_{30}-DNA coated gold nanoparticles for signal amplification before the signal is eventually measured with SPR imaging. Based on this approach, they achieved a limit-of-detection of 10fM. In contrast, unlabeled miRNA can only be detected down to a concentration of 1 nm. In other words, the signal amplification produced a remarkable 10^5 signal enhancement. In another work by Zhang et al., streptavidin was used instead of nanoparticles for signal amplification [323]. In this case, target miRNAs first bind to short-stranded DNA capture probes on the sensing surface. A streptavidin-oligonucleotide complex is then added to hybridize with the exposed nucleotide fragments of the captured miRNAs before the SPR signal is acquired. A similar approach was adopted by Ding et al., whereby instead of hybridizing directly to a streptavidin-oligonucleotide complex, the exposed fragments of the captured miRNA was first hybridized with biotinylated auxiliary probes, to achieve a DNA supersandwich, before the addition of streptavidin and acquisition of the SPR signal [324]. Along this line, it is worthy to note that, unlike signal amplification using gold nanoparticles, which was capable of producing femtomolar limits of detection, signal amplification using DNA supersandwich and streptavidin only produced a limit of detection in the

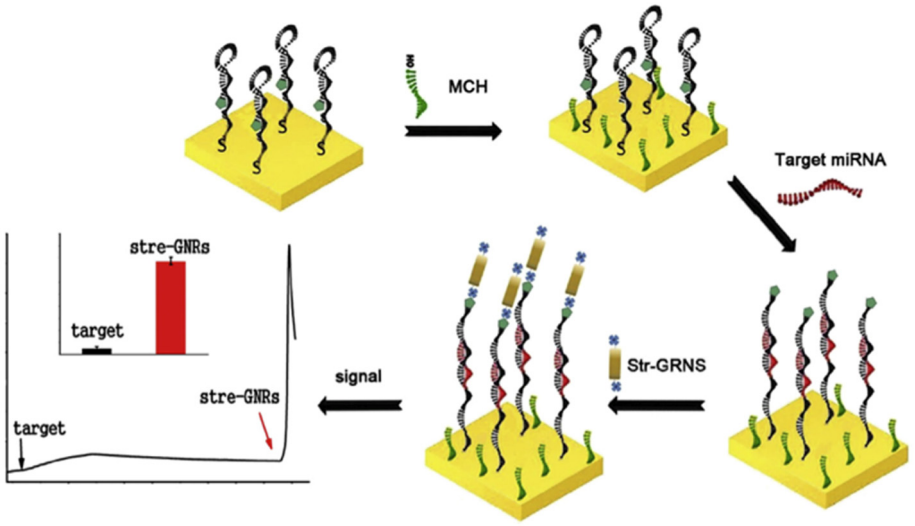

Fig. 1. Schematic illustration of the proposed method of miRNA detection based on Stre-GNRs enhanced SPR response. Adapted from Analytica Chimica Acta 954 (2017) 114–120.

picomolar range, suggesting the advantage of using a hard, plasmon active nanomaterial for signal amplification. Wang et al. then adopted the DNA super-sandwich amplification step but replaced streptavidin with gold nanoparticles [325]. They employed the scheme to detect miR-21 and, as expected, achieved a detection limit of 8 fM. Most recently, Hao et al. described the utilization of biotinylated thiolated DNA molecular beacon as the capture probe [326] (Fig. 1). In this case, when target miRNA hybridizes with the molecular beacon, the biotinylated group becomes accessible and will then bind to streptavidin functionalized gold nanorods, which served to significantly amplify the SERS signal. Under optimal conditions, they obtained a limit of detection of 0.045 pM. Besides achieving a detection limit in the femtomolar range, another advantage of this approach compared to the ones described previously is that amplification is performed in a single-step, which simplifies the detection procedure and greatly reduces reproducibility issues arising from human error. In essence, there is a relatively huge degree of

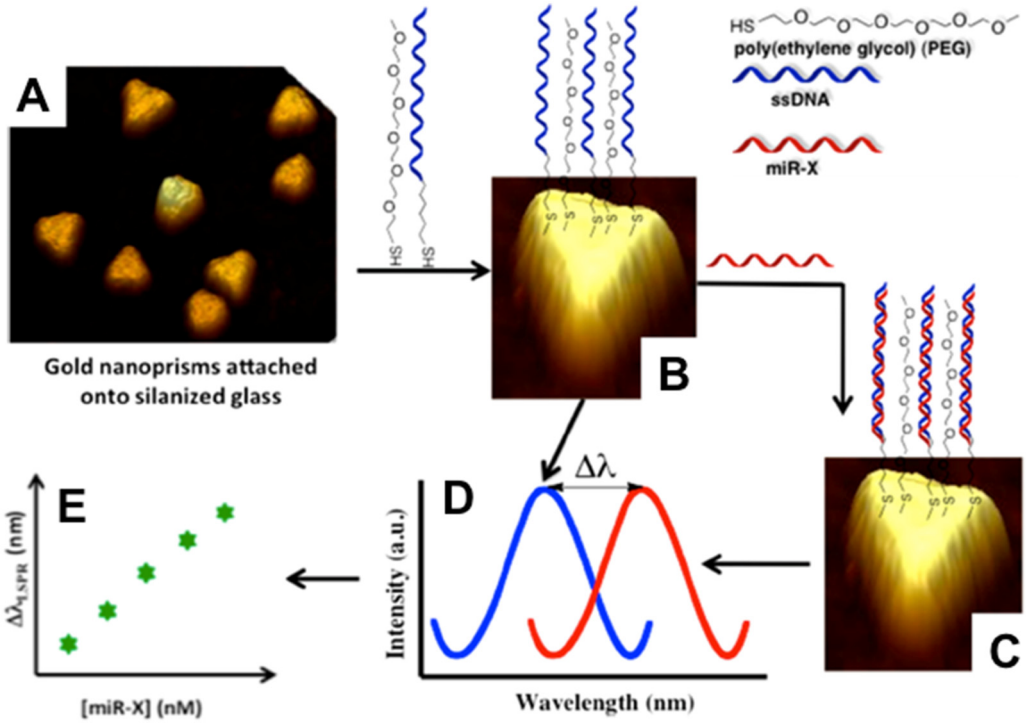

Fig. 2. Design of plasmonic biosensors and detecting miR-X in various physiological media. (A) Chemically synthesized and freshly prepared gold nanoprisms were covalently attached onto a 3-mercaptopropyltriethoxysilane-functionalized glass coverslip (substrate). (B) Surface of gold nanoprisms was chemically modified with a 1.0 μM 1:1 mixture of SH-C6-ssDNA-X and PEG6-SH in PBS buffer (pH 7.4) to prepare the plasmonic biosensor. (C) Incubation of sensor in miR-X solution and formation of DNA duplex. (D) Schematic of the extinction spectrum of the biosensor collected in PBS buffer after modification with a 1.0 μM 1:1 mixture of SH-C6-ssDNA-X and PEG6-SH (blue curve). The extinction spectrum was again collected after incubation in miR-X solution and careful rinsing with PBS buffer to determine the new peak position (red curve). The extent of LSPR dipole peak shift (ΔλLSPR) depends on the concentration of miR-X used during the incubation in (C), which ranged from 100 nM to 50 fM. (E) Plot of ΔλLSPR versus log of miR-X concentrations used to determine the limit of detection. The image is not to scale.
Adapted with permission from Nano Lett. 2014, 14, 6955–6963.

freedom in designing the amplification step, including the use of other biomacromolecules [327–329] and nanomaterials [330] as well as employing more than one amplification strategy [321]. On top of that, the detection performance can also be improved through better passivation of the sensing surface [331] as well as better SPR instrumentation and detection formats [329,332]. In a notable example, by combining SPR with a DNA-RNA antibody based assay, Sipova et al. achieved subfemtomole level detection of miRNA using a novel high-performance portable SPR sensor instrument for spectroscopy of surface plasmons based on a special diffraction grating called a surface plasmon coupler and disperser (SPRCD) [329]. Most recently, Yang et al. employed SPR to enhance light scattering from gold nanoparticle (AuNP) tags conjugated with a monoclonal antibody with high affinity for DNA-RNA hybrids [332]. In the presence of target miRNA, DNA-RNA hybrids are formed on the sensing surface when target miRNA hybridizes with the capture DNA. AuNP tags are then added to bind to the DNA-RNA hybrids and subsequent illumination with the laser beam lead to surface plasmon enhanced light scattering (SP-LS). They employed this detection scheme for the detection of miR-122 and achieved a limit of detection of 60 fM.

Unlike ctDNA, which has higher tendency to form stable secondary structures due to its length, miRNA remains stretched since they are much shorter. This provides better access for hybridization with probe complementary sequences and provides greater flexibility in terms of designing LSPR-based detection schemes. Since the length of miRNA (6–8 nm) closely matches the sensing depth of LSPR (5–20 nm), direct detection on isolated nanostructures is possible even without any signal amplification step. This was first reported by Joshi et al., whereby gold nanoprisms deposited onto silanized glass and functionalized with a probe ssDNA act as the LSPR transducer in the detection of miR-21 and miR-10b in human plasma obtained from pancreatic cancer patients [333] (Fig. 2). Due to the remarkable refractive index sensitivity of the gold nanoprisms, the direct capture of miRNAs resulted in quantifiable peak shifts down to the subfemtomolar range. Besides exhibiting excellent sensitivity and selectivity, this approach is extremely simple and do not require any sample preparation step, making it highly promising for use in point-of-care settings. In a follow-up work, they employed the same platform for direct detection of miR-10b in biological fluids and exosomes [334]. Most notably, they achieved single nucleotide specificity at the attomolar concentration level. The remarkable detection sensitivity was attributed to charge transport and/or delocalization of free electrons on the gold nanoprism surface through DNA backbone when the ssDNA probe forms the duplex with the target miRNA. It is also worthy to note that this work represents the first demonstration of a label-free technique for the quantification of miRNAs in exosomes. Consequently, it was the first work that revealed that miR-10b is abundant in circulating exosomes in pancreatic ductal adenocarcinoma (PDAC) patients. Along this line, it becomes clear that with an appropriate design, solid-phase LSPR detection platforms have huge a potential in prognostic and therapeutic applications. Apart from the possibility of direct detection, the short length of miRNA also facilitates the bridging of nanoparticles in solution, which paves way for detection based on the plasmonic coupling effect and colorimetry [335–338]. For example, Guo et al. demonstrated detection based on the formation of nanoparticle dimers in the presence of the target miRNA [335]. Briefly, an enzyme-mediated signal amplification step was first performed in which target miRNA was hybridized with cDNA and, in the presence of duplex specific nuclease (DSN), resulted in cleaved fragments of cDNA. Intact cDNA is then hybridized with two different probes that have been asymmetrically functionalized onto two different groups of AuNPs, respectively, resulting in a Y-shape DNA duplex that would assemble the AuNPs into dimers. Consequently, the color of the solution would gradually change from purple to red with increasing miRNA concentration (i.e. decreasing intact cDNA concentration). Due to the highly controlled formation of the AuNP dimers, sub-femtomolar circulating miRNAs can be directly visualized in serum via unaided eye. The formation of AuNP dimers as opposed to random aggregates also ensured a high level of colloidal stability and contributed to a wide dynamic range. The rearrangement of nanoparticles for the purpose of miRNA detection is not only restricted to the solution phase. Detection based on the formation of nanoparticle dimers [338] as well as core-satellite-assemblies [336,339] have also been demonstrated on a solid support whereby measurements are based on the LSPR scattering spectra obtained using a darkfield setup. In this case, existing microfabrication techniques can be exploited to obtain well-defined nanostructures on a solid support. For example, Lee et al. demonstrated the fabrication of side-edge prefunctionalized gold nanostructure arrays on a flexible polyethylene terepthalate (PET) substrate using contact transfer printing [339]. In the presence of target miRNAs, heteroassemblies of nanostructure and nanoparticles are formed, which is translated to a significant change in LSPR scattering spectra. Aside from obtaining a femtomolar limit of detection, this work particularly demonstrates the possibility of developing LSPR-based miRNA sensors on plastic supports, aside from conventional materials such as glass and silicon oxide, which can lead to lower production costs. While plasmonic coupling have been largely employed to effect greater shifts in the absorbance and scattering spectra, thereby enabling visual detection of the target binding event, the change in color of scattered light as a result of small refractive index changes around a single nanostructure in the presence of small molecules such as miRNA can be intensified via an appropriate post-processing technique. This was recently demonstrated by Zhou et al., in which the color of single light scattering of plasmonic nanoparticles obtained from darkfield images is automatically coded with the hue values of the standard 'hue-saturation-intensity' (HSI) color model, before it is amplified using a MATLAB program even for minute spectral changes [340] (Fig. 3). This resulted in a significant increase in color resolution of the darkfield images, facilitating detection via unaided eye.

The detection of miRNA via SERS can either be achieved directly on a SERS active substrate or indirectly with the aid of SERS nanoprobes. For example, in the work by Driskell et al., target miRNAs directly adsorb onto silver nanorod arrays before their respective SERS spectra are acquired [341]. They revealed that SERS spectra of related and unrelated miRNAs can be distinguished almost in real-time and that miRNA patterns can be classified with high accuracy. Similarly, Abell et al. reported direct miRNA detection using highly reproducible silver nanorod SERS substrate [342]. In this work, the importance of an appropriate quantification technique in order to achieve better sensing resolution was discussed. In particularly, they noted the difficulty in distinguishing miRNA in a freely adsorbed state versus a hybridized state and overcome it by using a straightforward least-squares analysis technique to determine the relative ratios of four nucleotide components A, C, G, and T/U before and after hybridization. In the indirect detection format, target miRNA is first captured on a solid support, usually by means of hybridization with a complementary short-stranded nucleic acid probe. SERS nanotags, which are functionalized with a second nucleic acid probe, is then added and the SERS signal is acquired. In this case, the SERS spectrum originates from the SERS reporter molecule contained within the SERS nanotags instead of the target miRNA. There are plenty of variants to the indirect detection scheme, since the attachment, arrangement and configuration of SERS nanotags with respect to the target miRNA can all be customized. Along this line, it is important to note that slight variations to the detection scheme can result in significant changes to the SERS response. Guven et al. revealed this in a work employing two closely similar indirect SERS assay configurations to detect mir-21 [343]. In the first configuration, mir-21 was covalently immobilized on the sensing surface before hybridization with SERS nanotags functionalized with nucleic acid probes complementary to mir-21. In the second configuration, instead of covalent attachment to the sensing surface, mir-21 was hybridized to complementary nucleic probes functionalized on the sensing surface. The subsequent hybridization step with the SERS nanotags was maintained. The detection limits for the first and second configurations were found to be 0.36 and

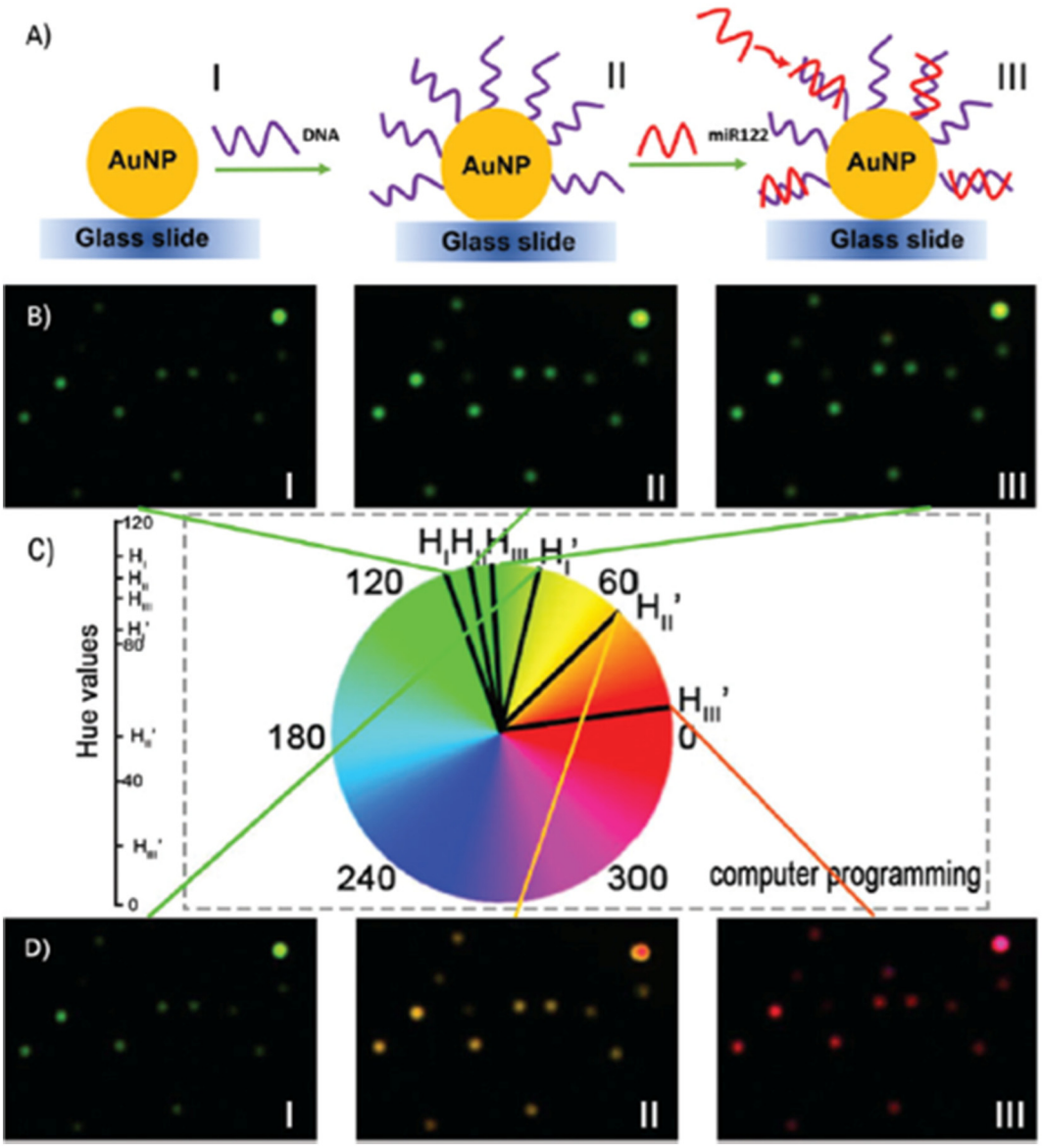

Fig. 3. Schematic illustration of the color analytical method for improving the resolution and its further application for the detection of HCC-associated miRNA. (A) Biosensing scheme for the detection of HCC-associated miRNA by hybridization between the DNA-functionalizedAuNP probe and miR-122. (B) Characteristic DFM images of AuNPs (B—I), DNA-functionalized AuNPs (B-II), and hybridization between probe molecules and miR-122 on the AuNP surface (B-III). (C) Hue diagram of the HSI color model and improvement of the color resolution of the DFM images by computer programming (H_I, H_{II}, and H_{III} are the hue values of the DFM images in (B), and the amplification values are H'_I, H'_{II}, and H'_{III}). (D) Improvement of the color resolution of the DFM images corresponding to (B) by amplifying the color difference signals.
Adapted with permission from Nanoscale, 2017, 9, 4593–4600.

0.85 nM, respectively, highlighting the importance of precise control over the spatial arrangement of SERS nanotags in optimizing the overall detection performance. However, compared to the control over their arrangement, there is perhaps greater freedom to design and fabricate novel SERS nanotags that can allow multiplex detection and at the same time improve the overall detection performance. Indeed, there are many current works that have achieved multiplex miRNA detection using a wide variety of SERS nanotags [344–348]. For example, the group of Vo-Dinh introduced the inverse molecular sentinel (iMS) nanoprobes for multiplex detection of miRNA cancer biomarkers directly from biological samples [344,346]. The iMS basically acts as an "off-to-on" signal switch based on a non-enzymatic strand displacement process and the conformational change of hairpin oligonucleotide probes upon target binding. In the absence of target miRNA, the oligonucleotide probe with a nanostructure at one end and a Raman reporter molecule at the other end is kept in a stretched configuration by means of hybridization with a partially complementary single-stranded DNA containing an overhanging toehold sequence (i.e. exposed sequence that later bind to the target miRNA), otherwise referred to as the placeholder strand. The sequence of the placeholder DNA strand is fully complementary to the target miRNA such that upon introduction of the target miRNA, the oligonucleotide probe is displaced and assumes a hairpin configuration, which brings the Raman reporter close to the nanostructure resulting in a SERS signal. Since iMS probes targeting different miRNAs can be easily tagged with different Raman reporter molecules, multiplex detection can be conveniently achieved. Most recently, Zhou et al. described the utilization of Raman dye encoded gold nanoparticles with narrow intra-nanogap structures (Au-RNNPs) as SERS nanotags and hollow silver microspheres (Ag-HMSs) as capturing substrates [348]. In a detection event, the miRNA will bind to both Ag-HMSs and Au-RNNPs to form a sandwich configuration. Excellent sensitivity and selectivity during the multiplex detection of 3 types of miRNA biomarkers (miRNA-21, miRNA-122, and miRNA-223), which is associated with hepatocellular carcinoma (HCC), was mainly

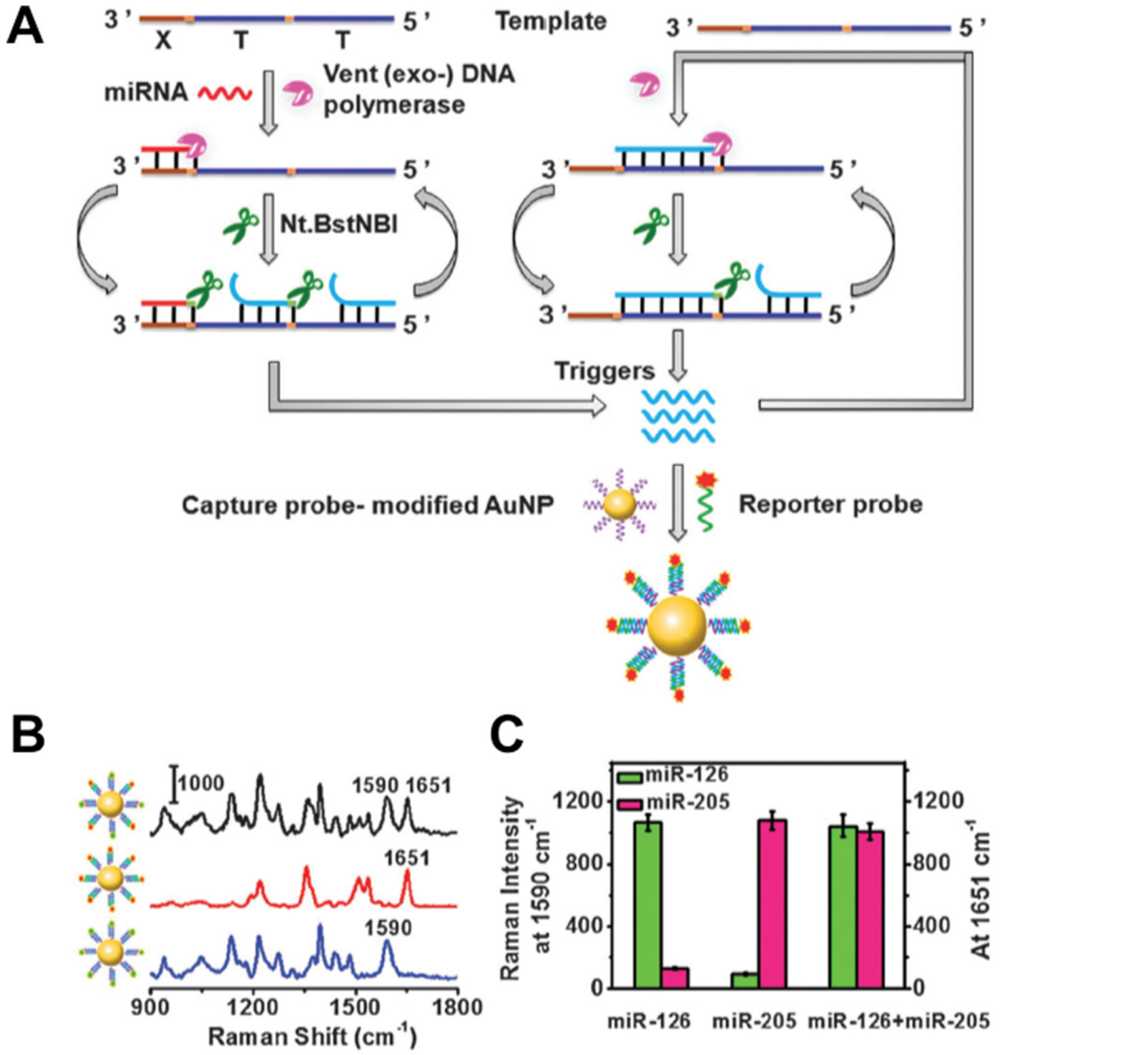

Fig. 4. (A) Schematic illustration of EXPAR-based SERS formicroRNA assay. Multiplexed miRNA assay. (B) Raman spectra of amplification products in the presence of miR-126 (blue line), miR-205 (red line), and a mixture of miR-126 and miR-205 (black line), respectively. The concentration of miR-126 is 1 pM, and the concentration of miR-205 is 1 pM. (C) Simultaneous detection of miR-126 (green column) and miR-205 (purple column) by measuring Raman intensity at 1590 cm^{-1} for miR-126 and 1651 cm^{-1} for miR-205. Error bars show the standard deviation of three experiments.
Adapted with permission from Chem. Commun., 2014, 50, 11,883–11,886.

attributed to the surface roughness of the Au-RNNPs. Finally, the SERS signals can also be amplified by means of generating an abundance of target miRNA or associated triggers that would bind to the SERS nanotags [333,349]. Although this involves an additional step prior to detection, it has proven to be remarkably successful in improving the detection sensitivity and selectivity. For example, in the work by Ye et al., whereby a circular exponential reaction (EXPAR)-based SERS was employed for the multiplex detection of several miRNAs associated with lung cancer, a detection limit of as low as 0.5 fM was obtained [333] (Fig. 4). This translated to a 6 order of magnitude improvement compared to the case without EXPAR amplification.

3.2. ctDNA

Circulating tumor DNA (ctDNA) are relatively small molecules with short length of around 100–200 nucleic acid base pairs (i.e. around 30–60 nm in length) [350,351]. Specific sequences point to different types of cancer (cancer-associated genes) and can be easily detected through highly specific hybridization reactions with nucleic acid probes bearing complementary sequences. Generally, the detection of cancer via ctDNA relies on the presence of mutations [51,352,353], although there are other types of abnormalities associated with genetic alteration such as microsatellite instability and loss of heterozygosity [354–356].

Since the size of ctDNA is within the sensing depth of LSPR, there is seemingly huge prospect for the technique to be used for ctDNA detection. Furthermore, LSPR transducers can be easily functionalized with complementary nucleic acid detection probes via well-established thiolation strategies [357,358]. Surprisingly, there exist only few works describing detection of ctDNA via LSPR-based detection schemes. This is possibly due to two main reasons. Firstly, typical ctDNA fragments are relatively long, consisting of around 150 bases [350]. It is therefore difficult to detect via solution-based aggregation strategies since the attachment of ctDNA will hinder nanoparticles from approaching each other to a distance close enough for effective plasmonic coupling to occur [359]. Secondly, at such lengths, they have the tendency to form secondary structures (e.g. hairpin, internal and bulge loops) that can conceal the mutated fragment [360]. As such, most works describing LSPR-based detection of ctDNA rely on single nanoparticles

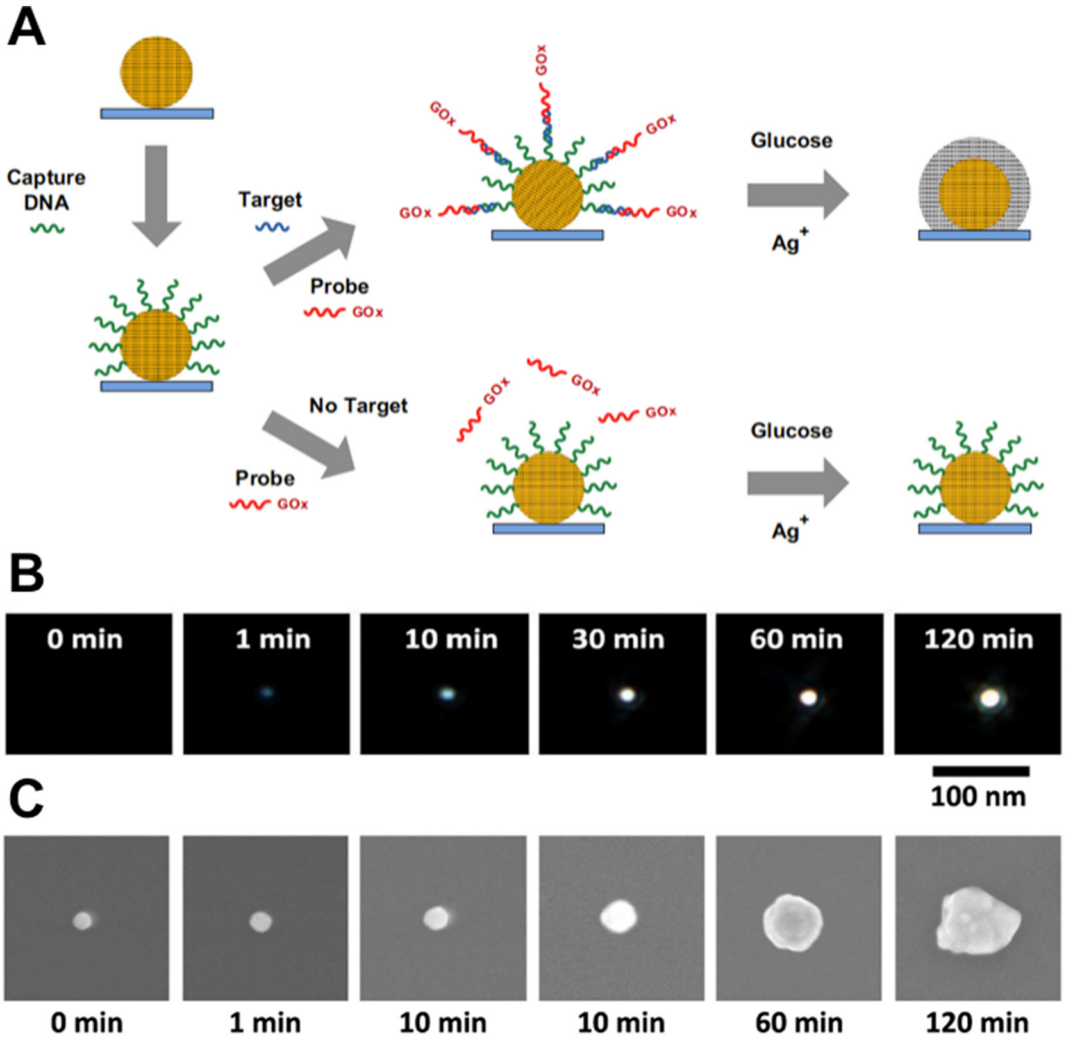

Fig. 5. (A) Schematic illustration of the enzyme-enhanced optical DNA sensor. Darkfield images (B) and SEM images (C) of GOx-guided time-dependent growth of an AuNP seed. Adapted with permission from Biosensors and Bioelectronics 79 (2016) 266–272.

with measurements performed in a dark-field setup. One of the earliest examples of mutant DNA detection using single nanoparticles was demonstrated by Ma et al., whereby gold nanoparticles (AuNPs) measuring around 50 nm in diameter is functionalized with thiol-oligonucleotide probes [334]. Upon the introduction of the sample solution, both in buffer and serum, the mutant DNA hybridizes with the oligonucleotide probe on the AuNP surface, resulting in a slight red shift of the LSPR scattering spectra to a higher wavelength. In order to amplify this shift, they employed cell-derived DNA mismatch repair protein MutS, which recognizes and binds specifically to the mutant fragment of the DNA. By using this strategy, they were able to distinguish mutant from normal genes and quantify the amount of mutant DNA down to picomolar levels. In a separate work by Nguyen et al., both mutation and methylation of ctDNA of PIK3CA gene is detected by means of hybridization with peptide nucleic acid (PNA) probe on single AuNPs [361]. In this case, signal amplification is performed via the addition of immunogold colloids that specifically detect methylation sites on the target ctDNA. While the primary detection event (i.e. ctDNA-PNA hybridization) led to a LSPR peak shift of around 4.3 nm, the secondary detection event (i.e. immunogold attachment to the ctDNA) led to a LSPR peak shift of around 11.4 nm. This eventually translated to a four times enhancement in terms detection sensitivity, reducing the limit of detection from 200 fM to 50 fM. More importantly, their work demonstrated the capability of LSPR to detect not only hot-spot mutations but also epigenetic changes on the ctDNA. While these works have demonstrated signal amplification, they do not result in a significant change to the appearance of scattered light observed under the dark-field microscope. Recently, Guo et al. demonstrated the possibility of distinguishing the mutant from wild-type phenotypes of the breast cancer gene BRCA1 by means of direct observation of the scattered light under the microscope [362] (Fig. 5). They employed a unique detection scheme involving an enzyme-guided enlargement of AuNPs. In brief, small AuNPs (25 nm in diameter) that are typically invisible under the dark-field microscope act as the target-binding sites. Upon target binding, Ag deposition is triggered via an enzyme-mediated reaction leading to an enlargement of the AuNP beyond its diffraction limit, making it visible. Quantitatively, a limit of detection of 5.0×10^{-21} M was obtained following this scheme. In other words, that is the lowest concentration that can transform the darkfield image of the nanoparticle from a completely dark to a blue dot. With regard to the detection of ctDNA based on an ensemble of nanoparticles, Sanroman-Iglesias et al. recently revealed a strategy involving sequential bridging of DNA-functionalized AuNPs. They noted that while the direct addition of ctDNA to a solution mixture containing two sets of probe DNA-functionalized AuNPs (65 nm in diameter) did not result in any aggregation, pre-incubation of the target with one set of DNA-functionalized AuNPs followed by the addition of the second set led to appreciable increase in AuNP cluster size. This is attributed to the extension of non-hybridized bases of

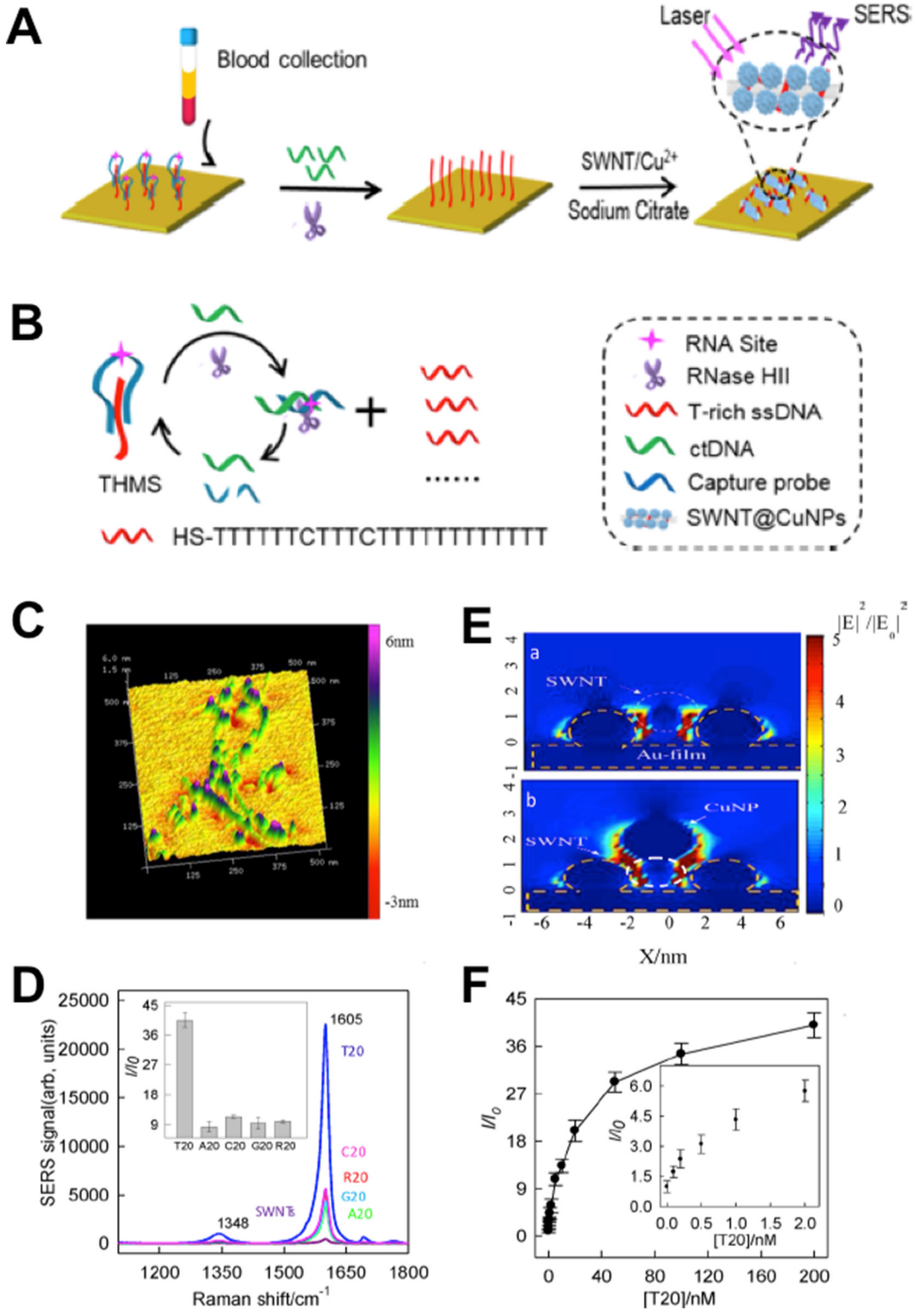

Fig. 6. (A) Construction of SWNT-based SERS assay coupling with RNase HII-assisted amplification for highly sensitive detection of ctDNA in human blood. The enlarged image illustrates T-rich DNA mediated growth of CuNPs to enhance the SERS signal of SWNTs. (B) Mechanism of RNase HII-assisted THMS-based amplified recognition to produce numerous T-rich ssDNAs. (C) Representative AFM image of T20-mediated growth of CuNPs on the SWNT surface. (D) SERS spectra of SWNTs and DNAmediated SWNT@CuNPs with A20, T20, C20, G20, and random DNA. [$CuSO_4$] = 150 μM and [$Na_3C_6H_5O_7$] = 2 mM. The concentration of SWNTs was excessive. (E) FDTD simulation of the normalized EM-field intensity distribution ($|E|^2/|E_0|^2$) for T20-mediated SWNT@CuNPs: (a) XZ plane views of T20-mediated SWNTs and (b) XZ plane views of T20-mediated SWNT@CuNPs on the surface of a Au film. (D) SERS intensity enhancements of the 1605 cm^{-1}-band of SWNTs, I/I_0, plotted against the concentration of T20.
Adapted with permission from Anal. Chem. 2016, 88, 4759–4765.

the target upon hybridization with the short-sequence probe DNA in the first set of AuNPs, highlighting the importance of unravelling the secondary structure of the ctDNA for successful detection based on AuNP aggregation. With this strategy, they demonstrated the colorimetric detection of single-based mutations in ctDNA containing 70 and 140 bases.

Besides LSPR-based detection platforms, SERS-based detection platforms have also been used to detect ctDNA. As earlier described, SERS nanotags have an outer layer of dielectric material, which can likewise be functionalized to present short-strand nucleic acid probes. Another advantage of SERS-based detection platforms is that it allows multiplex sensing and it is capable of direct detection in human blood without the need for a separate purification or separation step. For example, Wee et al. combined the simplicity of a standard polymerase chain reaction (PCR) procedure with the multiplexing capability of a SERS-based detection scheme to develop a PCR/SERS assay for the detection of ctDNA [363]. Briefly, PCR amplicons obtained from target DNA sequences is enriched on magnetic beads and attached with mutation-specific SERS nanotags. Since the nanotags employ dedicated reporter molecules for different mutation sequences, the presence of several mutation sequences can be detected simultaneously from a single SERS spectrum in the output signal. As a proof-of-concept, they first utilized the assay for triplex detection of 3 clinically important DNA point mutations in melanoma (BRAF V600E, c-Kit L576P and NRAS Q61K) and as few as 10 mutant alleles were successfully detected from a background of 10,000 wild-type sequences. By using <5 ng of genomic DNA, the assay can accurately genotype cell lines and serum-derived ctDNA from cancer patients. As these procedures are essentially performed in a single-tube, its simplicity and multiplexing capability makes it suitable for translation to a clinical setting. In another work, Zhou et al. described SERS detection of ctDNA directly in human blood by employing single-walled carbon nanotubes [364] (Fig. 6). In their approach, the specific identification of ctDNA was achieved using a triple-helix molecular switch (THMS) structure as the recognition element. The thymine-rich ssDNA fragment of the THMS structure was used as the signal transduction probe while an RNA site embedded in the sequence produce numerous T-rich ssDNA in the presence of target ctDNA, mediated by the enzyme RNase HII. The T-rich ssDNA fragments then adsorb onto single-walled carbon nanotubes (SWNTs) to form ssDNA/SWNT complex, which served as a template for the growth of copper nanoparticles (CuNPs) in the presence of copper (Cu^{2+}) ions and sodium citrate. The CuNPs on ssDNA/SWNT complex gave rise to SERS enhancement of the G-band peak of SWNTs, the intensity of which is dependent on the T-rich ssDNA concentration. Following this detection scheme, they could identify KRAS G12DM mutation down to femtomolar levels from microliter blood sample volumes.

3.3. Proteins

Proteins are generally large and complex biomacromolecules measuring around tens to hundreds of nm [365]. Generally, they can be detected by specific interaction with antibodies [366,367] or aptamers [368,369], which are protein-specific nucleic acid sequences. Disease detection is usually inferred from an elevated concentration (due to over-expression) of cancer biomarker proteins [370,371].

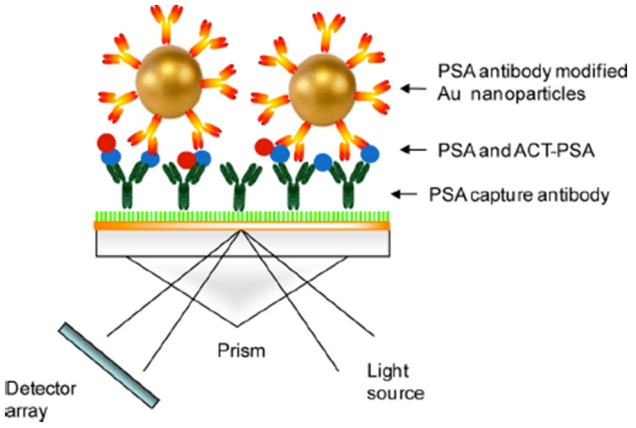

Fig. 7. Schematic representation of the PSA sandwich assay on a SPR platform using PSA detection antibody-modified Au nanoparticles.
Adapted with permission from Anal. Chem. 2012, 84, 5898–5904.

Within the general context of protein sensing, the SPR technique has been widely employed for the real-time characterization of protein-protein [372,373], protein-ligand [374,375] and protein-surface interactions [376–378], providing information on the binding kinetics and affinity of the interactions. As such, protocols for protein assay developments and concentration measurements have also been well-established, facilitating its adaptation for the detection of cancer biomarker proteins. In a typical SPR-based detection format, the sensing surface is functionalized with antibodies or aptamers that serve as the biorecognition element for the target protein of interest. However, considering the fact that cancer biomarker proteins are usually present at ultralow concentration levels in the blood, an additional step is usually needed to amplify the signal. For example, Krishnan et al. relied on the labeling of targets captured on the SPR sensing surface with superparamagnetic nanoparticle clusters to achieve an ultralow detection limit (around 300 attomolar) for cancer biomarker prostate specific antigen (PSA) in serum [379]. In a separate work, Uludag et al. also described the development of a point-of-care immunosensor for the detection of total PSA (tPSA) using SPR with an amplification step involving gold nanoparticles [380] (Fig. 7). In this case, a detection limit of 8.5 pM tPSA was obtained in 75% serum. In another work, Eletxigerra et al. also employed gold nanoparticles to amplify SPR responses for the detection of ErbB2 cancer biomarker protein in serum samples and raw cell lysates [381]. They obtained a limit of detection of 180 pg/mL in 50% human serum. In the detection of tumor necrosis factor alpha (TNF-α) Law et al. reported a 40-fold enhancement by employing a sandwich type configuration involving gold nanorods functionalized with a secondary antibody that binds to captured target [143]. The capture of target proteins on the SPR sensing surface can also be achieved without functionalizing the SPR sensing surface with a biorecognition element. This was recently demonstrated by Erturk et al. by using the microcontact imprinting method, which introduced PSA imprints directly onto the SPR sensor chip surface [382]. The system was used for the detection of PSA from clinical samples and the results were compared with those obtained using conventional ELISA. When the response linearity was compared between the two methods, no significant difference was found for PSA detection in serum samples from prostate cancer patients, highlighting its suitability for use in a clinical setting. Other ways to promote the use of SPR in a clinical setting include simplifying the instrumentation such as using a plastic optical fiber configuration [383].

Unlike SPR sensors, which utilizes planar substrates as the sensing surface and have sensing penetration depths of around 100–200 nm [115,116], LSPR sensors utilizes nanostructures as the signal transducer with sensing penetration depths of around 10–30 nm [113,140,158,160]. This represents an important consideration within the context of cancer biomarker protein sensing. In particular, the use of antibodies as the biorecognition element will not yield an appreciable response during the target detection step since antibodies would already occupy a large section of the sensing depth and the captured target would effectively lie beyond the sensing depth. Along this line, aptamers, which are oligonucleotide strands with specific recognition towards a particular protein, are often used instead of antibodies. In fact, the use of aptamer-conjugated nanomaterials represents a primary enabling factor that contributes to the success of LSPR-based detection schemes for protein sensing [384]. Due to the spatial and configurational flexibility of the nanostructure transducers, as well as the small size of aptamers, the detection of cancer biomarker proteins can be achieved through a variety of detection formats ranging from direct protein binding to nanoparticles adsorbed onto a solid support [385–389] to target-induced nanoparticle rearrangement in solution [390]. The captured target can also be further labelled with other nanoparticles for signal amplification [391] and LSPR-based detection schemes can also be

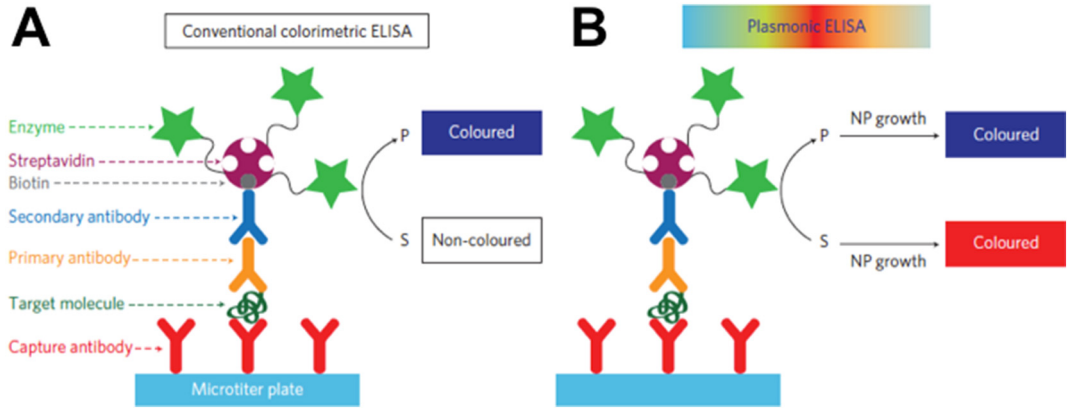

Fig. 8. Schematic representation of conventional ELISA versus Plasmonic ELISA. (A) In conventional colorimetric ELISA, enzymatic biocatalysis generates a colored compound. (B) In plasmonic ELISA the biocatalytic cycle of the enzyme generates colored nanoparticle solutions of characteristic tonality (S, substrate; P, product; NP, nanoparticle). Adapted with permission from Nature Nanotechnology, 7, 2012.

linked to other forms of detection schemes such as fluorescence detection using quantum dots [392]. Recent efforts aimed towards the application of LSPR-based sensing platforms in clinical settings have focused on developing their multiplexing capabilities [385,393]. In another exciting development, LSPR has been increasingly used in combination with conventional enzyme-linked immunosorbent assay (ELISA), in an approach often referred to as plasmonic ELISA [243]. This approach was first developed by the Stevens group. In their first report, they described how the catalytic cycle in the final step of ELISA can be used to control the growth of nanoparticles and generate colored solutions with distinct tonality in the presence of the target protein [240] (Fig. 8). They employed their system for the detection of PSA in whole serum and achieved successful detection down to an ultralow concentration of 1×10^{-18} g/mL. Since then, several other variants of the technique have been reported [394–399].

Similar to the case of LSPR-based detection platforms, cancer biomarker proteins can also be detected via SERS through a variety of detection schemes performed either on a substrate [400–402] or in solution [403]. For SERS-based direct detection of cancer biomarker proteins on a substrate, it is crucial to ensure that the surface can produce significant SERS enhancement (high efficiency SERS substrate) since the natural Raman signatures produced by some target proteins are weak. Such surfaces are usually roughened, highly corrugated or possess intricate nanostructures [345,364,404]. In the most recent example, Song et al. described the detection of a tumor marker, carcinoembryonic antigen (CEA) on Au-coated butterfly wings possessing natural three-dimensional hierarchical sub-micrometer structures [345]. Aside from the ability to effectively enhance Raman signals, these structures are extremely stable leading to high signal reproducibility. Compared to the direct detection approach, the detection of protein biomarkers involving the addition of SERS nanotags, conducted either on a solid support [400,402] or in solution [403], is generally more favorable since a sharper spectra can be obtained through the use of spectrally rich Raman reporter molecule. Recent efforts have focused on improving these strategies through various aspects such as probe design and instrumentation in order to obtain better detection performance. For example, Li et al. described the use of bifunctional nanocomposite probes in a flow-through system [405]. The nanocomposite probes, which comprised of a magnetic nickel iron core and a gold shell, served to enhance the SERS signals as well as to allow magnetic focusing of the bound target to the laser excitation spot. The use of magnetic focusing combined with microfluidics has also been reported in other SERS-based detection schemes [406,407]. In terms of improving the detection platform, additional functionalities can also be presented on the SERS substrate by means of introducing an electrical field. For example, Wang et al. introduced an electric field to the substrate to generate nanoscaled shear forces that facilitate transport of the target proteins to the surface, resulting in a rapid and specific SERS immunoassay [402]. SERS-active substrate properties can also be tuned through the use of hybrid materials or coatings, in order enhance functionalization with Raman reporter molecule, promote surface passivation and enhance the SERS response. For example, Zhou et al. reported the detection of tumor markers in human serum using SiO_2-coated silica nanoparticles as Raman probes and silver-coated SiC sandpaper as SERS active substrates [364]. They detected prostate specific antigen (PSA), alpha-fetoprotein (AFP), and carbohydrate antigen 19-9 (CA19-9) and obtained detection limits of 1.79 fg/mL, 0.46 fg/mL and 1.3×10^{-3} U/mL, respectively. The use of hybrid materials as SERS tags has been gaining traction in the context of both bioimaging and biosensing [408,409]. In the most recent development, Ali et al. demonstrated the controlled clustering of gold nanoparticles induced by graphene oxide and obtained SERS signal enhancements up to 3- to 4-fold higher compared to individual nanoparticles when used as SERS tags for the detection of antibodies [408]. Such design can likewise be adopted for the detection of cancer antigens in the near future. Besides variations to the detection platform, the detection performance can also be improved though better instrumentation and analysis techniques. For example, Dinish et al. described a highly sensitive SERS detection for epidermal growth factor receptors (EGFRs) in low sample volume using a hollow core photonic crystal fiber [410]. Chang et al. described an area-scanning method for the analysis of SERS responses and achieved PSA detection with femtomolar sensitivity and a broad dynamic range [411]. Most recently, Cheng et al. developed a SERS-based immunoassay for the determination of free to total (f/t) PSA ratio to improve the diagnostic performance of prostate cancer [403] (Fig. 9). Simultaneous dual detection of the two markers was performed using two SERS tags for clinical samples between 4.0 and 10.0 ng/mL (i.e. gray zone) and their results showed a good linear correlation with those measured using an electrochemiluminescene (ECL) system used in a clinical laboratory. Besides employing SERS for the detection of cancer biomarker proteins for the purpose of disease diagnosis, it can also be employed to monitor responses to drug treatments. This was demonstrated by Chung et al., whereby a SERS-based imaging technique was utilized to quantify the expression of EGFR before and after cetuximab treatment [412]. Finally, SERS can also be combined with ELISA to produce SERS-ELISA detection platforms whereby the catalytic cycle in the last step of ELISA is linked to the aggregation of silver nanoparticle SERS nanotags [302].

3.4. Exosomes

Exosomes are relatively small extracellular vesicles measuring around 30–120 nm in diameter [413,414]. They carry cargo that reflects the genetic or signaling alterations in cancer cells of origin [415–417].

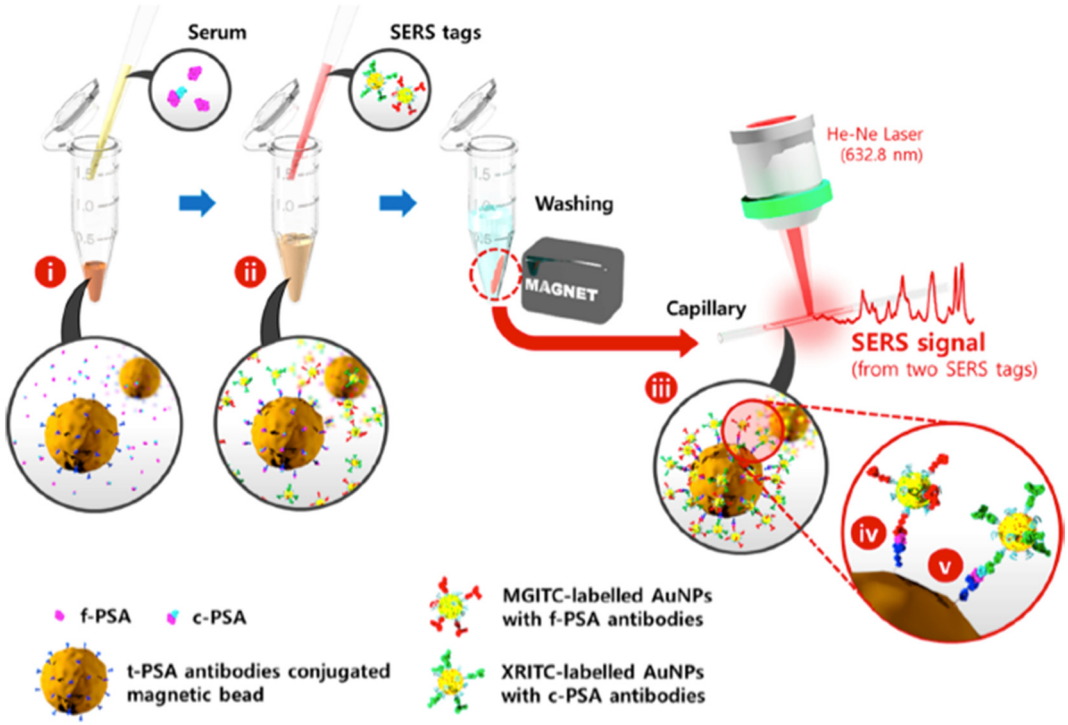

Fig. 9. Sequential SERS-based assay process for the simultaneous detection of f-PSA and c-PSA. (i) Mixing of f-PSA, c-PSA, and t-PSA antibody-conjugated magnetic beads. (ii) Addition of SERS nano tags to form sandwich immunocomplexes. (iii) Separation of magnetic immunocomplexes using a magnetic bar. Simultaneous detection of (iv) f-PSA and (v) c-PSA. Adapted with permission from ACS Nano 2017, 11, 4926–4933.

Generally, the detection of a specific type of cancer is based on an increased amount of exosomes in circulation [418–420].

The detection of exosomes via SPR based on a direct, label-free detection format is generally feasible [421–425] since the size of exosomes closely matches the SPR sensing depth. In one of the earliest reports of SPR-based exosome detection, an antibody microarray was combined with SPR imaging to achieve a label-free detection platform (Fig. 10). In brief, antibodies specific to exosome transmembrane proteins are functionalized on gold surfaces of the microarray chip. The reflected laser beam exiting the prism directly underneath the chip is recorded by a CCD camera. When the sample is injected, exosomes are directly captured by the antibodies on the microarray chip resulting in a refractive index change and a drop in the intensity of reflected laser beam. The intensity recorded by the CCD camera can therefore be directly correlated to the amount of captured exosomes. Since then, various techniques have been introduced to improve the detection performance. For example, Di Noto described the combination of colloidal gold merging colloidal plasmonics and SPR to achieve enhanced profiling of multiple

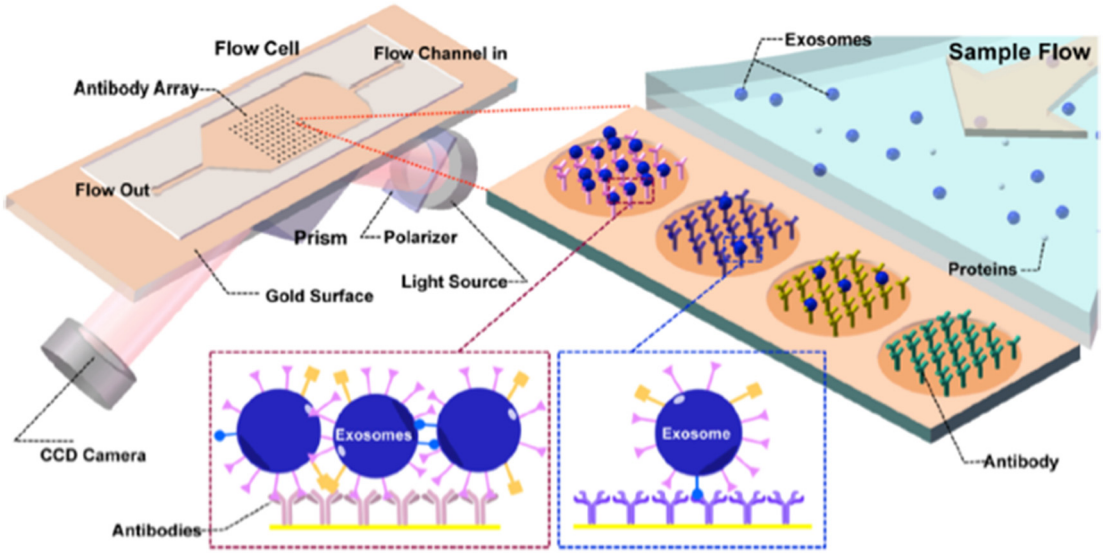

Fig. 10. Schematic view of SPRi in combination with antibody microarray to capture and detect exosomes in cell culture supernatant. Antibodies specific to exosome transmembrane proteins were printed on the gilded gold chip. The optical path from the laser passes through the coupling prism at a fixed angle of incidence, and the reflection is recorded by a CCD camera. Upon injection of sample into the flow cell, exosomes can be captured by antibodies on the chip, resulting in changes in the refractive index and therefore changes in the reflection intensities, which is monitored by the CCD camera.
Adapted with permission from Anal. Chem. 2014, 86, 8857–8864.

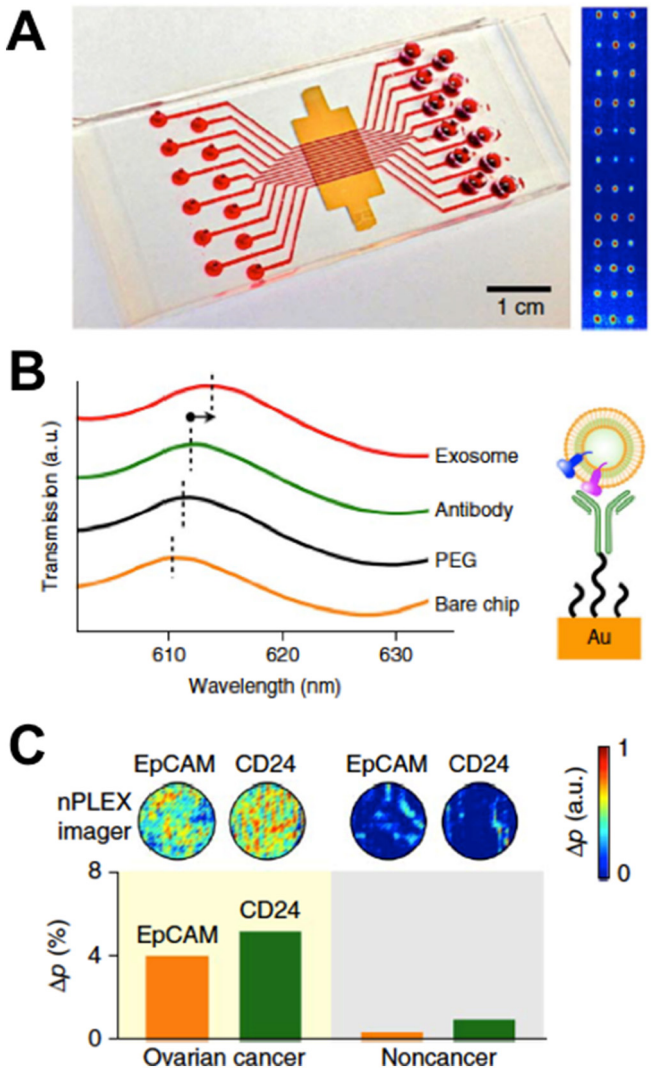

Fig. 11. Profiling of ovarian cancer patient exosomes with nPLEX. (A) A photograph of nPLEX chip integrated with a multichannel microfluidic cell for independent and parallel analyses. (Right) Transmission intensities of 12 by 3 nanohole arrays were measured simultaneously using the imaging setup. (B) A representative schematic of changes in transmission spectra showing exosome detection with nPLEX. The gold surface is pre-functionalized by a layer of polyethylene glycol (PEG), and antibody conjugation and specific exosome binding were monitored by transmission spectral shifts as measured by nPLEX (not drawn to scale). (C) Exosomal protein levels of EpCAM and CD24 in ascites samples from patients were measured by nPLEX. Ovarian cancer patient samples ($n = 20$) were associated with elevated EpCAM and CD24 levels, whereas noncancer patients ($n = 10$) showed negligible signals.
Adapted with permission from Nature Biotechnology 32, 5, 2014.

myeloma-derived exosomes [426]. Rupert et al. described a dual-wavelength SPR for determining not only the presence, but also the size and concentration of sub-populations of extracellular vesicles [424]. More recently, Sina et al. described an approach to quantify the proportion of clinically relevant exosomes (CREs) within the bulk exosome population isolated from patient serum [427]. The quantification began with the isolation of bulk exosome population followed by the detection CREs within the captured bulk exosomes using tumor specific markers. Following this approach, they successfully isolated exosomes from a small cohort of breast cancer patient samples and identified that approximately 14–35% of their bulk population express HER2.

The detection as well as quantitative profiling of exosomes via LSPR has been performed on gold nanoholes, nanopores and nanoislands. In the first demonstration of exosome detection on a nanoplasmonic platform, Im et al. employed a periodic gold nanohole array as the sensing substrate and conducted measurements based on transmission surface plasmon resonance [428] (Fig. 11). Each array is functionalized with antibodies that specifically bind to exosome surface proteins as well as proteins present in exosome lysates. Unlike conventional LSPR devices, which measure responses based on absorbance or scattering and produce absorbance and scattering spectra respectively, their nanoplasmonic exosome (nPLEX) assay measure light transmitted through the nanohole arrays and produce a transmission spectra. When exosomes specifically bind to the nPLEX sensor, the local refractive index will change. This event can be monitored by measuring either wavelength shifts in light spectrum or intensity changes at a fixed wavelength. The nPLEX sensor was used to analyze ascites samples from ovarian cancer patients and their results revealed that there was an increased expression of CD24 and EpCAM on exosomes derived from ovarian cancer patients. A significant advantage of transmission-based measurements is that it facilitates device miniaturization. In this case, the nPLEX sensor is integrated with a laser diode and a complementary metal-oxide semiconductor (CMOS) imager, forming a portable device capable of rapid and large scale sensing, which is suitable for use in the clinical setting. Following up on this work and adopting the same detection principle, Yang et al. employed nanopore arrays for multiparametric plasma extracellular vesicle profiling, which was aimed at facilitating diagnosis of pancreatic malignancy [429]. In a separate work, Thakur et al. utilized self-assembled gold nanoislands to detect and distinguish exosomes from multivesicular vesicles isolated from cells, blood serum and urine from a mouse model [430]. Most recently, Liang et al. described the nanoplasmonic quantification of tumor-derived extracellular vesicles in plasma microsamples based on light scattering [431]. In brief, a nanoplasmon-enhanced scattering (nPES) assay was used. The assay relied on the binding of antibody-conjugated gold nanospheres and nanorods to extracellular vesicles (EV) by EV-specific antibodies functionalized on a sensor chip to produce a local plasmon effect that enhances tumor-derived EV detection sensitivity and specificity.

The detection of exosomes using a SERS-based detection platform was mostly conducted in solution, with the aid of SERS nanoprobes. For example, Zong et al. described the facile detection of tumor-derived exosomes using magnetic nanobeads and SERS nanoprobes [432]. In the presence of exosomes, the magnetic nanobeads and SERS nanoprobes captured the exosomes by forming a sandwich-type immunocomplex, which was precipitated by a magnet. As a result, high intensity SERS signals were detected in the precipitates. In the absence of exosomes, there will be no immunocomplex formed and the SERS signals will be very weak (i.e. background). In another work, Stremersch et al. described a method to distinguish between exosome-like vesicles derived from different cellular origins by using partial least squares discriminant analysis on the obtained SERS spectra [433]. This study highlights the importance of combining SERS fingerprinting with an appropriate statistical analysis approach to develop effective cancer diagnostic tools for clinical applications. At the same time, SERS fingerprinting can be conducted either through the identification of specific peaks or through analysis of the entire SERS spectra. In the most recent work, Park et al. described exosome classification by pattern analysis for lung cancer diagnosis [434] (Fig. 12). In this case, the detection was performed on a solid support in which exosome directly attaches to gold nanoparticle coated glass slides without any biorecognition element. In other words, the SERS spectra originate from the exosomes. After detection, whole SERS spectra were analyzed using principle component analysis (PCA). By applying this methodology for pattern analysis, exosomes from lung cancer cells were clearly distinguished from exosomes from normal cells by 95.3% sensitivity and 97.3% specificity. With this approach, cancer diagnosis and identification can be performed in real-time using exosome as a cancer marker.

3.5. CTCs

Circulating tumor cells (CTCs) are cells that are shed off from the primary tumor into the blood circulation [435]. They typically measure

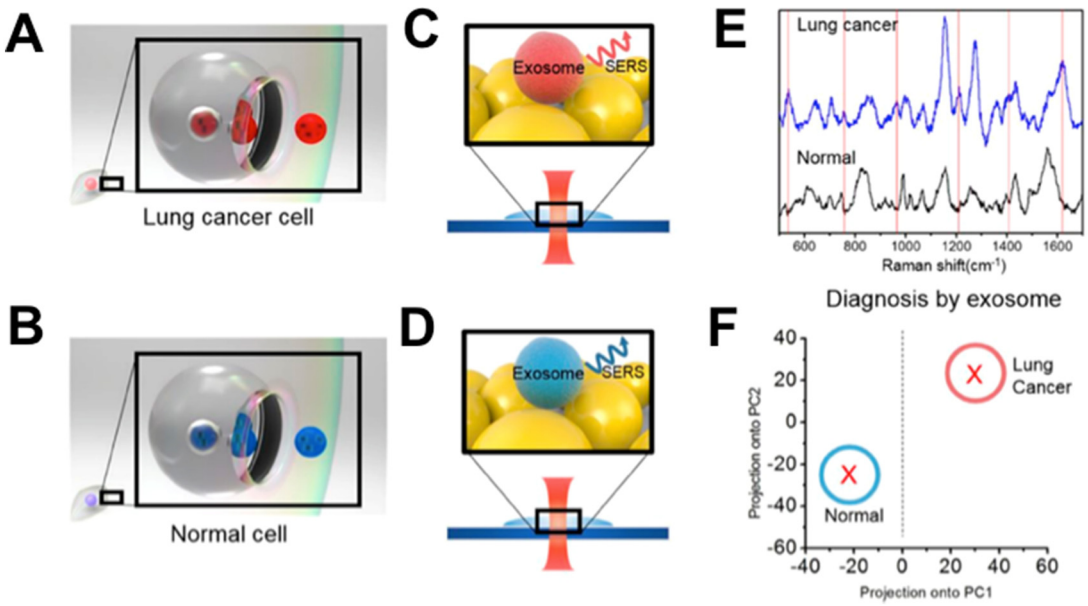

Fig. 12. Schematic diagram of lung cancer diagnosis by SERS classification of exosome. (A, B) Lung cancer cell and normal cell release exosomes to the extracellular environment having their own profiles by fusing multivesicular endosomes to plasma membrane, respectively. (C, D) Raman spectra of lung cancer cell and normal cell derived exosomes were achieved by SERS respectively. (E) SERS spectra achieved by methods of panels c and d are shown. Red lines indicate specific peaks of lung cancer derived exosomes. (F) Exosome classification is done by PCA of SERS spectra. Identifying the origin of the exosome is done by checking the location of the plotted X-marked dots. Dot plotted inside of the red circle indicates lung cancer cell derived exosome, and dot plotted inside of the blue circle indicates normal cell derived exosome.
Adapted with permission from DOI: https://doi.org/10.1021/acs.analchem.7b00911.

around 20–30 μm in diameter [436,437] and are present in blood at extremely low levels or copy number [438]. Since CTC-based cancer diagnosis essentially relies on the quantification of CTC concentration, it is often necessary to enrich the CTCs before it can be detected via conventional biosensing schemes. Along this line, most recent works have been dedicated to improve the efficiency of CTC capture and ensure a high

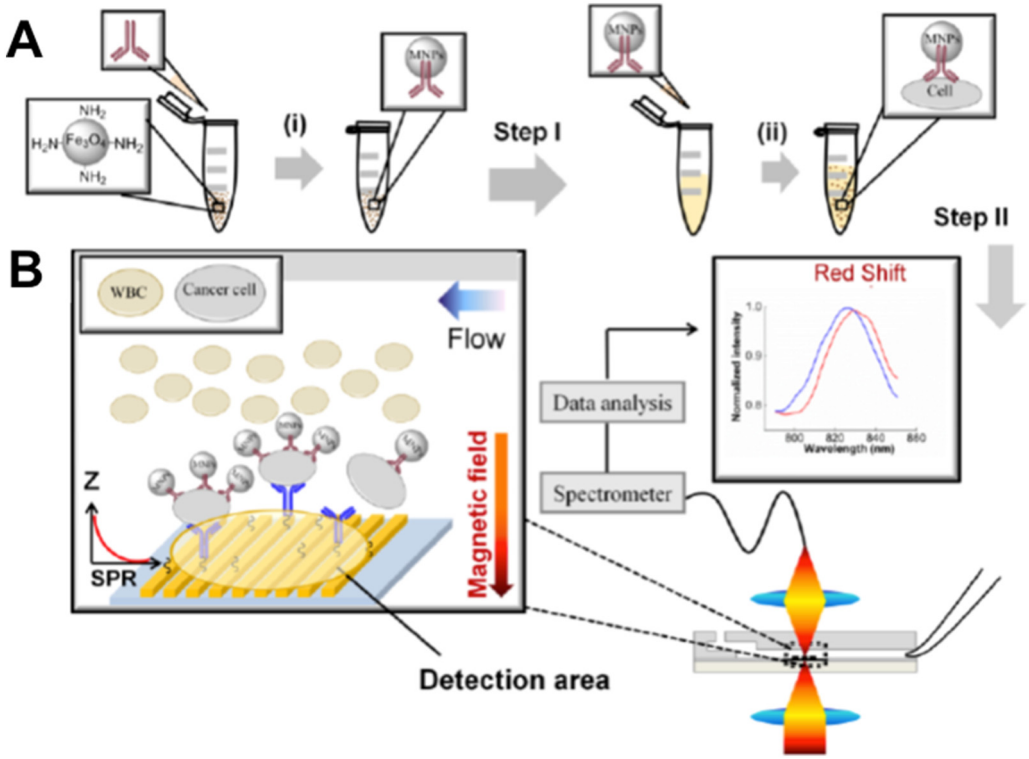

Fig. 13. SPR-based cancer cell detection with signal amplification with magnetic nanoparticles (MNPs). (A) The first step includes: (i) Functionalizing the MNPs with antibody I; (ii) Mixing the functionalized MNPs (carrying antibody I) with the sample to capture the target cells. (B) The second step includes introducing the mixture of blood sample and MNPs to the microfluidic chip and capturing the MNPs-cells to binds to the antibody II on the gold nanoslits. The cell binding on the gold nanoslits was monitored by the wavelength shift of the SPR spectrum generated by the gold nanoslits. The detection area of the nanoslits is defined by the focal spot of the probe light.
Adapted with permission from Biosensors 2015, 5, 98–117.

level of purity of captured cells [71,77]. These approaches rely on several distinguishing features of CTCs with respect to red and white blood cells. Aside from differentiating the different cells based on their physical properties such as size and stiffness [64,439,440], the expression of specific surface antigens on the CTCs is usually exploited for the purpose of CTC isolation and enrichment [441,442].

While there exists several SPR-based strategies for the general characterization of cell attachment to surfaces, including real-time tracking of cell-cell and cell-substrate interactions [443], detecting variations in cell layer morphology [444] and monitoring cell viability [445], the detection of CTCs using SPR detection platforms is still rare. Hiragun et al. first revealed the possibility of identifying different cancer cells lines through the different patterns of their respective SPR signals [446]. In a more recent work, Mousavi et al. demonstrated the detection of CTCs using a gold nanoslit SPR detection platform integrated with microfluidics. The detection was achieved following two steps [447] (Fig. 13). Firstly, CTCs from whole blood are captured on magnetic nanoparticles (MNPs) functionalized with a first set of antibodies recognizing specific antigens on the CTC surface. The suspension containing the CTC-bound MNPs was then introduced via microfluidics to the detection chip comprising of gold nanoslits that have been pre-functionalized with a second set of antibodies specific to the CTCs. Furthermore, a needle magnet was also placed beneath the sensing area to facilitate transport of CTC-bound MNPs to the surface of the gold nanoslits. In effect, this resulted in a highly selective capture of CTCs on the sensing area while eliminating non-specific adsorption of other cells present in whole blood, leading to a detection limit of 13 cells/mL of whole blood.

While the detection of CTCs using SPR-based platforms has been achieved by means of CTC accumulation on a planar or nanostructured bulk surface, detection of CTCs relying on LSPR has been performed almost exclusively in solution. Although it is not entirely clear why LSPR-based detection of CTCs has not been achieved on discrete nanostructures deposited on a solid support, one possible reason is that the dimension of the CTCs far exceeds the dimension of LSPR transducer (i.e. metal nanostructures). As such, a single CTC can adsorb onto several discrete nanostructures, making it difficult to directly correlate the LSPR signal response to the actual CTC surface coverage and concentration. Most reports describing CTC detection based on LSPR therefore depend on nanoparticle aggregation, which is either directly triggered in the presence of CTC, or mediated by an enzymatic signal amplification step. In of the earliest works describing the employment of LSPR for the detection of cancer cells, Medley et al. utilized aptamer-conjugated gold nanoparticles, which specifically bind to proteins and receptors that are uniquely present on the surfaces of cancer cells [448]. Conversely, nanoparticle accumulation and aggregation occurred only in the presence of cancer cells. Aside from observing significant changes to the LSPR absorption spectra, a color change is also visible to the unaided eye during the detection event. Excellent sensitivity and selectivity was maintained even in fetal bovine serum (FBS), which can be attributed to the application of highly specific aptamers as the cell recognition element. This also meant that the approach can differentiate between different types of cells, suggesting its wide applicability in cancer diagnosis. Having recognized the advantages of aptamer conjugation, especially within the context of cell detection by means of nanoparticle aggregation, several other closely-related detection schemes employing aptamer conjugation have been demonstrated. For example, Liu et al. described the detection of cancer cells on a lateral flow device by employing the same principle. In this case, cancer cells are first captured on the 'test zone' before the addition of aptamer-conjugated nanoparticle [449]. The attachment of the aptamer-conjugated nanoparticle to the cancer cells will result in a visible test line, the intensity of which can be quantified with a portable strip reader. Compared to the work by Medley et al., the main advantage of the sensor designed by Liu et al. is its operation simplicity and portability, which makes it highly suitable for point-of-care diagnostics. Aside from the direct accumulation and aggregation of nanoparticles on the surfaces of cancer cells, the aggregation of nanoparticles can also be mediated by cell-triggered cyclic enzymatic signal amplification (CTCESA) [450] (Fig. 14). There are two primary components in this scheme, namely linker DNA, which serve to link gold nanoparticles via hybridization with complementary sequences present on the nanoparticle surface, and hairpin aptamer probes, which specifically bind to the target cells. In the absence of target cells, no hybridization occurs between the linker DNA and hairpin aptamer probes and the linker DNA assembles the gold nanoparticles into relative large clusters, which produces a purple solution. In the presence of target cells, the hairpin aptamer probes specifically bind to the surface of the cells. This triggers a conformational switch that leads to linker DNA hybridization and cleavage by nicking endonuclease strand scission cycles. As a result, the cleaved fragments of the linker DNA can no longer assemble the nanoparticles, thereby producing a red solution. It is interesting to note that following this scheme, the presence of target cell is actually inferred through nanoparticle de-aggregation, instead of nanoparticle aggregation, highlighting the flexibility of colorimetric-based LSPR sensing. The cyclic enzymatic signal amplification step can also be performed more than once to achieve even greater signal enhancement.

Unlike LSPR-based colorimetric detection schemes employed for cancer cell detection that require a re-arrangement of an ensemble of nanoparticles to provide effective signal readout, SERS-based detection schemes can operate even by using discrete or isolated SERS nanotags since the signals essentially originate from the SERS reporter molecules, simplifying the detection protocol. On a related note, the presence of interfering molecules is less likely to affect the signal response as long as the SERS nanotags are appropriately functionalized with a

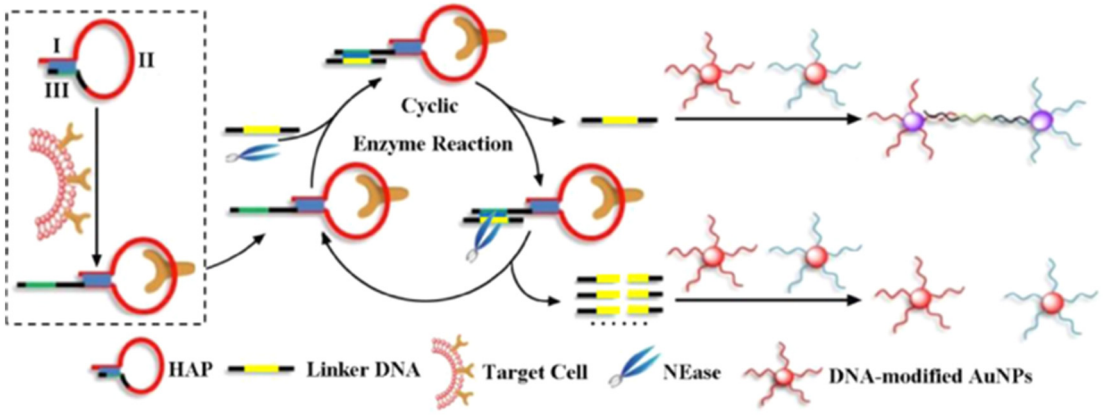

Fig. 14. Schematic illustration of a highly sensitive colorimetric method for the detection of rare cancer cells based on cell-triggered cyclic enzymatic signal amplification (CTCESA). Adapted with permission from Anal. Chem. 2014, 86, 5567–5572.

biorecognition element that binds to the target cell with a high level of specificity. This facilitates direct detection from whole blood. Furthermore, due to the narrow bandwidths of the SERS peaks, signals arising from a wide variety of SERS reporter molecules can be distinguished with relatively good precision when used simultaneously, paving the way for highly multiplexed detection formats. The first example of CTC detection employing SERS nanotags was reported almost a decade ago and even then, the detection was already performed in whole blood. It described the use of magnetic beads conjugated with epithelial cell-specific antibody (epithelial cell adhesion molecule, anti-EpCAM) and SERS nanotags conjugated to an anti-her2 antibody (human epidermal growth factor receptor-2) for the detection of SKBR3 cells from the breast cancer cell line. During detection, a mixture containing the antibody-conjugated magnetic beads and SERS nanotags was added to the blood sample containing the target cell in a reaction tube. The EpCAM antibody-conjugated magnetic beads only bind to cancer cells enabling its effective separation from other regular circulating cells (including red and white blood cells) in the presence of a magnetic field. At the same time anti-her2 antibody-conjugated SERS nanotags binds to the target cells in significant quantities due to the abundance of her2 receptors on the cell surface, ensuring not only specific recognition but also high intensity SERS peaks. The mixture is then subjected to a magnetic field to concentrate the magnetic beads along with the target cells and SERS nanotags to a single spot at the side of the tube where the SERS spectrum is acquired. The limit of detection obtained using 100 μL of blood sample was about 50 cells/mL. Clearly, a major advantage of this technique is its simplicity and the fact that it does not require any washing step. Since then, other similar detection schemes have been developed with slight variations [60,391,451,452]. For example, instead of using antibodies as the cell recognition element on the magnetic beads and SERS nanotags, aptamers can also be used [60]. More recently, several works have moved away from direct detection from solution and developed solid-based protocols, which are deemed to be more practical when used in a clinical setting. For example, Zhang et al. described the capture of target cells in the bloodstream by the SERS nanotags followed by their attachment on an antibody-functionalized nitrocellulose membrane substrate [453]. This approach eliminates the need for magnetic nanobeads and relies on the high density of antibodies on the nitrocellulose membrane to concentrate the SERS nanotag-decorated target cells within the sensing area. Following this line, there are also reports that have paid particular attention to the development of microfluidics-based SERS detection platforms [454,455]. In a notable example, Pallaoro et al. recently described a fully integrated microfluidic SERS system that is capable of identifying and quantifying cancer cells from a population of cells flowing through a microfluidic channel [455] (Fig. 15). There are two important features to this system. Firstly, two types of SERS nanotags (defined in their work as SERS biotags or SBTs) are employed such that one will only bind to cancerous cells while the other will universally bind to both cancerous and normal cells, serving as a non-cell-specific control. Each type of SBT contains a reporter molecule that presents a unique SERS spectrum with distinct Raman bands that can be easily deconvoluted from a composite SERS spectrum. Secondly, cells are forced by hydrodynamic forces to flow in a single file so that it crosses a focused laser beam at the interrogation region, allowing SERS signals to be acquired one cell at a time as they flow through the system. Prior to detection, the sample solution is incubated with both types of SBTs. When the samples pass through the laser beam, the SERS spectrum is acquired and deconvoluted using two strategies namely principle component analysis and classical least-squares, to identify the cancer cells and determine its amount. Owing to the spectroscopic richness of the Raman bands of the reporter molecules in each type of SBT, they were successful in detecting down to one cancer cell per 100 noncancerous cells under an interrogation time of 20 ms. This approach requires only one-step labeling, enable high-throughput continuous analysis and can be fabricated into a low-cost device, making it highly promising for point-of-care diagnostics. Apart from using spherical gold nanoparticles as SERS nanotags, nanorods with different metal compositions can also be employed to refine the signal responses. This was demonstrated by Nima et al., whereby the detection and imaging of single breast cancer cells in unprocessed human blood, representing CTCs, were achieved using tunable, silver-decorated, gold nanorods as SERS nanotags [456]. In essence, the decoration of gold nanorods with silver led to narrower bandwidths of the SERS peaks, providing higher spectral specificity. Compared to conventional gold nanorods, the use of silver gold nanorods resulted in an improvement in SERS signal enhancement by more than two orders of magnitude. The surface modification procedures of the SERS nanotags can also be varied to optimize the intensity of the SERS signal. For example, Wu et al. demonstrated the use of reductive bovine serum albumin (rBSA) as an alternative to the more conventional polyethylene glycol (PEG) for the purpose of bio-passivation and protective coating [457]. Since rBSA formed a thinner outer coating than PEG, SERS signals from the underlying SERS reporter molecules can be obtained with higher intensities, ultimately improving the detection performance. In a separate work, they applied the same strategy to SERS nanotags of different shapes specifically gold nanoparticles, gold nanorods and gold nanostars [458]. They revealed that gold nanostars produced the best sensing capability, with a detection limit of 1 cell/mL without requiring any enrichment process. Based on these recent efforts, it is clear that there is plenty of room for continual improvements to the detection

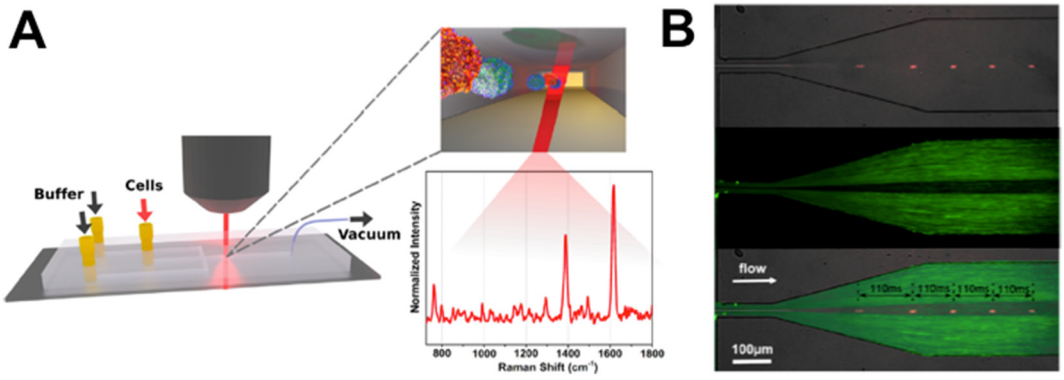

Fig. 15. Graphical depiction of a highly focused flow-through SERS detection system for sensing CTCs. (A) Schematic of setup and concept. Cells, prelabeled with a cocktail of cancer-specific (NRP) and control (UC) SBTs (the latter binding both cell types), are injected into the device, where they are flow-focused before passing through the Raman laser. (B) Simultaneous bright-field and epifluorescence (Cy3 channel, colorized orange) image of a single cell in the channel as a function of time illustrating the efficacy of flow focusing (top). Epifluorescence image (FITC channel, colorized green) of 200 nm polymer beads separately injected into the buffer channels, to highlight the sheath flow (center). Montage merging the two former images (bottom), showing the overall flow dynamics in the device.
Adapted with permission from ACS Nano 2015, 9, 4328–4336.

sensitivity and specificity of SERS-based CTC detection schemes, which can be achieved through the fabrication of novel SERS nanotags.

4. Conclusions & future outlook

Nanoplasmonic sensing techniques have been proven useful for the detection of a wide variety of circulating cancer biomarkers. This has been facilitated by well-established nanofabrication, surface modification and bio-functionalization techniques, which are routinely utilized in the nanoplasmonic sensing field for the general purpose of biomolecular detection beyond circulating cancer biomarkers. In particular, the protocols for wet-chemical synthesis or fabrication of nanoparticles and nanostructures are well-established and are widely available such that the nanostructures can be obtained with relatively good precision. At the same time, a wide selection of surface functionalization protocols is available for the attachment of biorecognition elements on the sensor surface. Clearly, this has accelerated the progress in sensor development for the detection of cancer biomarkers since it encourages the development of novel detection schemes.

However, it is worthy to note that while most works have focused on the development of novel detection schemes, or improvement of existing detection schemes, there exists only a few works that have attempted to design an integrated sensing platform for the purpose of device development. In other words, most works have mainly focused on the improvement of the detection performance. While progress in this aspect is encouraging, the translation of nanoplasmonic sensing techniques will not be possible without efforts to demonstrate its applicability as an integrated device. In order to achieve this, there needs to be greater combined efforts encompassing the development of sensing platform as well as instrumentation design. For example, while LSPR sensors based on darkfield microscopy can achieve excellent specificity and sensitivity, their translation into a clinical setting is still beyond the horizon due to their difficulty in miniaturization. In this respect, ensemble average LSPR sensors are more promising. Likewise, while conventional SPR sensors represent the gold standard for protein interaction studies, its utilization in the clinical setting cannot be achieved without significant modifications to the instrumentation setup, for example through the use of optical waveguides and optical fibers.

At the same time, while current works have focused almost entirely on improving detection specificity and sensitivity, it needs to be realized that effective detection of cancer biomarkers for purpose of proper analysis goes beyond singular detection events. Most often, relative concentration variations need to be monitored in real time and compared against several variants of the biomarker or in parallel with other biomarkers, instead of determining the absolute concentration of a single biomarker. To satisfy this requirement, novel techniques need to be demonstrated for the analysis of multiple or an ensemble of measurement signals.

Acknowledgements

This work was financially supported by a National Research Foundation of Korea (NRF) grant funded by the Ministry of Education, Science and Technology (NRF-2016R1A2B4007209), and by the National Research Foundation of Singapore through a Competitive Research Programme grant (NRF-CRP10-2012-07) and a Proof-of-Concept grant (NRF2015NRF-POC0001-19) as well as through the Centre for Precision Biology at Nanyang Technological University.

References

[1] J.A. Ludwig, J.N. Weinstein, Biomarkers in cancer staging, prognosis and treatment selection, Nat. Rev. Cancer 5 (2005) 845–856.
[2] L. Wu, X. Qu, Cancer biomarker detection: recent achievements and challenges, Chem. Soc. Rev. 44 (2015) 2963–2997.
[3] N.L. Henry, D.F. Hayes, Cancer biomarkers, Mol. Oncol. 6 (2012) 140–146.
[4] J. Kononen, L. Bubendorf, A. Kallionimeni, M. Barlund, P. Schraml, S. Leighton, J. Torhorst, M.J. Mihatsch, G. Sauter, O.-P. Kallionimeni, Tissue microarrays for high-throughput molecular profiling of tumor specimens, Nat. Med. 4 (1998) 844–847.
[5] A.A. Bravo, S.G. Sheth, S. Chopra, Liver biopsy, N. Engl. J. Med. 344 (2001) 495–500.
[6] M. Borghesi, H. Ahmed, R. Nam, E. Schaeffer, R. Schiavina, S. Taneja, W. Weidner, S. Loeb, Complications after systematic, random, and image-guided prostate biopsy, Eur. Urol., 71, 353–365.
[7] S. Loeb, A. Vellekoop, H.U. Ahmed, J. Catto, M. Emberton, R. Nam, D.J. Rosario, V. Scattoni, Y. Lotan, Systematic review of complications of prostate biopsy, Eur. Urol., 64, 876–892.
[8] M. Greaves, C.C. Maley, Clonal evolution in cancer, Nature 481 (2012) 306–313.
[9] N. Murugaesu, S.K. Chew, C. Swanton, Adapting clinical paradigms to the challenges of cancer clonal evolution, Am. J. Pathol. 182 (2013) 1962–1971.
[10] F.D.S.E. Melo, L. Vermeulen, E. Fessler, J.P. Medema, Cancer heterogeneity—a multifaceted view, EMBO Rep. 14 (2013) 686–695.
[11] P. Eirew, A. Steif, J. Khattra, G. Ha, D. Yap, H. Farahani, K. Gelmon, S. Chia, C. Mar, A. Wan, E. Laks, J. Biele, K. Shumansky, J. Rosner, A. McPherson, C. Nielsen, A.J.L. Roth, C. Lefebvre, A. Bashashati, C. de Souza, C. Siu, R. Aniba, J. Brimhall, A. Oloumi, T. Osako, A. Bruna, J.L. Sandoval, T. Algara, W. Greenwood, K. Leung, H. Cheng, H. Xue, Y. Wang, D. Lin, A.J. Mungall, R. Moore, Y. Zhao, J. Lorette, L. Nguyen, D. Huntsman, C.J. Eaves, C. Hansen, M.A. Marra, C. Caldas, S.P. Shah, S. Aparicio, Dynamics of genomic clones in breast cancer patient xenografts at single-cell resolution, Nature 518 (2015) 422–426.
[12] S. Gupta, K. Seaberg, M.J. Wallace, D.C. Madoff, J. Frank, A. Morello, K. Ahrar, R. Murthy, M.E. Hicks, Imaging-guided percutaneous biopsy of mediastinal lesions: different approaches and anatomic considerations, Radiographics 25 (2005) 763–786.
[13] D.M. Lerman, Biopsy considerations, in: R.L. Randall (Ed.), Metastatic Bone Disease: An Integrated Approach to Patient Care, Springer New York, New York, NY 2016, pp. 111–117.
[14] J.H. Burkhardt, J.H. Sunshine, Core-needle and surgical breast biopsy: comparison of three methods of assessing cost, Radiology 212 (1999) 181–188.
[15] R. Kang, P.P. Goodney, S.L. Wong, Importance of cost-effectiveness and value in cancer care and healthcare policy, J. Surg. Oncol. 114 (2016) 275–280.
[16] I.A. Cree, Liquid biopsy for cancer patients: principles and practice, Pathogenesis 2 (2015) 1–4.
[17] E. Crowley, F. Di Nicolantonio, F. Loupakis, A. Bardelli, Liquid biopsy: monitoring cancer-genetics in the blood, Nat. Rev. Clin. Oncol. 10 (2013) 472–484.
[18] C. Fumagalli, F. Bianchi, P.R. Raviele, D. Vacirca, G. Bertalot, C. Rampinelli, M. Lazzeroni, B. Bonanni, G. Veronesi, N. Fusco, M. Barberis, E. Guerini-Rocco, Circulating and tissue biomarkers in early-stage non-small cell lung cancer, ecancermedicalscience 11 (2017) 717.
[19] R.M. Bremnes, R. Sirera, C. Camps, Circulating tumor-derived DNA and RNA markers in blood: a tool for early detection, diagnostics, and follow-up?, Lung Cancer, 49, 1–12.
[20] D. Konforte, E.P. Diamandis, Is early detection of cancer with circulating biomarkers feasible? Clin. Chem. 59 (2013) 35.
[21] J.C.M. Wan, C. Massie, J. Garcia-Corbacho, F. Mouliere, J.D. Brenton, C. Caldas, S. Pacey, R. Baird, N. Rosenfeld, Liquid biopsies come of age: towards implementation of circulating tumor DNA, Nat. Rev. Cancer 17 (2017) 223–238.
[22] B. Gold, M. Cankovic, L.V. Furtado, F. Meier, C.D. Gocke, Do circulating tumor cells, exosomes, and circulating tumor nucleic acids have clinical utility? J. Mol. Diagn. 17 (2015) 209–224.
[23] G. Attard, J.S. de Bono, Utilizing circulating tumor cells: challenges and pitfalls, Curr. Opin. Genet. Dev. 21 (2011) 50–58.
[24] Y. Ming, Y. Li, H. Xing, M. Luo, Z. Li, J. Chen, J. Mo, S. Shi, Circulating tumor cells: from theory to nanotechnology-based detection, Front. Pharmacol. 8 (2017).
[25] M.G. Krebs, R.L. Metcalf, L. Carter, G. Brady, F.H. Blackhall, C. Dive, Molecular analysis of circulating tumor cells—biology and biomarkers, Nat. Rev. Clin. Oncol. 11 (2014) 129–144.
[26] C. Sheridan, Exosome cancer diagnostic reaches market, Nat. Biotechnol. 34 (2016) 359–360.
[27] Y. Soung, S. Ford, V. Zhang, J. Chung, Exosomes in cancer diagnostics, Cancer 9 (2017) 8.
[28] Y.L. Jia, Y.X. Chen, Q.C. Wang, U. Jayasinghe, X. Luo, Q. Wei, J. Wang, H.C. Xiong, C. Chen, B. Xu, W.X. Hu, L.B. Wang, W.H. Zhao, J.C. Zhou, Exosome: emerging biomarker in breast cancer, Oncotarget 8 (2017) 41717–41733.
[29] H.J. Lee, A.W. Wark, R.M. Corn, Microarray methods for protein biomarker detection, Analyst 133 (2008) 975–983.
[30] G. Mor, I. Visintin, Y. Lai, H. Zhao, P. Schwartz, T. Rutherford, L. Yue, P. Bray-Ward, D.C. Ward, Serum protein markers for early detection of ovarian cancer, Proc. Natl. Acad. Sci. U. S. A. 102 (2005) 7677–7682.
[31] J.F. Rusling, C.V. Kumar, J.S. Gutkind, V. Patel, Measurement of biomarker proteins for point-of-care early detection and monitoring of cancer, Analyst 135 (2010) 2496–2511.
[32] N. Krishnamurthy, E. Spencer, A. Torkamani, L. Nicholson, Liquid biopsies for cancer: coming to a patient near you, J. Clin. Med. 6 (2017) 3.
[33] K. Pantel, Blood-based analysis of circulating cell-free dna and tumor cells for early cancer detection, PLoS Med. 13 (2016), e1002205.
[34] P.T. Spellman, J.W. Gray, Detecting cancer by monitoring circulating tumor DNA, Nat. Med. 20 (2014) 474–475.
[35] G. Cheng, Circulating miRNAs: roles in cancer diagnosis, prognosis and therapy, Adv. Drug Deliv. Rev. 81 (2015) 75–93.
[36] S.W. Fu, W. Lee, C. Coffey, A. Lean, X. Wu, X. Tan, Y.-g. Man, R.F. Brem, miRNAs as potential biomarkers in early breast cancer detection following mammography, Cell Biosci. 6 (2016) 6.
[37] S. Rachagani, M.A. Macha, N. Heimann, P. Seshacharyulu, D. Haridas, S. Chugh, S.K. Batra, Clinical implications of miRNAs in the pathogenesis, diagnosis and therapy of pancreatic cancer, Adv. Drug Deliv. Rev. 81 (2015) 16–33.

[38] Y. Hong, F. Fang, Q. Zhang, Circulating tumor cell clusters: what we know and what we expect (Review), Int. J. Oncol. 49 (2016) 2206–2216.
[39] J.T. Kaifi, M. Kunkel, J. Zhu, D.T. Dicker, N. Gusani, Z. Yang, N.E. Sarwani, G. Li, E.T. Kimchi, K.F. Staveley-O'Carroll, W.S. El-Deiry, Circulating tumor cells are associated with diffuse spread in stage IV colorectal cancer patients, Cancer Biol. Ther. 14 (2013) 1174–1181.
[40] J.T. Kaifi, M. Kunkel, D.T. Dicker, J. Joude, J.E. Allen, A. Das, J. Zhu, Z. Yang, N.E. Sarwani, G. Li, K.F. Staveley-O'Carroll, W.S. El-Deiry, Circulating tumor cell levels are elevated in colorectal cancer patients with high tumor burden in the liver, Cancer Biol. Ther. 16 (2015) 690–698.
[41] N. Aceto, A. Bardia, D.T. Miyamoto, M.C. Donaldson, B.S. Wittner, J.A. Spencer, M. Yu, A. Pely, A. Engstrom, H. Zhu, B.W. Brannigan, R. Kapur, S.L. Stott, T. Shioda, S. Ramaswamy, D.T. Ting, C.P. Lin, M. Toner, D.A. Haber, S. Maheswaran, Circulating tumor cell clusters are oligoclonal precursors of breast cancer metastasis, Cell 158 (2014) 1110–1122.
[42] A. Fabisiewicz, E. Grzybowska, CTC clusters in cancer progression and metastasis, Med. Oncol. 34 (2016) 12.
[43] A. Beach, H.-G. Zhang, M.Z. Ratajczak, S.S. Kakar, Exosomes: an overview of biogenesis, composition and role in ovarian cancer, J. Ovarian Res. 7 (2014) (14–14).
[44] C.Y. Wu, S.L. Du, J. Zhang, A.L. Liang, Y.J. Liu, Exosomes and breast cancer: a comprehensive review of novel therapeutic strategies from diagnosis to treatment, Cancer Gene Ther. 24 (2017) 6–12.
[45] C. Corrado, S. Raimondo, A. Chiesi, F. Ciccia, G. De Leo, R. Alessandro, Exosomes as intercellular signaling organelles involved in health and disease: basic science and clinical applications, Int. J. Mol. Sci. 14 (2013) 5338–5366.
[46] H.J. Huber, P. Holvoet, Exosomes: emerging roles in communication between blood cells and vascular tissues during atherosclerosis, Curr. Opin. Lipidol. 26 (2015) 412–419.
[47] M.K.S. Tang, A.S.T. Wong, Exosomes: emerging biomarkers and targets for ovarian cancer, Cancer Lett. 367 (2015) 26–33.
[48] Q. Wang, R. Chaerkady, J. Wu, H.J. Hwang, N. Papadopoulos, L. Kopelovich, A. Maitra, H. Matthaei, J.R. Eshleman, R.H. Hruban, K.W. Kinzler, A. Pandey, B. Vogelstein, Mutant proteins as cancer-specific biomarkers, Proc. Natl. Acad. Sci. 108 (2011) 2444–2449.
[49] K.A. Sato, T. Hachiya, T. Iwaya, K. Kume, T. Matsuo, K. Kawasaki, Y. Abiko, R. Akasaka, T. Matsumoto, K. Otsuka, S.S. Nishizuka, Individualized mutation detection in circulating tumor DNA for monitoring colorectal tumor burden using a cancer-associated gene sequencing panel, PLoS One 11 (2016), e0146275.
[50] X. Yi, J. Ma, Y. Guan, R. Chen, L. Yang, X. Xia, The feasibility of using mutation detection in ctDNA to assess tumor dynamics, Int. J. Cancer 140 (2017) 2642–2647.
[51] C. Bettegowda, M. Sausen, R.J. Leary, I. Kinde, Y. Wang, N. Agrawal, B.R. Bartlett, H. Wang, B. Luber, R.M. Alani, E.S. Antonarakis, N.S. Azad, A. Bardelli, H. Brem, J.L. Cameron, C.C. Lee, L.A. Fecher, G.L. Gallia, P. Gibbs, D. Le, R.L. Giuntoli, M. Goggins, M.D. Hogarty, M. Holdhoff, S.-M. Hong, Y. Jiao, H.H. Juhl, J.J. Kim, G. Siravegna, D.A. Laheru, C. Lauricella, M. Lim, E.J. Lipson, S.K.N. Marie, G.J. Netto, K.S. Oliner, A. Olivi, L. Olsson, G.J. Riggins, A. Sartore-Bianchi, K. Schmidt, I.-M. Shih, S.M. Oba-Shinjo, S. Siena, D. Theodorescu, J. Tie, T.T. Harkins, S. Veronese, T.-L. Wang, J.D. Weingart, C.L. Wolfgang, L.D. Wood, D. Xing, R.H. Hruban, J. Wu, P.J. Allen, C.M. Schmidt, M.A. Choti, V.E. Velculescu, K.W. Kinzler, B. Vogelstein, N. Papadopoulos, L.A. Diaz, Detection of circulating tumor DNA in Early- and Late-stage human malignancies, Sci. Transl. Med. 6 (2014), 224ra224.
[52] A.M. Newman, S.V. Bratman, J. To, J.F. Wynne, N.C.W. Eclov, L.A. Modlin, C.L. Liu, J.W. Neal, H.A. Wakelee, R.E. Merritt, J.B. Shrager, B.W. Loo Jr., A.A. Alizadeh, M. Diehn, An ultrasensitive method for quantitating circulating tumor DNA with broad patient coverage, Nat. Med. 20 (2014) 548–554.
[53] C. Catalanotto, C. Cogoni, G. Zardo, MicroRNA in control of gene expression: an overview of nuclear functions, Int. J. Mol. Sci. 17 (2016) 1712.
[54] A.E. Pasquinelli, MicroRNAs and their targets: recognition, regulation and an emerging reciprocal relationship, Nat. Rev. Genet. 13 (2012) 271–282.
[55] S. Mukherji, M.S. Ebert, G.X.Y. Zheng, J.S. Tsang, P.A. Sharp, A. van Oudenaarden, MicroRNAs can generate thresholds in target gene expression, Nat. Genet. 43 (2011) 854–859.
[56] R. Garzon, M. Fabbri, A. Cimmino, G.A. Calin, C.M. Croce, MicroRNA expression and function in cancer, Trends Mol. Med. 12 (2006) 580–587.
[57] K. Zhou, M. Liu, Y. Cao, New insight into microRNA functions in cancer: oncogene–microRNA–tumor suppressor gene network, Front. Mol. Biosci. 4 (2017) 46.
[58] K.-A. Hyun, J. Kim, H. Gwak, H.-I. Jung, Isolation and enrichment of circulating biomarkers for cancer screening, detection, and diagnostics, Analyst 141 (2016) 382–392.
[59] J. Ko, E. Carpenter, D. Issadore, Detection and isolation of circulating exosomes and microvesicles for cancer monitoring and diagnostics using micro-/nano-based devices, Analyst 141 (2016) 450–460.
[60] C. Sun, R. Zhang, M. Gao, X. Zhang, A rapid and simple method for efficient capture and accurate discrimination of circulating tumor cells using aptamer conjugated magnetic beads and surface-enhanced Raman scattering imaging, Anal. Bioanal. Chem. 407 (2015) 8883–8892.
[61] C. Jin, S.M. McFaul, S.P. Duffy, X. Deng, P. Tavassoli, P.C. Black, H. Ma, Technologies for label-free separation of circulating tumor cells: from historical foundations to recent developments, Lab Chip 14 (2014) 32–44.
[62] X. Qin, S. Park, S.P. Duffy, K. Matthews, R.R. Ang, T. Todenhofer, H. Abdi, A. Azad, J. Bazov, K.N. Chi, P.C. Black, H. Ma, Size and deformability based separation of circulating tumor cells from castrate resistant prostate cancer patients using resettable cell traps, Lab Chip 15 (2015) 2278–2286.
[63] A. Williams, M. Balic, R. Datar, R. Cote, Size-based enrichment technologies for CTC detection and characterization, in: M. Ignatiadis, C. Sotiriou, K. Pantel (Eds.), Minimal Residual Disease and Circulating Tumor Cells in Breast Cancer, Springer, Berlin Heidelberg, Berlin, Heidelberg 2012, pp. 87–95.
[64] M. Hosokawa, H. Kenmotsu, Y. Koh, T. Yoshino, T. Yoshikawa, T. Naito, T. Takahashi, H. Murakami, Y. Nakamura, A. Tsuya, T. Shukuya, A. Ono, H. Akamatsu, R. Watanabe, S. Ono, K. Mori, H. Kanbara, K. Yamaguchi, T. Tanaka, T. Matsunaga, N. Yamamoto, Size-based isolation of circulating tumor cells in lung cancer patients using a microcavity array system, PLoS One 8 (2013), e67466.
[65] M. Aghaamoo, Z. Zhang, X. Chen, J. Xu, Deformability-based circulating tumor cell separation with conical-shaped microfilters: concept, optimization, and design criteria, Biomicrofluidics 9 (2015), 034106.
[66] W.S. Low, W.A.B. Wan Abas, Benchtop technologies for circulating tumor cells separation based on biophysical properties, Biomed. Res. Int. 2015 (2015) 239362.
[67] S.d. Wit, G.v. Dalum, A.T.M. Lenferink, A.G.J. Tibbe, T.J.N. Hiltermann, H.J.M. Groen, C.J.M. van Rijn, L.W.M.M. Terstappen, The Detection of EpCAM + and EpCAM– Circulating Tumor Cells, vol. 5, 2015 12270.
[68] E. Rossi, U. Basso, R. Celadin, F. Zilio, S. Pucciarelli, M. Aieta, C. Barile, T. Sava, G. Bonciarelli, S. Tumolo, C. Ghiotto, C. Magro, A. Jirillo, S. Indraccolo, A. Amadori, R. Zamarchi, M30 neoepitope expression in epithelial cancer: quantification of apoptosis in circulating tumor cells by cell search analysis, Clin. Cancer Res. 16 (2010) 5233.
[69] A. Satelli, A. Mitra, Z. Brownlee, X. Xia, S. Bellister, M.J. Overman, S. Kopetz, L.M. Ellis, Q.H. Meng, S. Li, Epithelial–mesenchymal transitioned circulating tumor cells capture for detecting tumor progression, Clin. Cancer Res. 21 (2015) 899.
[70] R.L. Bitting, R. Boominathan, C. Rao, G. Kemeny, B. Foulk, M.A. Garcia-Blanco, M. Connelly, A.J. Armstrong, Development of a method to isolate circulating tumor cells using mesenchymal-based capture, Methods 64 (2013) 129–136.
[71] S. Nagrath, L.V. Sequist, S. Maheswaran, D.W. Bell, D. Irimia, L. Ulkus, M.R. Smith, E.L. Kwak, S. Digumarthy, A. Muzikansky, P. Ryan, U.J. Balis, R.G. Tompkins, D.A. Haber, M. Toner, Isolation of rare circulating tumor cells in cancer patients by microchip technology, Nature 450 (2007) 1235–1239.
[72] S. Yagi, Y. Koh, H. Akamatsu, K. Kanai, A. Hayata, N. Tokudome, K. Akamatsu, K. Endo, S. Nakamura, M. Higuchi, H. Kanbara, M. Nakanishi, H. Ueda, N. Yamamoto, Development of an automated size-based filtration system for isolation of circulating tumor cells in lung cancer patients, PLoS One 12 (2017), e0179744.
[73] A. Yusa, M. Toneri, T. Masuda, S. Ito, S. Yamamoto, M. Okochi, N. Kondo, H. Iwata, Y. Yatabe, Y. Ichinosawa, S. Kinuta, E. Kondo, H. Honda, F. Arai, H. Nakanishi, Development of a new rapid isolation device for circulating tumor cells (CTCs) using 3D palladium filter and its application for genetic analysis, PLoS One 9 (2014), e88821.
[74] J.A. Awe, J. Saranchuk, D. Drachenberg, S. Mai, Filtration-based enrichment of circulating tumor cells from all prostate cancer risk groups, Urol. Oncol. 35 (2017) 300–309.
[75] L. Hajba, A. Guttman, Circulating tumor-cell detection and capture using microfluidic devices, TrAC Trends Anal. Chem. 59 (2014) 9–16.
[76] M.C. Miller, G.V. Doyle, L.W.M.M. Terstappen, Significance of circulating tumor cells detected by the cell search system in patients with metastatic breast colorectal and prostate cancer, J. Oncol. 2010 (2010) 617421.
[77] S. Riethdorf, H. Fritsche, V. Müller, T. Rau, C. Schindlbeck, B. Rack, W. Janni, C. Coith, K. Beck, F. Jänicke, S. Jackson, T. Gornet, M. Cristofanilli, K. Pantel, Detection of circulating tumor cells in peripheral blood of patients with metastatic breast cancer: a validation study of the cell search System, Clin. Cancer Res. 13 (2007) 920.
[78] R.M. Lequin, Enzyme immunoassay (EIA)/enzyme-linked immunosorbent assay (ELISA), Clin. Chem. 51 (2005) 2415.
[79] C.Y. Soo, Y. Song, Y. Zheng, E.C. Campbell, A.C. Riches, F. Gunn-Moore, S.J. Powis, Nanoparticle tracking analysis monitors microvesicle and exosome secretion from immune cells, Immunology 136 (2012) 192–197.
[80] V. Palmieri, D. Lucchetti, I. Gatto, A. Maiorana, M. Marcantoni, G. Maulucci, M. Papi, R. Pola, M. De Spirito, A. Sgambato, Dynamic light scattering for the characterization and counting of extracellular vesicles: a powerful noninvasive tool, J. Nanopart. Res. 16 (2014) 2583.
[81] K.-T. Rim, S.-J. Kim, Quantitative analysis of exosomes from murine lung cancer cells by flow cytometry, J. Cancer Prev. 21 (2016) 194–200.
[82] C. Alix-Panabières, K. Pantel, Clinical applications of circulating tumor cells and circulating tumor DNA as liquid biopsy, Cancer Discov. 6 (2016) 479.
[83] O. Tokel, F. Inci, U. Demirci, Advances in plasmonic technologies for point of care applications, Chem. Rev. 114 (2014) 5728–5752.
[84] K.M. Mayer, J.H. Hafner, Localized surface plasmon resonance sensors, Chem. Rev. 111 (2011) 3828–3857.
[85] K.A. Willets, R.P.V. Duyne, Localized surface plasmon resonance spectroscopy and sensing, Annu. Rev. Phys. Chem. 58 (2007) 267–297.
[86] A.R. Ferhan, J.A. Jackman, N.-J. Cho, Integration of quartz crystal microbalance-dissipation and reflection-mode localized surface plasmon resonance sensors for biomacromolecular interaction analysis, Anal. Chem. 88 (2016) 12524–12531.
[87] A.R. Ferhan, J.A. Jackman, N.-J. Cho, Probing spatial proximity of supported lipid bilayers to silica surfaces by localized surface plasmon resonance sensing, Anal. Chem. 89 (2017) 4301–4308.
[88] A. Dahlin, M. Zäch, T. Rindzevicius, M. Käll, D.S. Sutherland, F. Höök, Localized surface plasmon resonance sensing of lipid-membrane-mediated biorecognition events, J. Am. Chem. Soc. 127 (2005) 5043–5048.
[89] M.P. Jonsson, P. Jönsson, A.B. Dahlin, F. Höök, Supported lipid bilayer formation and lipid-membrane-mediated biorecognition reactions studied with a new nanoplasmonic sensor template, Nano Lett. 7 (2007) 3462–3468.
[90] M.P. Jonsson, P. Jönsson, F. Höök, Simultaneous nanoplasmonic and quartz crystal microbalance sensing: analysis of biomolecular conformational changes and quantification of the bound molecular mass, Anal. Chem. 80 (2008) 7988–7995.
[91] A. Ferhan, G. Ma, J. Jackman, T. Sut, J. Park, N.-J. Cho, Probing the interaction of dielectric nanoparticles with supported lipid membrane coatings on nanoplasmonic arrays, Sensors 17 (2017) 1484.

[92] A.R. Ferhan, J.A. Jackman, N.-J. Cho, Investigating how vesicle size influences vesicle adsorption on titanium oxide: a competition between steric packing and shape deformation, Phys. Chem. Chem. Phys. 19 (2017) 2131–2139.
[93] J.A. Jackman, B. Spackova, E. Linardy, M.C. Kim, B.K. Yoon, J. Homola, N.-J. Cho, Nanoplasmonic ruler to measure lipid vesicle deformation, Chem. Commun. 52 (2016) 76–79.
[94] J.A. Jackman, S. Yorulmaz Avsar, A.R. Ferhan, D. Li, J.H. Park, V.P. Zhdanov, N.-J. Cho, Quantitative profiling of nanoscale liposome deformation by a localized surface plasmon resonance sensor, Anal. Chem. 89 (2017) 1102–1109.
[95] J.A. Jackman, V.P. Zhdanov, N.-J. Cho, Nanoplasmonic biosensing for soft matter adsorption: kinetics of lipid vesicle attachment and shape deformation, Langmuir 30 (2014) 9494–9503.
[96] M. Dacic, J.A. Jackman, S. Yorulmaz, V.P. Zhdanov, B. Kasemo, N.-J. Cho, Influence of divalent cations on deformation and rupture of adsorbed lipid vesicles, Langmuir 32 (2016) 6486–6495.
[97] E. Oh, J.A. Jackman, S. Yorulmaz, V.P. Zhdanov, H. Lee, N.-J. Cho, Contribution of temperature to deformation of adsorbed vesicles studied by nanoplasmonic biosensing, Langmuir 31 (2015) 771–781.
[98] M. Beseničar, P. Maček, J.H. Lakey, G. Anderluh, Surface plasmon resonance in protein–membrane interactions, Chem. Phys. Lipids 141 (2006) 169–178.
[99] V. Hodnik, G. Anderluh, Surface plasmon resonance for measuring interactions of proteins with lipid membranes, in: J.H. Kleinschmidt (Ed.), Lipid-protein Interactions: Methods and Protocols, Humana Press, Totowa, NJ 2013, pp. 23–36.
[100] H. Im, N.J. Wittenberg, A. Lesuffleur, N.C. Lindquist, S.-H. Oh, Membrane protein biosensing with plasmonic nanopore arrays and pore-spanning lipid membranes, Chem. Sci. 1 (2010) 688–696.
[101] R.E. Messersmith, G.J. Nusz, S.M. Reed, Using the localized surface plasmon resonance of gold nanoparticles to monitor lipid membrane assembly and protein binding, J. Phys. Chem. C 117 (2013) 26725–26733.
[102] H.-J. Wu, J. Henzie, W.-C. Lin, C. Rhodes, Z. Li, E. Sartorel, J. Thorner, P. Yang, J.T. Groves, Membrane-protein binding measured with solution-phase plasmonic nanocube sensors, Nat. Methods 9 (2012) 1189–1191.
[103] J.A. Jackman, E. Linardy, D. Yoo, J. Seo, W.B. Ng, D.J. Klemme, N.J. Wittenberg, S.-H. Oh, N.-J. Cho, Plasmonic nanohole sensor for capturing single virus-like particles towards virucidal drug evaluation, Small 12 (2016) 1159–1166.
[104] J.A. Jackman, A. Rahim Ferhan, N.-J. Cho, Nanoplasmonic sensors for biointerfacial science, Chem. Soc. Rev. 46 (2017) 3615–3660.
[105] J.-F. Masson, Surface plasmon resonance clinical biosensors for medical diagnostics, ACS Sensors 2 (2017) 16–30.
[106] J. Homola, Surface plasmon resonance sensors for detection of chemical and biological species, Chem. Rev. 108 (2008) 462–493.
[107] J.N. Anker, W.P. Hall, O. Lyandres, N.C. Shah, J. Zhao, R.P. Van Duyne, Biosensing with plasmonic nanosensors, Nat. Mater. 7 (2008) 442–453.
[108] R.T. Hill, Plasmonic biosensors, Wiley Interdiscip. Rev. Nanomed. Nanobiotechnol. 7 (2015) 152–168.
[109] J. Smolsky, S. Kaur, C. Hayashi, S. Batra, A. Krasnoslobodtsev, Surface-enhanced raman scattering-based immunoassay technologies for detection of disease biomarkers, Bios 7 (2017) 7.
[110] D. Cialla-May, X.S. Zheng, K. Weber, J. Popp, Recent progress in surface-enhanced Raman spectroscopy for biological and biomedical applications: from cells to clinics, Chem. Soc. Rev. 46 (2017) 3945–3961.
[111] A.-I. Henry, B. Sharma, M.F. Cardinal, D. Kurouski, R.P. Van Duyne, Surface-enhanced Raman spectroscopy biosensing: in vivo diagnostics and multimodal imaging, Anal. Chem. 88 (2016) 6638–6647.
[112] J. Homola, S.S. Yee, G. Gauglitz, Surface plasmon resonance sensors: review, Sensors Actuators B Chem. 54 (1999) 3–15.
[113] F. Mazzotta, T.W. Johnson, A.B. Dahlin, J. Shaver, S.-H. Oh, F. Höök, Influence of the evanescent field decay length on the sensitivity of plasmonic nanodisks and nanoholes, ACS Photonics 2 (2015) 256–262.
[114] H. Nguyen, J. Park, S. Kang, M. Kim, Surface plasmon resonance: a versatile technique for biosensor applications, Sensors 15 (2015) 10481.
[115] A. Otto, Excitation of nonradiative surface plasma waves in silver by the method of frustrated total reflection, Z. Phys. A: Hadrons Nucl. 216 (1968) 398–410.
[116] J. Homola, Present and future of surface plasmon resonance biosensors, Anal. Bioanal. Chem. 377 (2003) 528–539.
[117] M.A. Ordal, L.L. Long, R.J. Bell, S.E. Bell, R.R. Bell, R.W. Alexander, C.A. Ward, Optical properties of the metals Al, Co, Cu, Au, Fe, Pb, Ni, Pd, Pt, Ag, Ti, and W in the infrared and far infrared, Appl. Opt. 22 (1983) 1099–1119.
[118] E. Kretschmann, The determination of the optical constants of metals by excitation of surface plasmons, Z. Phys. A: Hadrons Nucl. 241 (1971) 313–324.
[119] H.N. Daghestani, B.W. Day, Theory and applications of surface plasmon resonance, resonant mirror, resonant waveguide grating, and dual polarization interferometry biosensors, Sensors 10 (2010) 9630.
[120] J. Guo, P.D. Keathley, J.T. Hastings, Dual-mode surface-plasmon-resonance sensors using angular interrogation, Opt. Lett. 33 (2008) 512–514.
[121] D.H. Jang, J.C. Yoo, Kretschman configuration surface plasmon resonance imaging using prism sheet, Electron. Lett. 47 (2011) 843–844.
[122] J. Homola, I. Koudela, S.S. Yee, Surface plasmon resonance sensors based on diffraction gratings and prism couplers: sensitivity comparison, Sensors Actuators B Chem. 54 (1999) 16–24.
[123] C. Hu, Surface plasmon resonance sensor based on diffraction grating with high sensitivity and high resolution, Optik 122 (2011) 1881–1884.
[124] S. Shi, L. Wang, A. Wang, R. Huang, L. Ding, R. Su, W. Qi, Z. He, Bioinspired fabrication of optical fiber SPR sensors for immunoassays using polydopamine-accelerated electroless plating, J. Mater. Chem. C 4 (2016) 7554–7562.
[125] Y. Liu, Q. Liu, S. Chen, F. Cheng, H. Wang, W. Peng, Surface Plasmon Resonance Biosensor Based on Smart Phone Platforms, vol. 5, 2015 12864.
[126] A. Suzuki, J. Kondoh, Y. Matsui, S. Shiokawa, K. Suzuki, Development of novel optical waveguide surface plasmon resonance (SPR) sensor with dual light emitting diodes, Sensors Actuators B Chem. 106 (2005) 383–387.
[127] S. Toyama, N. Doumae, A. Shoji, Y. Ikariyama, Design and fabrication of a waveguide-coupled prism device for surface plasmon resonance sensor, Sensors Actuators B Chem. 65 (2000) 32–34.
[128] A. Otto, A new method for exciting nonradioactive surface plasma oscillations, Phys. Status Solidi B 26 (1968) 99–101.
[129] E.K. Akowuah, T. Gorman, S. Haxha, Design and optimization of a novel surface plasmon resonance biosensor based on Otto configuration, Opt. Express 17 (2009) 23511–23521.
[130] J. Davies, Surface Analytical Techniques for Probing Biomaterial Processes, Taylor & Francis, 1996.
[131] S. Roh, T. Chung, B. Lee, Overview of the characteristics of micro- and nano-structured surface plasmon resonance sensors, Sensors 11 (2011) 1565.
[132] J.C. Love, L.A. Estroff, J.K. Kriebel, R.G. Nuzzo, G.M. Whitesides, Self-assembled monolayers of thiolates on metals as a form of nanotechnology, Chem. Rev. 105 (2005) 1103–1170.
[133] Y. Tang, R. Mernaugh, X. Zeng, Nonregeneration protocol for surface plasmon resonance: study of high-affinity interaction with high-density biosensors, Anal. Chem. 78 (2006) 1841–1848.
[134] J. Lahiri, L. Isaacs, J. Tien, G.M. Whitesides, A strategy for the generation of surfaces presenting ligands for studies of binding based on an active ester as a common reactive intermediate: a surface plasmon resonance study, Anal. Chem. 71 (1999) 777–790.
[135] T. Riedel, F. Surman, S. Hageneder, O. Pop-Georgievski, C. Noehammer, M. Hofner, E. Brynda, C. Rodriguez-Emmenegger, J. Dostálek, Hepatitis B plasmonic biosensor for the analysis of clinical serum samples, Biosens. Bioelectron. 85 (2016) 272–279.
[136] C. Blaszykowski, S. Sheikh, M. Thompson, A survey of state-of-the-art surface chemistries to minimize fouling from human and animal biofluids, Biomater. Sci. 3 (2015) 1335–1370.
[137] C. Blaszykowski, S. Sheikh, M. Thompson, Surface chemistry to minimize fouling from blood-based fluids, Chem. Soc. Rev. 41 (2012) 5599–5612.
[138] H. Lísalová, E. Brynda, M. Houska, I. Víšová, K. Mrkvová, X.C. Song, E. Gedeonová, F. Surman, T. Riedel, O. Pop-Georgievski, J. Homola, Ultralow-fouling behavior of biorecognition coatings based on carboxy-functional brushes of zwitterionic homo- and copolymers in blood plasma: functionalization matters, Anal. Chem. 89 (2017) 3524–3531.
[139] C.R. Yonzon, E. Jeoung, S. Zou, G.C. Schatz, M. Mrksich, R.P. Van Duyne, A comparative analysis of localized and propagating surface plasmon resonance sensors: the binding of concanavalin A to a monosaccharide functionalized self-assembled monolayer, J. Am. Chem. Soc. 126 (2004) 12669–12676.
[140] A.J. Haes, R.P. Van Duyne, A unified view of propagating and localized surface plasmon resonance biosensors, Anal. Bioanal. Chem. 379 (2004) 920–930.
[141] M. Svedendahl, S. Chen, A. Dmitriev, M. Käll, Refractometric sensing using propagating versus localized surface plasmons: a direct comparison, Nano Lett. 9 (2009) 4428–4433.
[142] S. Szunerits, J. Spadavecchia, R. Boukherroub, Surface plasmon resonance: signal amplification using colloidal gold nanoparticles for enhanced sensitivity, Rev. Anal. Chem. (2014) 153.
[143] W.-C. Law, K.-T. Yong, A. Baev, P.N. Prasad, Sensitivity improved surface plasmon resonance biosensor for cancer biomarker detection based on plasmonic enhancement, ACS Nano 5 (2011) 4858–4864.
[144] S. Mariani, S. Scarano, J. Spadavecchia, M. Minunni, A reusable optical biosensor for the ultrasensitive and selective detection of unamplified human genomic DNA with gold nanostars, Biosens. Bioelectron. 74 (2015) 981–988.
[145] J. Wang, A. Munir, Z. Li, H.S. Zhou, Aptamer–Au NPs conjugates-enhanced SPR sensing for the ultrasensitive sandwich immunoassay, Biosens. Bioelectron. 25 (2009) 124–129.
[146] L. He, M.D. Musick, S.R. Nicewarner, F.G. Salinas, S.J. Benkovic, M.J. Natan, C.D. Keating, Colloidal Au-enhanced surface plasmon resonance for ultrasensitive detection of DNA hybridization, J. Am. Chem. Soc. 122 (2000) 9071–9077.
[147] M.J. Kwon, J. Lee, A.W. Wark, H.J. Lee, Nanoparticle-enhanced surface plasmon resonance detection of proteins at attomolar concentrations: comparing different nanoparticle shapes and sizes, Anal. Chem. 84 (2012) 1702–1707.
[148] S. Kim, H.J. Lee, Gold nanostar enhanced surface plasmon resonance detection of an antibiotic at attomolar concentrations via an aptamer-antibody sandwich assay, Anal. Chem. 89 (2017) 6624–6630.
[149] Z. Yingying, L. Jiancheng, Y. Cheng, L. Zhenhua, Determination of effective complex refractive index of a turbid liquid with surface plasmon resonance phase detection, Appl. Opt. 48 (2009) 1262–1267.
[150] R. Karlsson, SPR for molecular interaction analysis: a review of emerging application areas, J. Mol. Recognit. 17 (2004) 151–161.
[151] J. Lu, D. Spasic, F. Delport, T. Van Stappen, I. Detrez, D. Daems, S. Vermeire, A. Gils, J. Lammertyn, Immunoassay for detection of infliximab in whole blood using a fiber-optic surface plasmon resonance biosensor, Anal. Chem. 89 (2017) 3664–3671.
[152] S.K. Vashist, E.M. Schneider, J.H.T. Luong, Surface plasmon resonance-based immunoassay for human fetuin A, Analyst 139 (2014) 2237–2242.
[153] S.K. Vashist, E.M. Schneider, J.H.T. Luong, Surface plasmon resonance-based immunoassay for human C-reactive protein, Analyst 140 (2015) 4445–4452.
[154] M. Piliarik, M. Bocková, J. Homola, Surface plasmon resonance biosensor for parallelized detection of protein biomarkers in diluted blood plasma, Biosens. Bioelectron. 26 (2010) 1656–1661.

[155] S.A. Vance, M.G. Sandros, Zeptomole detection of C-reactive protein in serum by a nanoparticle amplified surface plasmon resonance imaging aptasensor, Sci. Rep. 4 (2014) 5129.
[156] M.E. Stewart, C.R. Anderton, L.B. Thompson, J. Maria, S.K. Gray, J.A. Rogers, R.G. Nuzzo, Nanostructured plasmonic sensors, Chem. Rev. 108 (2008) 494–521.
[157] J. Yang, H. Giessen, P. Lalanne, Simple analytical expression for the peak-frequency shifts of plasmonic resonances for sensing, Nano Lett. 15 (2015) 3439–3444.
[158] E.M. Larsson, M.E.M. Edvardsson, C. Langhammer, I. Zorić, B. Kasemo, A combined nanoplasmonic and electrodeless quartz crystal microbalance setup, Rev. Sci. Instrum. 80 (2009) 125105.
[159] A.J. Haes, S. Zou, G.C. Schatz, R.P. Van Duyne, A nanoscale optical biosensor: the long range distance dependence of the localized surface plasmon resonance of noble metal nanoparticles, J. Phys. Chem. B 108 (2004) 109–116.
[160] A.V. Whitney, J.W. Elam, S. Zou, A.V. Zinovev, P.C. Stair, G.C. Schatz, R.P. Van Duyne, Localized surface plasmon resonance nanosensor: a high-resolution distance-dependence study using atomic layer deposition, J. Phys. Chem. B 109 (2005) 20522–20528.
[161] M. Potara, A.-M. Gabudean, S. Astilean, Solution-phase, dual LSPR-SERS plasmonic sensors of high sensitivity and stability based on chitosan-coated anisotropic silver nanoparticles, J. Mater. Chem. 21 (2011) 3625–3633.
[162] F.H. Ho, Y.-H. Wu, M. Ujihara, T. Imae, A solution-based nano-plasmonic sensing technique by using gold nanorods, Analyst 137 (2012) 2545–2548.
[163] A.R. Ferhan, D.-H. Kim, Nanoparticle polymer composites on solid substrates for plasmonic sensing applications, Nano Today 11 (2016) 415–434.
[164] K. Ode, M. Honjo, Y. Takashima, T. Tsuruoka, K. Akamatsu, Highly sensitive plasmonic optical sensors based on gold core–satellite nanostructures immobilized on glass substrates, ACS Appl. Mater. Interfaces 8 (2016) 20522–20526.
[165] S.M. Marinakos, S. Chen, A. Chilkoti, Plasmonic detection of a model analyte in serum by a gold nanorod sensor, Anal. Chem. 79 (2007) 5278–5283.
[166] N. Nath, A. Chilkoti, A colorimetric gold nanoparticle sensor to interrogate biomolecular interactions in real time on a surface, Anal. Chem. 74 (2002) 504–509.
[167] W.J. Galush, S.A. Shelby, M.J. Mulvihill, A. Tao, P. Yang, J.T. Groves, A nanocube plasmonic sensor for molecular binding on membrane surfaces, Nano Lett. 9 (2009) 2077–2082.
[168] P. Chen, M.T. Chung, W. McHugh, R. Nidetz, Y. Li, J. Fu, T.T. Cornell, T.P. Shanley, K. Kurabayashi, Multiplex serum cytokine immunoassay using nanoplasmonic biosensor microarrays, ACS Nano 9 (2015) 4173–4181.
[169] S.-W. Lee, K.-S. Lee, J. Ahn, J.-J. Lee, M.-G. Kim, Y.-B. Shin, Highly sensitive biosensing using arrays of plasmonic Au nanodisks realized by nanoimprint lithography, ACS Nano 5 (2011) 897–904.
[170] C.L. Haynes, R.P. Van Duyne, Nanosphere lithography: a versatile nanofabrication tool for studies of size-dependent nanoparticle optics, J. Phys. Chem. B 105 (2001) 5599–5611.
[171] M. Duval Malinsky, K.L. Kelly, G.C. Schatz, R.P. Van Duyne, Nanosphere lithography: effect of substrate on the localized surface plasmon resonance spectrum of silver nanoparticles, J. Phys. Chem. B 105 (2001) 2343–2350.
[172] H. Duan, H. Hu, K. Kumar, Z. Shen, J.K.W. Yang, Direct and reliable patterning of plasmonic nanostructures with sub-10-nm gaps, ACS Nano 5 (2011) 7593–7600.
[173] J. Henzie, J. Lee, M.H. Lee, W. Hasan, T.W. Odom, Nanofabrication of plasmonic structures, Annu. Rev. Phys. Chem. 60 (2009) 147–165.
[174] B. Sepúlveda, P.C. Angelomé, L.M. Lechuga, L.M. Liz-Marzán, LSPR-based nanobiosensors, Nano Today 4 (2009) 244–251.
[175] D. Vilela, M.C. González, A. Escarpa, Sensing colorimetric approaches based on gold and silver nanoparticles aggregation: chemical creativity behind the assay. A review, Anal. Chim. Acta 751 (2012) 24–43.
[176] A.R. Ferhan, L. Guo, X. Zhou, P. Chen, S. Hong, D.-H. Kim, Solid-phase colorimetric sensor based on gold nanoparticle-loaded polymer brushes: lead detection as a case study, Anal. Chem. 85 (2013) 4094–4099.
[177] S. Shinohara, D. Tanaka, K. Okamoto, K. Tamada, Colorimetric plasmon sensors with multilayered metallic nanoparticle sheets, Phys. Chem. Chem. Phys. 17 (2015) 18606–18612.
[178] I. Ruach-Nir, T.A. Bendikov, I. Doron-Mor, Z. Barkay, A. Vaskevich, I. Rubinstein, Silica-stabilized gold island films for transmission localized surface plasmon sensing, J. Am. Chem. Soc. 129 (2007) 84–92.
[179] G. Cappi, F.M. Spiga, Y. Moncada, A. Ferretti, M. Beyeler, M. Bianchessi, L. Decosterd, T. Buclin, C. Guiducci, Label-free detection of tobramycin in serum by transmission-localized surface plasmon resonance, Anal. Chem. 87 (2015) 5278–5285.
[180] W.-S. Liao, X. Chen, T. Yang, E.T. Castellana, J. Chen, P.S. Cremer, Benchtop chemistry for the rapid prototyping of label-free biosensors: transmission localized surface plasmon resonance platforms, Biointerphases 4 (2009) 80–85.
[181] L.J. Sherry, R. Jin, C.A. Mirkin, G.C. Schatz, R.P. Van Duyne, Localized surface plasmon resonance spectroscopy of single silver triangular nanoprisms, Nano Lett. 6 (2006) 2060–2065.
[182] M. Hu, C. Novo, A. Funston, H. Wang, H. Staleva, S. Zou, P. Mulvaney, Y. Xia, G.V. Hartland, Dark-field microscopy studies of single metal nanoparticles: understanding the factors that influence the linewidth of the localized surface plasmon resonance, J. Mater. Chem. 18 (2008) 1949–1960.
[183] A.D. McFarland, R.P. Van Duyne, Single silver nanoparticles as real-time optical sensors with zeptomole sensitivity, Nano Lett. 3 (2003) 1057–1062.
[184] G. Raschke, S. Kowarik, T. Franzl, C. Sönnichsen, T.A. Klar, J. Feldmann, A. Nichtl, K. Kürzinger, Biomolecular recognition based on single gold nanoparticle light scattering, Nano Lett. 3 (2003) 935–938.
[185] T. Huang, X.-H.N. Xu, Synthesis and characterization of tunable rainbow colored colloidal silver nanoparticles using single-nanoparticle plasmonic microscopy and spectroscopy, J. Mater. Chem. 20 (2010) 9867–9876.
[186] C.L. Nehl, J.H. Hafner, Shape-dependent plasmon resonances of gold nanoparticles, J. Mater. Chem. 18 (2008) 2415–2419.
[187] V. Juvé, M.F. Cardinal, A. Lombardi, A. Crut, P. Maioli, J. Pérez-Juste, L.M. Liz-Marzán, N. Del Fatti, F. Vallée, Size-dependent surface plasmon resonance broadening in nonspherical nanoparticles: single gold nanorods, Nano Lett. 13 (2013) 2234–2240.
[188] T.A. El-Brolossy, T. Abdallah, M.B. Mohamed, S. Abdallah, K. Easawi, S. Negm, H. Talaat, Shape and size dependence of the surface plasmon resonance of gold nanoparticles studied by photoacoustic technique, Eur. Phys. J. Spec. Top. 153 (2008) 361–364.
[189] W.-S. Chang, J.W. Ha, L.S. Slaughter, S. Link, Plasmonic nanorod absorbers as orientation sensors, Proc. Natl. Acad. Sci. 107 (2010) 2781–2786.
[190] M.B. Ross, C.A. Mirkin, G.C. Schatz, Optical properties of one-, two-, and three-dimensional arrays of plasmonic nanostructures, J. Phys. Chem. C 120 (2016) 816–830.
[191] J.M. McMahon, Y. Wang, L.J. Sherry, R.P. Van Duyne, L.D. Marks, S.K. Gray, G.C. Schatz, Correlating the structure, optical spectra, and electrodynamics of single silver nanocubes, J. Phys. Chem. C 113 (2009) 2731–2735.
[192] H. Chen, X. Kou, Z. Yang, W. Ni, J. Wang, Shape- and size-dependent refractive index sensitivity of gold nanoparticles, Langmuir 24 (2008) 5233–5237.
[193] T. Karakouz, D. Holder, M. Goomanovsky, A. Vaskevich, I. Rubinstein, Morphology and refractive index sensitivity of gold island films, Chem. Mater. 21 (2009) 5875–5885.
[194] A.J. Haes, S. Zou, G.C. Schatz, R.P. Van Duyne, Nanoscale optical biosensor: short range distance dependence of the localized surface plasmon resonance of noble metal nanoparticles, J. Phys. Chem. B 108 (2004) 6961–6968.
[195] C. Wang, Z. Ma, T. Wang, Z. Su, Synthesis, assembly, and biofunctionalization of silica-coated gold nanorods for colorimetric biosensing, Adv. Funct. Mater. 16 (2006) 1673–1678.
[196] V. Pavlov, Y. Xiao, B. Shlyahovsky, I. Willner, Aptamer-functionalized Au nanoparticles for the amplified optical detection of thrombin, J. Am. Chem. Soc. 126 (2004) 11768–11769.
[197] M. Oliverio, S. Perotto, G.C. Messina, L. Lovato, F. De Angelis, Chemical functionalization of plasmonic surface biosensors: a tutorial review on issues, strategies, and costs, ACS Appl. Mater. Interfaces 9 (2017) 29394–29411.
[198] J. Li, J. Ye, C. Chen, Y. Li, N. Verellen, V.V. Moshchalkov, L. Lagae, P. Van Dorpe, Revisiting the surface sensitivity of nanoplasmonic biosensors, ACS Photonics 2 (2015) 425–431.
[199] P.D. Howes, R. Chandrawati, M.M. Stevens, Colloidal nanoparticles as advanced biological sensors, Science 346 (2014).
[200] S. Zeng, K.-T. Yong, I. Roy, X.-Q. Dinh, X. Yu, F. Luan, A review on functionalized gold nanoparticles for biosensing applications, Plasmonics 6 (2011) 491.
[201] N. Nath, A. Chilkoti, Label-free biosensing by surface plasmon resonance of nanoparticles on glass: optimization of nanoparticle size, Anal. Chem. 76 (2004) 5370–5378.
[202] M. Sriram, K. Zong, S. Vivekchand, J. Gooding, Single nanoparticle plasmonic sensors, Sensors 15 (2015) 25774.
[203] T. Xie, C. Jing, Y.-T. Long, Single plasmonic nanoparticles as ultrasensitive sensors, Analyst 142 (2017) 409–420.
[204] L. Guo, A.R. Ferhan, K. Lee, D.-H. Kim, Nanoarray-based biomolecular detection using individual Au nanoparticles with minimized localized surface plasmon resonance variations, Anal. Chem. 83 (2011) 2605–2612.
[205] L. Guo, X. Zhou, D.-H. Kim, Facile fabrication of distance-tunable Au-nanorod chips for single-nanoparticle plasmonic biosensors, Biosens. Bioelectron. 26 (2011) 2246–2251.
[206] J. Ye, K. Bonroy, D. Nelis, F. Frederix, J. D'Haen, G. Maes, G. Borghs, Enhanced localized surface plasmon resonance sensing on three-dimensional gold nanoparticles assemblies, Colloids Surf. A Physicochem. Eng. Asp. 321 (2008) 313–317.
[207] L. Guo, G. Chen, D.-H. Kim, Three-dimensionally assembled gold nanostructures for plasmonic biosensors, Anal. Chem. 82 (2010) 5147–5153.
[208] L. Guo, D.-H. Kim, LSPR biomolecular assay with high sensitivity induced by aptamer–antigen–antibody sandwich complex, Biosens. Bioelectron. 31 (2012) 567–570.
[209] W.P. Hall, S.N. Ngatia, R.P. Van Duyne, LSPR biosensor signal enhancement using nanoparticle–antibody conjugates, J. Phys. Chem. C 115 (2011) 1410–1414.
[210] J. Spadavecchia, A. Barras, J. Lyskawa, P. Woisel, W. Laure, C.-M. Pradier, R. Boukherroub, S. Szunerits, Approach for plasmonic based DNA sensing: amplification of the wavelength shift and simultaneous detection of the plasmon modes of gold nanostructures, Anal. Chem. 85 (2013) 3288–3296.
[211] D.-Z. Lin, P.-C. Chuang, P.-C. Liao, J.-P. Chen, Y.-F. Chen, Increasing the spectral shifts in LSPR biosensing using DNA-functionalized gold nanorods in a competitive assay format for the detection of interferon-γ, Biosens. Bioelectron. 81 (2016) 221–228.
[212] S.K. Ghosh, T. Pal, Interparticle coupling effect on the surface plasmon resonance of gold nanoparticles: from theory to applications, Chem. Rev. 107 (2007) 4797–4862.
[213] N. Hooshmand, J.A. Bordley, M.A. El-Sayed, The sensitivity of the distance dependent plasmonic coupling between two nanocubes to their orientation: edge-to-edge versus face-to-face, J. Phys. Chem. C 120 (2016) 4564–4570.
[214] P.K. Jain, M.A. El-Sayed, Plasmonic coupling in noble metal nanostructures, Chem. Phys. Lett. 487 (2010) 153–164.
[215] M. Li, S.K. Cushing, N. Wu, Plasmon-enhanced optical sensors: a review, Analyst 140 (2015) 386–406.
[216] H. Lange, B.H. Juárez, A. Carl, M. Richter, N.G. Bastús, H. Weller, C. Thomsen, R. von Klitzing, A. Knorr, Tunable plasmon coupling in distance-controlled gold nanoparticles, Langmuir 28 (2012) 8862–8866.
[217] L. Tang, J. Li, Plasmon-based colorimetric nanosensors for ultrasensitive molecular diagnostics, ACS Sensors 2 (2017) 857–875.
[218] R. Elghanian, J.J. Storhoff, R.C. Mucic, R.L. Letsinger, C.A. Mirkin, Selective colorimetric detection of polynucleotides based on the distance-dependent optical properties of gold nanoparticles, Science 277 (1997) 1078.

[219] F. Xia, X. Zuo, R. Yang, Y. Xiao, D. Kang, A. Vallée-Bélisle, X. Gong, J.D. Yuen, B.B.Y. Hsu, A.J. Heeger, K.W. Plaxco, Colorimetric detection of DNA, small molecules, proteins, and ions using unmodified gold nanoparticles and conjugated polyelectrolytes, Proc. Natl. Acad. Sci. 107 (2010) 10837–10841.
[220] T. Zhang, H. Li, S. Hou, Y. Dong, G. Pang, Y. Zhang, Construction of plasmonic core–satellite nanostructures on substrates based on DNA-directed self-assembly as a sensitive and reproducible biosensor, ACS Appl. Mater. Interfaces 7 (2015) 27131–27139.
[221] J.R. Waldeisen, T. Wang, B.M. Ross, L.P. Lee, Disassembly of a core–satellite nanoassembled substrate for colorimetric biomolecular detection, ACS Nano 5 (2011) 5383–5389.
[222] L. Guo, Y. Xu, A.R. Ferhan, G. Chen, D.-H. Kim, Oriented gold nanoparticle aggregation for colorimetric sensors with surprisingly high analytical figures of merit, J. Am. Chem. Soc. 135 (2013) 12338–12345.
[223] J.I.L. Chen, Y. Chen, D.S. Ginger, Plasmonic nanoparticle dimers for optical sensing of DNA in complex media, J. Am. Chem. Soc. 132 (2010) 9600–9601.
[224] J.I.L. Chen, H. Durkee, B. Traxler, D.S. Ginger, Optical detection of protein in complex media with plasmonic nanoparticle dimers, Small 7 (2011) 1993–1997.
[225] A.B. Taylor, P. Zijlstra, Single-molecule plasmon sensing: current status and future prospects, ACS Sensors 2 (2017) 1103–1122.
[226] M.M. Kathryn, H. Feng, L. Seunghyun, N. Peter, H.H. Jason, A single molecule immunoassay by localized surface plasmon resonance, Nanotechnology 21 (2010) 255503.
[227] J.J. Mock, D.R. Smith, S. Schultz, Local refractive index dependence of plasmon resonance spectra from individual nanoparticles, Nano Lett. 3 (2003) 485–491.
[228] R. Giannini, C.V. Hafner, J.F. Löffler, Scaling behavior of individual nanoparticle plasmon resonances, J. Phys. Chem. C 119 (2015) 6138–6147.
[229] G.J. Nusz, A.C. Curry, S.M. Marinakos, A. Wax, A. Chilkoti, Rational selection of gold nanorod geometry for label-free plasmonic biosensors, ACS Nano 3 (2009) 795–806.
[230] K. Park, S. Biswas, S. Kanel, D. Nepal, R.A. Vaia, Engineering the optical properties of gold nanorods: independent tuning of surface plasmon energy, Extinction Coefficient, and Scattering Cross Section, J. Phys. Chem. C 118 (2014) 5918–5926.
[231] C.J. Orendorff, T.K. Sau, C.J. Murphy, Shape-dependent plasmon-resonant gold nanoparticles, Small 2 (2006) 636–639.
[232] H.-Y. Jin, D.-W. Li, N. Zhang, Z. Gu, Y.-T. Long, Analyzing carbohydrate–protein interaction based on single plasmonic nanoparticle by conventional dark field microscopy, ACS Appl. Mater. Interfaces 7 (2015) 12249–12253.
[233] K.-M. Lo, C.-Y. Lai, H.-M. Chan, D.-L. Ma, H.-W. Li, Monitoring of DNA–protein interaction with single gold nanoparticles by localized scattering plasmon resonance spectroscopy, Methods 64 (2013) 331–337.
[234] C. Langhammer, E.M. Larsson, B. Kasemo, I. Zorić, Indirect nanoplasmonic sensing: ultrasensitive experimental platform for nanomaterials science and optical nanocalorimetry, Nano Lett. 10 (2010) 3529–3538.
[235] S. Szunerits, M.R. Das, R. Boukherroub, Short- and long-range sensing on gold nanostructures, deposited on glass, coated with silicon oxide films of different thicknesses, J. Phys. Chem. C 112 (2008) 8239–8243.
[236] E.D. Gaspera, M. Karg, J. Baldauf, J. Jasieniak, G. Maggioni, A. Martucci, Au nanoparticle monolayers covered with sol–gel oxide thin films: optical and morphological study, Langmuir 27 (2011) 13739–13747.
[237] E. Galopin, J. Niedziółka-Jönsson, A. Akjouj, Y. Pennec, B. Djafari-Rouhani, A. Noual, R. Boukherroub, S. Szunerits, Sensitivity of plasmonic nanostructures coated with thin oxide films for refractive index sensing: experimental and theoretical investigations, J. Phys. Chem. C 114 (2010) 11769–11775.
[238] G.H. Zan, J.A. Jackman, S.-O. Kim, N.-J. Cho, Controlling lipid membrane architecture for tunable nanoplasmonic biosensing, Small 10 (2014) 4828–4832.
[239] D.-S. Wang, S.-K. Fan, Microfluidic surface plasmon resonance sensors: from principles to point-of-care applications, Sensors 16 (2016) 1175.
[240] R. de la Rica, M.M. Stevens, Plasmonic ELISA for the ultrasensitive detection of disease biomarkers with the naked eye, Nat. Nanotechnol. 7 (2012) 821–824.
[241] S. Chen, M. Svedendahl, R.P. Van Duyne, M. Käll, Plasmon-enhanced colorimetric ELISA with single molecule sensitivity, Nano Lett. 11 (2011) 1826–1830.
[242] Z. Xuan, M. Li, P. Rong, W. Wang, Y. Li, D. Liu, Plasmonic ELISA based on the controlled growth of silver nanoparticles, Nano 8 (2016) 17271–17277.
[243] J. Satija, N. Punjabi, D. Mishra, S. Mukherji, Plasmonic-ELISA: expanding horizons, RSC Adv. 6 (2016) 85440–85456.
[244] G.C. Schatz, M.A. Young, R.P. Van Duyne, Electromagnetic mechanism of SERS, in: K. Kneipp, M. Moskovits, H. Kneipp (Eds.), Surface-enhanced Raman Scattering: Physics and Applications, Springer, Berlin Heidelberg, Berlin, Heidelberg 2006, pp. 19–45.
[245] A. Campion, J.E. Ivanecky, C.M. Child, M. Foster, On the mechanism of chemical enhancement in surface-enhanced raman scattering, J. Am. Chem. Soc. 117 (1995) 11807–11808.
[246] H. Xu, J. Aizpurua, M. Käll, P. Apell, Electromagnetic contributions to single-molecule sensitivity in surface-enhanced Raman scattering, Phys. Rev. E 62 (2000) 4318–4324.
[247] P. Alonso-González, P. Albella, M. Schnell, J. Chen, F. Huth, A. García-Etxarri, F. Casanova, F. Golmar, L. Arzubiaga, L.E. Hueso, J. Aizpurua, R. Hillenbrand, Resolving the Electromagnetic Mechanism of Surface-enhanced Light Scattering at Single Hot Spots, 3, 2012 684.
[248] K. Kneipp, Chemical contribution to SERS enhancement: an experimental study on a series of polymethine dyes on silver nanoaggregates, J. Phys. Chem. C 120 (2016) 21076–21081.
[249] N. Valley, N. Greeneltch, R.P. Van Duyne, G.C. Schatz, A look at the origin and magnitude of the chemical contribution to the enhancement mechanism of surface-enhanced raman spectroscopy (SERS): theory and experiment, J. Phys. Chem. Lett. 4 (2013) 2599–2604.
[250] A. Otto, The 'chemical' (electronic) contribution to surface-enhanced Raman scattering, J. Raman Spectrosc. 36 (2005) 497–509.
[251] B.N.J. Persson, K. Zhao, Z. Zhang, Chemical contribution to surface-enhanced raman scattering, Phys. Rev. Lett. 96 (2006) 207401.
[252] P.L. Stiles, J.A. Dieringer, N.C. Shah, R.P.V. Duyne, Surface-enhanced Raman spectroscopy, Annu. Rev. Anal. Chem. 1 (2008) 601–626.
[253] S. Mahajan, J.J. Baumberg, A.E. Russell, P.N. Bartlett, Reproducible SERRS from structured gold surfaces, Phys. Chem. Chem. Phys. 9 (2007) 6016–6020.
[254] B. Sharma, M. Fernanda Cardinal, S.L. Kleinman, N.G. Greeneltch, R.R. Frontiera, M.G. Blaber, G.C. Schatz, R.P. Van Duyne, High-performance SERS substrates: Advances and challenges, MRS Bull. 38 (2013) 615–624.
[255] X.Y. Lang, L.Y. Chen, P.F. Guan, T. Fujita, M.W. Chen, Geometric effect on surface enhanced Raman scattering of nanoporous gold: improving Raman scattering by tailoring ligament and nanopore ratios, Appl. Phys. Lett. 94 (2009) 213109.
[256] D. Radziuk, H. Moehwald, Prospects for plasmonic hot spots in single molecule SERS towards the chemical imaging of live cells, Phys. Chem. Chem. Phys. 17 (2015) 21072–21093.
[257] J.P. Camden, J.A. Dieringer, Y. Wang, D.J. Masiello, L.D. Marks, G.C. Schatz, R.P. Van Duyne, Probing the structure of single-molecule surface-enhanced Raman scattering hot spots, J. Am. Chem. Soc. 130 (2008) 12616–12617.
[258] W. Li, P.H.C. Camargo, X. Lu, Y. Xia, Dimers of silver nanospheres: facile synthesis and their use as hot spots for surface-enhanced Raman scattering, Nano Lett. 9 (2009) 485–490.
[259] H.-Y. Chen, M.-H. Lin, C.-Y. Wang, Y.-M. Chang, S. Gwo, Large-scale hot spot engineering for quantitative SERS at the single-molecule scale, J. Am. Chem. Soc. 137 (2015) 13698–13705.
[260] G. Yang, J. Nanda, B. Wang, G. Chen, D.T. Hallinan, Self-assembly of large gold nanoparticles for surface-enhanced raman spectroscopy, ACS Appl. Mater. Interfaces 9 (2017) 13457–13470.
[261] R. Gill, E.C. Le Ru, Fluorescence enhancement at hot-spots: the case of Ag nanoparticle aggregates, Phys. Chem. Chem. Phys. 13 (2011) 16366–16372.
[262] K.D. Alexander, M.J. Hampton, S. Zhang, A. Dhawan, H. Xu, R. Lopez, A high-throughput method for controlled hot-spot fabrication in SERS-active gold nanoparticle dimer arrays, J. Raman Spectrosc. 40 (2009) 2171–2175.
[263] Y.-W. Wang, K.-C. Kao, J.-K. Wang, C.-Y. Mou, Large-scale uniform two-dimensional hexagonal arrays of gold nanoparticles templated from mesoporous silica film for surface-enhanced Raman spectroscopy, J. Phys. Chem. C 120 (2016) 24382–24388.
[264] Q. Yang, M. Deng, H. Li, M. Li, C. Zhang, W. Shen, Y. Li, D. Guo, Y. Song, Highly reproducible SERS arrays directly written by inkjet printing, Nano 7 (2015) 421–425.
[265] M.J. Banholzer, J.E. Millstone, L. Qin, C.A. Mirkin, Rationally designed nanostructures for surface-enhanced Raman spectroscopy, Chem. Soc. Rev. 37 (2008) 885–897.
[266] J. Huang, Y. Zhu, M. Lin, Q. Wang, L. Zhao, Y. Yang, K.X. Yao, Y. Han, Site-specific growth of Au–Pd alloy horns on Au nanorods: a platform for highly sensitive monitoring of catalytic reactions by surface enhancement Raman spectroscopy, J. Am. Chem. Soc. 135 (2013) 8552–8561.
[267] Q. Zhang, N. Large, H. Wang, Gold nanoparticles with tipped surface structures as substrates for single-particle surface-enhanced raman spectroscopy: concave nanocubes, nanotrisoctahedra, and nanostars, ACS Appl. Mater. Interfaces 6 (2014) 17255–17267.
[268] L.-F. Zhang, S.-L. Zhong, A.-W. Xu, Highly branched concave Au/Pd bimetallic nanocrystals with superior electrocatalytic activity and highly efficient SERS enhancement, Angew. Chem. Int. Ed. 52 (2013) 645–649.
[269] S.S.R. Dasary, A.K. Singh, D. Senapati, H. Yu, P.C. Ray, Gold nanoparticle based label-free SERS probe for ultrasensitive and selective detection of trinitrotoluene, J. Am. Chem. Soc. 131 (2009) 13806–13812.
[270] A. Campion, P. Kambhampati, Surface-enhanced Raman scattering, Chem. Soc. Rev. 27 (1998) 241–250.
[271] M. Moskovits, Surface-enhanced Raman spectroscopy: a brief retrospective, J. Raman Spectrosc. 36 (2005) 485–496.
[272] R.A. Álvarez-Puebla, Effects of the excitation wavelength on the SERS spectrum, J. Phys. Chem. Lett. 3 (2012) 857–866.
[273] F.S. Ameer, Y. Zhou, S. Zou, D. Zhang, Wavelength-dependent correlations between ultraviolet–visible intensities and surface enhanced raman spectroscopic enhancement factors of aggregated gold and silver nanoparticles, J. Phys. Chem. C 118 (2014) 22234–22242.
[274] J.M. Hermida-Ramon, L. Guerrini, R.A. Alvarez-Puebla, Analysis of the SERS spectrum by theoretical methodology: evaluating a classical dipole model and the detuning of the excitation frequency, J. Phys. Chem. A 117 (2013) 4584–4590.
[275] M. Sinwani, M. Muallem, Y.R. Tischler, The effect of excitation wavelength and metallic nanostructure on SERS spectra of C60, J. Raman Spectrosc. 48 (2017) 829–836.
[276] D. Naumenko, L. Stolzer, A.S. Quick, D. Abt, M. Wegener, C. Barner-Kowollik, S.D. Zilio, B. Marmiroli, H. Amenitsch, L. Fruk, M. Lazzarino, Design of broadband SERS substrates by the laser-induced aggregation of gold nanoparticles, J. Mater. Chem. C 4 (2016) 6152–6159.
[277] S.S. Sinha, S. Jones, A. Pramanik, P.C. Ray, Nanoarchitecture based SERS for biomolecular fingerprinting and label-free disease markers diagnosis, Acc. Chem. Res. 49 (2016) 2725–2735.
[278] S. Jones, A. Pramanik, R. Kanchanapally, B.P. Viraka Nellore, S. Begum, C. Sweet, P.C. Ray, Multifunctional three-dimensional chitosan/gold nanoparticle/graphene oxide architecture for separation, label-free SERS identification of pharmaceutical contaminants, and effective killing of superbugs, ACS Sustain. Chem. Eng. 5 (2017) 7175–7187.

[279] X.X. Han, G.G. Huang, B. Zhao, Y. Ozaki, Label-free highly sensitive detection of proteins in aqueous solutions using surface-enhanced Raman scattering, Anal. Chem. 81 (2009) 3329–3333.
[280] Y. Wang, B. Yan, L. Chen, SERS tags: novel optical nanoprobes for bioanalysis, Chem. Rev. 113 (2013) 1391–1428.
[281] L. Fabris, SERS tags: the next promising tool for personalized cancer detection? ChemNanoMat 2 (2016) 249–258.
[282] X. Qian, X.-H. Peng, D.O. Ansari, Q. Yin-Goen, G.Z. Chen, D.M. Shin, L. Yang, A.N. Young, M.D. Wang, S. Nie, In vivo tumor targeting and spectroscopic detection with surface-enhanced Raman nanoparticle tags, Nat. Biotechnol. 26 (2008) 83–90.
[283] M.Y. Sha, H. Xu, M.J. Natan, R. Cromer, Surface-enhanced raman scattering tags for rapid and homogeneous detection of circulating tumor cells in the presence of human whole blood, J. Am. Chem. Soc. 130 (2008) 17214–17215.
[284] A.J. Driscoll, M.H. Harpster, P.A. Johnson, The development of surface-enhanced Raman scattering as a detection modality for portable in vitro diagnostics: progress and challenges, Phys. Chem. Chem. Phys. 15 (2013) 20415–20433.
[285] J.-y. Lim, J.-s. Nam, S.-e. Yang, H. Shin, Y.-h. Jang, G.-U. Bae, T. Kang, K.-i. Lim, Y. Choi, Identification of newly emerging influenza viruses by surface-enhanced Raman spectroscopy, Anal. Chem. 87 (2015) 11652–11659.
[286] A.M. Paul, Z. Fan, S.S. Sinha, Y. Shi, L. Le, F. Bai, P.C. Ray, Bioconjugated gold nanoparticle based SERS probe for ultrasensitive identification of mosquito-borne viruses using raman fingerprinting, J. Phys. Chem. C 119 (2015) 23669–23675.
[287] L.A. Lane, X. Qian, S. Nie, SERS nanoparticles in medicine: from label-free detection to spectroscopic tagging, Chem. Rev. 115 (2015) 10489–10529.
[288] R.A. Alvarez-Puebla, L.M. Liz-Marzán, SERS-based diagnosis and biodetection, Small 6 (2010) 604–610.
[289] Y. Zhang, X. Li, B. Xue, X. Kong, X. Liu, L. Tu, Y. Chang, A facile and General Route to Synthesize Silica-coated SERS Tags with the Enhanced Signal Intensity, vol. 5, 2015 14934.
[290] K. Yang, Y. Hu, N. Dong, A novel biosensor based on competitive SERS immunoassay and magnetic separation for accurate and sensitive detection of chloramphenicol, Biosens. Bioelectron. 80 (2016) 373–377.
[291] B.-H. Jun, M.S. Noh, J. Kim, G. Kim, H. Kang, M.-S. Kim, Y.-T. Seo, J. Baek, J.-H. Kim, J. Park, S. Kim, Y.-K. Kim, T. Hyeon, M.-H. Cho, D.H. Jeong, Y.-S. Lee, Multifunctional silver-embedded magnetic nanoparticles as SERS nanoprobes and their applications, Small 6 (2010) 119–125.
[292] F. Bao, J.-L. Yao, R.-A. Gu, Synthesis of magnetic Fe_2O_3/Au core/shell nanoparticles for bioseparation and immunoassay based on surface-enhanced Raman spectroscopy, Langmuir 25 (2009) 10782–10787.
[293] M.R. Bailey, A.M. Pentecost, A. Selimovic, R.S. Martin, Z.D. Schultz, Sheath-flow microfluidic approach for combined surface enhanced Raman scattering and electrochemical detection, Anal. Chem. 87 (2015) 4347–4355.
[294] X. Niu, H. Chen, Y. Wang, W. Wang, X. Sun, L. Chen, Upconversion fluorescence-SERS dual-mode tags for cellular and in vivo imaging, ACS Appl. Mater. Interfaces 6 (2014) 5152–5160.
[295] F. Tian, J. Conde, C. Bao, Y. Chen, J. Curtin, D. Cui, Gold nanostars for efficient in vitro and in vivo real-time SERS detection and drug delivery via plasmonic-tunable Raman/FTIR imaging, Biomaterials 106 (2016) 87–97.
[296] K.K. Maiti, U.S. Dinish, C.Y. Fu, J.-J. Lee, K.-S. Soh, S.-W. Yun, R. Bhuvaneswari, M. Olivo, Y.-T. Chang, Development of biocompatible SERS nanotag with increased stability by chemisorption of reporter molecule for in vivo cancer detection, Biosens. Bioelectron. 26 (2010) 398–403.
[297] L. Ming, K.C. Scott, Z. Jianming, L. Jessica, P.A. Zoraida, M. Dongling, W. Nianqiang, Shape-dependent surface-enhanced Raman scattering in gold–Raman-probe–silica sandwiched nanoparticles for biocompatible applications, Nanotechnology 23 (2012) 115501.
[298] H. Yuan, Y. Liu, A.M. Fales, Y.L. Li, J. Liu, T. Vo-Dinh, Quantitative surface-enhanced resonant Raman scattering multiplexing of biocompatible gold nanostars for in vitro and ex vivo detection, Anal. Chem. 85 (2013) 208–212.
[299] X. Huang, X. Peng, Y. Wang, Y. Wang, D.M. Shin, M.A. El-Sayed, S. Nie, A reexamination of active and passive tumor targeting by using rod-shaped gold nanocrystals and covalently conjugated peptide ligands, ACS Nano 4 (2010) 5887–5896.
[300] S. Laing, L.E. Jamieson, K. Faulds, D. Graham, Surface-enhanced Raman Spectroscopy for In Vivo Biosensing, vol. 1, 2017 0060.
[301] N. Guarrotxena, B. Liu, L. Fabris, G.C. Bazan, Antitags: nanostructured tools for developing SERS-based ELISA analogs, Adv. Mater. 22 (2010) 4954–4958.
[302] J. Liang, H. Liu, C. Huang, C. Yao, Q. Fu, X. Li, D. Cao, Z. Luo, Y. Tang, Aggregated silver nanoparticles based surface-enhanced raman scattering enzyme-linked immunosorbent assay for ultrasensitive detection of protein biomarkers and small molecules, Anal. Chem. 87 (2015) 5790–5796.
[303] C.L. Zavaleta, B.R. Smith, I. Walton, W. Doering, G. Davis, B. Shojaei, M.J. Natan, S.S. Gambhir, Multiplexed imaging of surface enhanced Raman scattering nanotags in living mice using noninvasive Raman spectroscopy, Proc. Natl. Acad. Sci. 106 (2009) 13511–13516.
[304] H. Jang, E.Y. Hwang, Y. Kim, J. Choo, J. Jeong, D.W. Lim, Surface-enhanced Raman scattering and fluorescence-based dual nanoprobes for multiplexed detection of bacterial pathogens, J. Biomed. Nanotechnol. 12 (2016) 1938–1951.
[305] . F. Zou, H. Zhou, T.V. Tan, J. Kim, K. Koh, J. Lee, Dual-mode SERS-fluorescence immunoassay using graphene quantum dot labeling on one-dimensional aligned magnetoplasmonic nanoparticles, ACS Appl. Mater. Interfaces 7 (2015) 12168–12175.
[306] S. Lee, H. Chon, S.-Y. Yoon, E.K. Lee, S.-I. Chang, D.W. Lim, J. Choo, Fabrication of SERS-fluorescence dual modal nanoprobes and application to multiplex cancer cell imaging, Nano 4 (2012) 124–129.
[307] V. Ambros, B. Bartel, D.P. Bartel, C.B. Burge, J.C. Carrington, X. Chen, G. Dreyfuss, S.R. Eddy, S. Griffiths-Jones, M. Marshall, M. Matzke, G. Ruvkun, T. Tuschl, A uniform system for microRNA annotation, RNA 9 (2003) 277–279.
[308] F. Wahid, A. Shehzad, T. Khan, Y.Y. Kim, MicroRNAs: synthesis, mechanism, function, and recent clinical trials, Biochim. Biophys. Acta (BBA) - Mol. Cell Res. 1803 (2010) 1231–1243.
[309] J. Hayes, P.P. Peruzzi, S. Lawler, MicroRNAs in cancer: biomarkers, functions and therapy, Trends Mol. Med. 20 (2014) 460–469.
[310] R. Ma, T. Jiang, X. Kang, Circulating microRNAs in cancer: origin, function and application, J. Exp. Clin. Cancer Res. 31 (2012) 38.
[311] M.S. Scott, M. Ono, From snoRNA to miRNA: Dual function regulatory non-coding RNAs, Biochimie 93 (2011) 1987–1992.
[312] G.A. Calin, C.D. Dumitru, M. Shimizu, R. Bichi, S. Zupo, E. Noch, H. Aldler, S. Rattan, M. Keating, K. Rai, L. Rassenti, T. Kipps, M. Negrini, F. Bullrich, C.M. Croce, Frequent deletions and down-regulation of micro- RNA genes miR15 and miR16 at 13q14 in chronic lymphocytic leukemia, Proc. Natl. Acad. Sci. 99 (2002) 15524–15529.
[313] J. Krol, I. Loedige, W. Filipowicz, The widespread regulation of microRNA biogenesis, function and decay, Nat. Rev. Genet. 11 (2010) 597–610.
[314] Y. He, J. Lin, D. Kong, M. Huang, C. Xu, T.-K. Kim, A. Etheridge, Y. Luo, Y. Ding, K. Wang, Current state of circulating microRNAs as cancer biomarkers, Clin. Chem. 61 (2015) 1138.
[315] Y. Gusev, D.J. Brackett, MicroRNA expression profiling in cancer from a bioinformatics prospective, Expert. Rev. Mol. Diagn. 7 (2007) 787–792.
[316] W. Li, K. Ruan, MicroRNA detection by microarray, Anal. Bioanal. Chem. 394 (2009) 1117–1124.
[317] R.-Q. Liang, W. Li, Y. Li, C.-y. Tan, J.-X. Li, Y.-X. Jin, K.-C. Ruan, An oligonucleotide microarray for microRNA expression analysis based on labeling RNA with quantum dot and nanogold probe, Nucleic Acids Res. 33 (2005) (e17–e17).
[318] T. Ueno, T. Funatsu, Label-free quantification of MicroRNAs using ligase-assisted sandwich hybridization on a DNA microarray, PLoS One 9 (2014), e90920.
[319] H. Arata, H. Komatsu, A. Han, K. Hosokawa, M. Maeda, Rapid microRNA detection using power-free microfluidic chip: coaxial stacking effect enhances the sandwich hybridization, Analyst 137 (2012) 3234–3237.
[320] Y.-X. Chen, K.-J. Huang, K.-X. Niu, Recent advances in signal amplification strategy based on oligonucleotide and nanomaterials for microRNA detection-a review, Biosens. Bioelectron. 99 (2018) 612–624.
[321] R. Liu, Q. Wang, Q. Li, X. Yang, K. Wang, W. Nie, Surface plasmon resonance biosensor for sensitive detection of microRNA and cancer cell using multiple signal amplification strategy, Biosens. Bioelectron. 87 (2017) 433–438.
[322] S. Fang, H.J. Lee, A.W. Wark, R.M. Corn, Attomole microarray detection of microRNAs by nanoparticle-amplified SPR imaging measurements of surface polyadenylation reactions, J. Am. Chem. Soc. 128 (2006) 14044–14046.
[323] D. Zhang, Y. Yan, W. Cheng, W. Zhang, Y. Li, H. Ju, S. Ding, Streptavidin-enhanced surface plasmon resonance biosensor for highly sensitive and specific detection of microRNA, Microchim. Acta 180 (2013) 397–403.
[324] X. Ding, Y. Yan, S. Li, Y. Zhang, W. Cheng, Q. Cheng, S. Ding, Surface plasmon resonance biosensor for highly sensitive detection of microRNA based on DNA supersandwich assemblies and streptavidin signal amplification, Anal. Chim. Acta 874 (2015) 59–65.
[325] Q. Wang, R. Liu, X. Yang, K. Wang, J. Zhu, L. He, Q. Li, Surface plasmon resonance biosensor for enzyme-free amplified microRNA detection based on gold nanoparticles and DNA supersandwich, Sensors Actuators B Chem. 223 (2016) 613–620.
[326] K. Hao, Y. He, H. Lu, S. Pu, Y. Zhang, H. Dong, X. Zhang, High-sensitive surface plasmon resonance microRNA biosensor based on streptavidin functionalized gold nanorods-assisted signal amplification, Anal. Chim. Acta 954 (2017) 114–120.
[327] J. Li, P. Lei, S. Ding, Y. Zhang, J. Yang, Q. Cheng, Y. Yan, An enzyme-free surface plasmon resonance biosensor for real-time detecting microRNA based on allosteric effect of mismatched catalytic hairpin assembly, Biosens. Bioelectron. 77 (2016) 435–441.
[328] S. Schmieder, J. Weißpflog, N. Danz, U. Klotzbach, F. Sonntag, Detection of miRNA using a surface plasmon resonance biosensor and antibody amplification, Curr. Dir. Biomed. Eng. (2016) 135.
[329] H. Šípová, S. Zhang, A.M. Dudley, D. Galas, K. Wang, J. Homola, Surface plasmon resonance biosensor for rapid label-free detection of microribonucleic acid at subfemtomole level, Anal. Chem. 82 (2010) 10110–10115.
[330] Q. Wang, Q. Li, X. Yang, K. Wang, S. Du, H. Zhang, Y. Nie, Graphene oxide–gold nanoparticles hybrids-based surface plasmon resonance for sensitive detection of microRNA, Biosens. Bioelectron. 77 (2016) 1001–1007.
[331] H. Vaisocherová, H. Šípová, I. Víšová, M. Bocková, T. Špringer, M. Laura Ermini, X. Song, Z. Krejčík, L. Chrastinová, O. Pastva, K. Pimková, M. Dostálová Merkerová, J.E. Dyr, J. Homola, Rapid and sensitive detection of multiple microRNAs in cell lysate by low-fouling surface plasmon resonance biosensor, Biosens. Bioelectron. 70 (2015) 226–231.
[332] C.-T. Yang, M. Pourhassan-Moghaddam, L. Wu, P. Bai, B. Thierry, Ultrasensitive detection of cancer prognostic miRNA biomarkers based on surface plasmon enhanced light scattering, ACS Sensors 2 (2017) 635–640.
[333] G.K. Joshi, S. Deitz-McElyea, M. Johnson, S. Mali, M. Korc, R. Sardar, Highly specific plasmonic biosensors for ultrasensitive MicroRNA detection in plasma from pancreatic cancer patients, Nano Lett. 14 (2014) 6955–6963.
[334] G.K. Joshi, S. Deitz-McElyea, T. Liyanage, K. Lawrence, S. Mali, R. Sardar, M. Korc, Label-free nanoplasmonic-based short noncoding RNA sensing at attomolar concentrations allows for quantitative and highly specific assay of microRNA-10b in biological fluids and circulating exosomes, ACS Nano 9 (2015) 11075–11089.
[335] L. Guo, Y. Lin, C. Chen, B. Qiu, Z. Lin, G. Chen, Direct visualization of sub-femtomolar circulating microRNAs in serum based on the duplex-specific nuclease-amplified oriented assembly of gold nanoparticle dimers, Chem. Commun. 52 (2016) 11347–11350.
[336] J. Park, J.-S. Yeo, Colorimetric detection of microRNA miR-21 based on nanoplasmonic core-satellite assembly, Chem. Commun. 50 (2014) 1366–1368.

[337] W. Shen, H. Deng, Y. Ren, Z. Gao, A real-time colorimetric assay for label-free detection of microRNAs down to sub-femtomolar levels, Chem. Commun. 49 (2013) 4959–4961.
[338] Y. Wang, E. MacLachlan, B.K. Nguyen, G. Fu, C. Peng, J.I.L. Chen, Direct detection of microRNA based on plasmon hybridization of nanoparticle dimers, Analyst 140 (2015) 1140–1148.
[339] J. Lee, J. Park, J.-Y. Lee, J.-S. Yeo, Contact transfer printing of side edge prefunctionalized nanoplasmonic arrays for flexible microRNA biosensor, Adv. Sci. 2 (2015) (1500121-n/a).
[340] J. Zhou, P.F. Gao, H.Z. Zhang, G. Lei, L.L. Zheng, H. Liu, C.Z. Huang, Color resolution improvement of the dark-field microscopy imaging of single light scattering plasmonic nanoprobes for microRNA visual detection, Nano 9 (2017) 4593–4600.
[341] J.D. Driskell, A.G. Seto, L.P. Jones, S. Jokela, R.A. Dluhy, Y.P. Zhao, R.A. Tripp, Rapid microRNA (miRNA) detection and classification via surface-enhanced Raman spectroscopy (SERS), Biosens. Bioelectron. 24 (2008) 917–922.
[342] J.L. Abell, J.M. Garren, J.D. Driskell, R.A. Tripp, Y. Zhao, Label-free detection of microRNA hybridization using surface-enhanced Raman spectroscopy and least-squares analysis, J. Am. Chem. Soc. 134 (2012) 12889–12892.
[343] B. Guven, F.C. Dudak, I.H. Boyaci, U. Tamer, M. Ozsoz, SERS-based direct and sandwich assay methods for mir-21 detection, Analyst 139 (2014) 1141–1147.
[344] B.M. Crawford, H.-N. Wang, A.M. Fales, M.L. Bowie, V.L. Seewaldt, T. Vo-Dinh, SERS-based Inverse Molecular Sentinel (iMS) Nanoprobes for Multiplexed Detection of microRNA Cancer Biomarkers in Biological Samples, 2017 (1008008-1008008-1008012).
[345] J. Su, D. Wang, L. Nörbel, J. Shen, Z. Zhao, Y. Dou, T. Peng, J. Shi, S. Mathur, C. Fan, S. Song, Multicolor gold–silver nano-mushrooms as ready-to-use SERS probes for ultrasensitive and multiplex DNA/miRNA detection, Anal. Chem. 89 (2017) 2531–2538.
[346] H.-N. Wang, B.M. Crawford, A.M. Fales, M.L. Bowie, V.L. Seewaldt, T. Vo-Dinh, Multiplexed detection of microRNA biomarkers using SERS-based inverse molecular sentinel (iMS) nanoprobes, J. Phys. Chem. C 120 (2016) 21047–21055.
[347] H. Zhang, Y. Liu, J. Gao, J. Zhen, A sensitive SERS detection of miRNA using a label-free multifunctional probe, Chem. Commun. 51 (2015) 16836–16839.
[348] W. Zhou, Y.-F. Tian, B.-C. Yin, B.-C. Ye, Simultaneous surface-enhanced raman spectroscopy detection of multiplexed MicroRNA biomarkers, Anal. Chem. 89 (2017) 6120–6128.
[349] Y. He, X. Yang, R. Yuan, Y. Chai, "Off" to "on" surface-enhanced Raman spectroscopy platform with padlock probe-based exponential rolling circle amplification for ultrasensitive detection of MicroRNA 155, Anal. Chem. 89 (2017) 2866–2872.
[350] H.R. Underhill, J.O. Kitzman, S. Hellwig, N.C. Welker, R. Daza, D.N. Baker, K.M. Gligorich, R.C. Rostomily, M.P. Bronner, J. Shendure, Fragment length of circulating tumor DNA, PLoS Genet. 12 (2016), e1006162.
[351] F. Mouliere, B. Robert, E. Arnau Peyrotte, M. Del Rio, M. Ychou, F. Molina, C. Gongora, A.R. Thierry, High fragmentation characterizes tumor-derived circulating DNA, PLoS One 6 (2011), e23418.
[352] K.M. Patel, D.W.Y. Tsui, The translational potential of circulating tumor DNA in oncology, Clin. Biochem. 48 (2015) 957–961.
[353] X. Han, J. Wang, Y. Sun, Circulating tumor DNA as biomarkers for cancer detection, Genomics Proteomics Bioinformatics 15 (2017) 59–72.
[354] D.M. Marzese, H. Hirose, D.S.B. Hoon, Diagnostic and prognostic value of circulating tumor-related DNA in cancer patients, Expert. Rev. Mol. Diagn. 13 (2013) 827–844.
[355] Z. Qin, V.A. Ljubimov, C. Zhou, Y. Tong, J. Liang, Cell-free circulating tumor DNA in cancer, Chin. J. Cancer 35 (2016) 36.
[356] H. Nawroz, W. Koch, P. Anker, M. Stroun, D. Sidransky, Microsatellite alterations in serum DNA of head and neck cancer patients, Nat. Med. 2 (1996) 1035–1037.
[357] L. Soares, A. Csaki, J. Jatschka, W. Fritzsche, O. Flores, R. Franco, E. Pereira, Localized surface plasmon resonance (LSPR) biosensing using gold nanotriangles: detection of DNA hybridization events at room temperature, Analyst 139 (2014) 4964–4973.
[358] T. Schneider, N. Jahr, J. Jatschka, A. Csaki, O. Stranik, W. Fritzsche, Localized surface plasmon resonance (LSPR) study of DNA hybridization at single nanoparticle transducers, J. Nanopart. Res. 15 (2013) 1531.
[359] P.K. Jain, W. Huang, M.A. El-Sayed, On the universal scaling behavior of the distance decay of plasmon coupling in metal nanoparticle pairs: a plasmon ruler equation, Nano Lett. 7 (2007) 2080–2088.
[360] M. Sanroman-Iglesias, C.H. Lawrie, L.M. Liz-Marzan, M. Grzelczak, Nanoparticle-based discrimination of single-nucleotide polymorphism in long DNA sequences, Bioconjug. Chem. 28 (2017) 903–906.
[361] A.H. Nguyen, S.J. Sim, Nanoplasmonic biosensor: detection and amplification of dual bio-signatures of circulating tumor DNA, Biosens. Bioelectron. 67 (2015) 443–449.
[362] L. Guo, L. Chen, S. Hong, D.-H. Kim, Single plasmonic nanoparticles for ultrasensitive DNA sensing: from invisible to visible, Biosens. Bioelectron. 79 (2016) 266–272.
[363] E.J.H. Wee, Y. Wang, S.C.-H. Tsao, M. Trau, Simple, sensitive and accurate multiplex detection of clinically important melanoma DNA mutations in circulating tumour DNA with SERS nanotags, Theranostics 6 (2016) 1506–1513.
[364] Q. Zhou, J. Zheng, Z. Qing, M. Zheng, J. Yang, S. Yang, L. Ying, R. Yang, Detection of circulating tumor DNA in human blood via DNA-mediated surface-enhanced raman spectroscopy of single-walled carbon nanotubes, Anal. Chem. 88 (2016) 4759–4765.
[365] H.P. Erickson, Size and Shape of Protein Molecules at the Nanometer Level Determined by Sedimentation, Gel Filtration, and Electron Microscopy, Biological Procedures Online, vol. 11, 2009 32–51.
[366] I. Sela-Culang, V. Kunik, Y. Ofran, The structural basis of antibody-antigen recognition, Front. Immunol. 4 (2013) 302.
[367] H.-P. Peng, K.H. Lee, J.-W. Jian, A.-S. Yang, Origins of specificity and affinity in antibody-protein interactions, Proc. Natl. Acad. Sci. 111 (2014) E2656–E2665.
[368] B. Strehlitz, N. Nikolaus, R. Stoltenburg, Protein detection with aptamer biosensors, Sensors 8 (2008) 4296–4307.
[369] Y. Seok Kim, N.H. Ahmad Raston, M. Bock Gu, Aptamer-based nanobiosensors, Biosens. Bioelectron. 76 (2016) 2–19.
[370] E. Stern, A. Vacic, N.K. Rajan, J.M. Criscione, J. Park, B.R. Ilic, D.J. Mooney, M.A. Reed, T.M. Fahmy, Label-free biomarker detection from whole blood, Nat. Nanotechnol. 5 (2010) 138–142.
[371] R. Etzioni, N. Urban, S. Ramsey, M. McIntosh, S. Schwartz, B. Reid, J. Radich, G. Anderson, L. Hartwell, The case for early detection, Nat. Rev. Cancer 3 (2003) 243–252.
[372] B. Douzi, Protein-protein interactions: surface plasmon resonance, in: L. Journet, E. Cascales (Eds.), Bacterial Protein Secretion Systems: Methods and Protocols, Springer New York, New York, NY 2017, pp. 257–275.
[373] C. Boozer, G. Kim, S. Cong, H. Guan, T. Londergan, Looking towards label-free biomolecular interaction analysis in a high-throughput format: a review of new surface plasmon resonance technologies, Curr. Opin. Biotechnol. 17 (2006) 400–405.
[374] S.G. Patching, Surface plasmon resonance spectroscopy for characterization of membrane protein–ligand interactions and its potential for drug discovery, Biochim. Biophys. Acta Biomembr. 1838 (2014) 43–55.
[375] A. Frostell, L. Vinterbeck, H. Sjobom, Protein-ligand interactions using SPR systems, in: M.A. Williams, T. Daviter (Eds.), Protein-ligand Interactions: Methods and Applications, Humana Press, Totowa, NJ 2013, pp. 139–165.
[376] Y. Arima, R. Ishii, I. Hirata, H. Iwata, High-throughput study of protein-surface interactions using a surface plasmon resonance imaging apparatus, proteins at interfaces III state of the art, Am. Chem. Soc. (2012) 695–708.
[377] R.J. Green, J. Davies, M.C. Davies, C.J. Roberts, S.J.B. Tendler, Surface plasmon resonance for real time in situ analysis of protein adsorption to polymer surfaces, Biomaterials 18 (1997) 405–413.
[378] R.J. Green, R.A. Frazier, K.M. Shakesheff, M.C. Davies, C.J. Roberts, S.J.B. Tendler, Surface plasmon resonance analysis of dynamic biological interactions with biomaterials, Biomaterials 21 (2000) 1823–1835.
[379] S. Krishnan, V. Mani, D. Wasalathanthri, C.V. Kumar, J.F. Rusling, Attomolar detection of a cancer biomarker protein in serum by surface plasmon resonance using superparamagnetic particle labels, Angew. Chem. Int. Ed. 50 (2011) 1175–1178.
[380] Y. Uludag, I.E. Tothill, Cancer biomarker detection in serum samples using surface plasmon resonance and quartz crystal microbalance sensors with nanoparticle signal amplification, Anal. Chem. 84 (2012) 5898–5904.
[381] U. Eletxigerra, J. Martinez-Perdiguero, R. Barderas, J.M. Pingarrón, S. Campuzano, S. Merino, Surface plasmon resonance immunosensor for ErbB2 breast cancer biomarker determination in human serum and raw cancer cell lysates, Anal. Chim. Acta 905 (2016) 156–162.
[382] G. Ertürk, H. Özen, M.A. Tümer, B. Mattiasson, A. Denizli, Microcontact imprinting based surface plasmon resonance (SPR) biosensor for real-time and ultrasensitive detection of prostate specific antigen (PSA) from clinical samples, Sensors Actuators B Chem. 224 (2016) 823–832.
[383] N. Cennamo, M. Pesavento, L. Lunelli, L. Vanzetti, C. Pederzolli, L. Zeni, L. Pasquardini, An easy way to realize SPR aptasensor: a multimode plastic optical fiber platform for cancer biomarkers detection, Talanta 140 (2015) 88–95.
[384] L. Yang, X. Zhang, M. Ye, J. Jiang, R. Yang, T. Fu, Y. Chen, K. Wang, C. Liu, W. Tan, Aptamer-conjugated nanomaterials and their applications, Adv. Drug Deliv. Rev. 63 (2011) 1361–1370.
[385] S.S. Ačimović, M.A. Ortega, V. Sanz, J. Berthelot, J.L. Garcia-Cordero, J. Renger, S.J. Maerkl, M.P. Kreuzer, R. Quidant, LSPR chip for parallel, rapid, and sensitive detection of cancer markers in serum, Nano Lett. 14 (2014) 2636–2641.
[386] S. Chen, Q. Zhao, L. Zhang, L. Wang, Y. Zeng, H. Huang, Combined detection of breast cancer biomarkers based on plasmonic sensor of gold nanorods, Sensors Actuators B Chem. 221 (2015) 1391–1397.
[387] W.S. Hwang, S.J. Sim, A strategy for the ultrasensitive detection of cancer biomarkers based on the LSPR response of a single AuNP, J. Nanosci. Nanotechnol. 11 (2011) 5651–5656.
[388] M. Soler, M.-C. Estevez, M. Alvarez, M. Otte, B. Sepulveda, L. Lechuga, Direct detection of protein biomarkers in human fluids using site-specific antibody immobilization strategies, Sensors 14 (2014) 2239.
[389] L. Tian, J.J. Morrissey, R. Kattumenu, N. Gandra, E.D. Kharasch, S. Singamaneni, Bioplasmonic paper as a platform for detection of kidney cancer biomarkers, Anal. Chem. 84 (2012) 9928–9934.
[390] M.H. Jazayeri, H. Amani, A.A. Pourfatollah, A. Avan, G.A. Ferns, H. Pazoki-Toroudi, Enhanced detection sensitivity of prostate-specific antigen via PSA-conjugated gold nanoparticles based on localized surface plasmon resonance: GNP-coated anti-PSA/LSPR as a novel approach for the identification of prostate anomalies, Cancer Gene Ther. 23 (2016) 365–369.
[391] Y. Hu, L. Li, L. Guo, The sandwich-type aptasensor based on gold nanoparticles/DNA/magnetic beads for detection of cancer biomarker protein AGR2, Sensors Actuators B Chem. 209 (2015) 846–852.
[392] H.Y. Song, T.I. Wong, A. Sadovoy, L. Wu, P. Bai, J. Deng, S. Guo, Y. Wang, W. Knoll, X. Zhou, Imprinted gold 2D nanoarray for highly sensitive and convenient PSA detection via plasmon excited quantum dots, Lab Chip 15 (2015) 253–263.
[393] J.U. Lee, A.H. Nguyen, Sang J. Sim, A nanoplasmonic biosensor for label-free multiplex detection of cancer biomarkers, Biosens. Bioelectron. 74 (2015) 341–346.
[394] J. Liang, C. Yao, X. Li, Z. Wu, C. Huang, Q. Fu, C. Lan, D. Cao, Y. Tang, Silver nanoprism etching-based plasmonic ELISA for the high sensitive detection of prostate-specific antigen, Biosens. Bioelectron. 69 (2015) 128–134.
[395] D. Liu, J. Yang, H.-F. Wang, Z. Wang, X. Huang, Z. Wang, G. Niu, A.R. Hight Walker, X. Chen, Glucose oxidase-catalyzed growth of gold nanoparticles enables quantitative detection of attomolar cancer biomarkers, Anal. Chem. 86 (2014) 5800–5806.

[396] L. Rodríguez-Lorenzo, R. de la Rica, R.A. Álvarez-Puebla, L.M. Liz-Marzán, M.M. Stevens, Plasmonic nanosensors with inverse sensitivity by means of enzyme-guided crystal growth, Nat. Mater. 11 (2012) 604–607.
[397] S. Chen, M. Svedendahl, M. Käll, L. Gunnarsson, A. Dmitriev, Ultrahigh sensitivity made simple: nanoplasmonic label-free biosensing with an extremely low limit-of-detection for bacterial and cancer diagnostics, Nanotechnology 20 (2009) 434015.
[398] X. Huang, R. Chen, H. Xu, W. Lai, Y. Xiong, Nanospherical brush as catalase container for enhancing the detection sensitivity of competitive plasmonic ELISA, Anal. Chem. 88 (2016) 1951–1958.
[399] X. Yang, Z. Gao, Enzyme-catalyzed deposition of ultrathin silver shells on gold nanorods: a universal and highly efficient signal amplification strategy for translating immunoassay into a litmus-type test, Chem. Commun. 51 (2015) 6928–6931.
[400] F. Domenici, A.R. Bizzarri, S. Cannistraro, Surface-enhanced Raman scattering detection of wild-type and mutant p53 proteins at very low concentration in human serum, Anal. Biochem. 421 (2012) 9–15.
[401] A.V. Krasnoslobodtsev, M.P. Torres, S. Kaur, I.V. Vlassiouk, R.J. Lipert, M. Jain, S.K. Batra, Y.L. Lyubchenko, Nano-immunoassay with improved performance for detection of cancer biomarkers, Nanomedicine 11 (2015) 167–173.
[402] Y. Wang, R. Vaidyanathan, M.J.A. Shiddiky, M. Trau, Enabling rapid and specific surface-enhanced Raman scattering immunoassay using nanoscaled surface shear forces, ACS Nano 9 (2015) 6354–6362.
[403] Z. Cheng, N. Choi, R. Wang, S. Lee, K.C. Moon, S.-Y. Yoon, L. Chen, J. Choo, Simultaneous detection of dual prostate specific antigens using surface-enhanced Raman scattering-based immunoassay for accurate diagnosis of prostate cancer, ACS Nano 11 (2017) 4926–4933.
[404] P. Owens, N. Phillipson, J. Perumal, G. O'Connor, M. Olivo, Sensing of p53 and EGFR biomarkers using high efficiency SERS substrates, Bios 5 (2015) 664.
[405] J. Li, Z. Skeete, S. Shan, S. Yan, K. Kurzatkowska, W. Zhao, Q.M. Ngo, P. Holubovska, J. Luo, M. Hepel, C.-J. Zhong, Surface enhanced Raman scattering detection of cancer biomarkers with bifunctional nanocomposite probes, Anal. Chem. 87 (2015) 10698–10702.
[406] R. Gao, Z. Cheng, A.J. deMello, J. Choo, Wash-free magnetic immunoassay of the PSA cancer marker using SERS and droplet microfluidics, Lab Chip 16 (2016) 1022–1029.
[407] Z. Rong, C. Wang, J. Wang, D. Wang, R. Xiao, S. Wang, Magnetic immunoassay for cancer biomarker detection based on surface-enhanced resonance Raman scattering from coupled plasmonic nanostructures, Biosens. Bioelectron. 84 (2016) 15–21.
[408] A. Ali, E.Y. Hwang, J. Choo, D.W. Lim, Nanoscale graphene oxide-induced metallic nanoparticle clustering for surface-enhanced Raman scattering-based IgG detection, Sensors Actuators B Chem. 255 (2018) 183–192.
[409] G. Jalani, S. Lee, C.W. Jung, H. Jang, J. Choo, D.W. Lim, Controlled biohybrid nanoprobes with silver nanoparticle clusters for Raman imaging, Analyst 138 (2013) 4756–4759.
[410] U.S. Dinish, G. Balasundaram, Y.-T. Chang, M. Olivo, Actively Targeted In Vivo Multiplex Detection of Intrinsic Cancer Biomarkers Using Biocompatible SERS Nanotags, vol. 4, 2014 4075.
[411] H. Chang, H. Kang, E. Ko, B.-H. Jun, H.-Y. Lee, Y.-S. Lee, D.H. Jeong, PSA detection with femtomolar sensitivity and a broad dynamic range using SERS nanoprobes and an area-scanning method, ACS Sensors 1 (2016) 645–649.
[412] E. Chung, J. Lee, J. Yu, S. Lee, J.H. Kang, I.Y. Chung, J. Choo, Use of surface-enhanced Raman scattering to quantify EGFR markers uninhibited by cetuximab antibodies, Biosens. Bioelectron. 60 (2014) 358–365.
[413] R.J. Simpson, J.W.E. Lim, R.L. Moritz, S. Mathivanan, Exosomes: proteomic insights and diagnostic potential, Expert Rev. Proteomics 6 (2009) 267–283.
[414] C. Thery, L. Zitvogel, S. Amigorena, Exosomes: composition, biogenesis and function, Nat. Rev. Immunol. 2 (2002) 569–579.
[415] G. Raposo, W. Stoorvogel, Extracellular vesicles: exosomes, microvesicles, and friends, J. Cell Biol. 200 (2013) 373–383.
[416] S. Mathivanan, H. Ji, R.J. Simpson, Exosomes: extracellular organelles important in intercellular communication, J. Proteome 73 (2010) 1907–1920.
[417] S. El Andaloussi, I. Mager, X.O. Breakefield, M.J.A. Wood, Extracellular vesicles: biology and emerging therapeutic opportunities, Nat. Rev. Drug Discov. 12 (2013) 347–357.
[418] A.S. Azmi, B. Bao, F.H. Sarkar, Exosomes in cancer development, metastasis, and drug resistance: a comprehensive review, Cancer Metastasis Rev. 32 (2013) 623–642.
[419] Z. Wang, J.-Q. Chen, J.-l. Liu, L. Tian, Exosomes in tumor microenvironment: novel transporters and biomarkers, J. Transl. Med. 14 (2016) 297.
[420] X. Zhang, X. Yuan, H. Shi, L. Wu, H. Qian, W. Xu, Exosomes in cancer: small particle, big player, J. Hematol. Oncol. 8 (2015) 83.
[421] L. Grasso, R. Wyss, L. Weidenauer, A. Thampi, D. Demurtas, M. Prudent, N. Lion, H. Vogel, Molecular screening of cancer-derived exosomes by surface plasmon resonance spectroscopy, Anal. Bioanal. Chem. 407 (2015) 5425–5432.
[422] B. Hosseinkhani, N. van den Akker, J. D'Haen, M. Gagliardi, T. Struys, I. Lambrichts, J. Waltenberger, I. Nelissen, J. Hooyberghs, D.G.M. Molin, L. Michiels, Direct detection of nano-scale extracellular vesicles derived from inflammation-triggered endothelial cells using surface plasmon resonance, Nanomedicine 13 (2017) 1663–1671.
[423] D.L.M. Rupert, C. Lässer, M. Eldh, S. Block, V.P. Zhdanov, J.O. Lotvall, M. Bally, F. Höök, Determination of exosome concentration in solution using surface plasmon resonance spectroscopy, Anal. Chem. 86 (2014) 5929–5936.
[424] D.L.M. Rupert, G.V. Shelke, G. Emilsson, V. Claudio, S. Block, C. Lässer, A. Dahlin, J.O. Lötvall, M. Bally, V.P. Zhdanov, F. Höök, Dual-wavelength surface plasmon resonance for determining the size and concentration of sub-populations of extracellular vesicles, Anal. Chem. 88 (2016) 9980–9988.
[425] L. Zhu, K. Wang, J. Cui, H. Liu, X. Bu, H. Ma, W. Wang, H. Gong, C. Lausted, L. Hood, G. Yang, Z. Hu, Label-free quantitative detection of tumor-derived exosomes through surface plasmon resonance imaging, Anal. Chem. 86 (2014) 8857–8864.
[426] G. Di Noto, A. Bugatti, A. Zendrini, E.L. Mazzoldi, A. Montanelli, L. Caimi, M. Rusnati, D. Ricotta, P. Bergese, Merging colloidal nanoplasmonics and surface plasmon resonance spectroscopy for enhanced profiling of multiple myeloma-derived exosomes, Biosens. Bioelectron. 77 (2016) 518–524.
[427] A.A.I. Sina, R. Vaidyanathan, S. Dey, L.G. Carrascosa, M.J.A. Shiddiky, M. Trau, Real time and label free profiling of clinically relevant exosomes, Sci. Rep. 6 (2016) 30460.
[428] H. Im, H. Shao, Y.I. Park, V.M. Peterson, C.M. Castro, R. Weissleder, H. Lee, Label-free detection and molecular profiling of exosomes with a nano-plasmonic sensor, Nat. Biotechnol. 32 (2014) 490–495.
[429] K.S. Yang, H. Im, S. Hong, I. Pergolini, A.F. del Castillo, R. Wang, S. Clardy, C.-H. Huang, C. Pille, S. Ferrone, R. Yang, C.M. Castro, H. Lee, C.F. del Castillo, R. Weissleder, Multiparametric plasma EV profiling facilitates diagnosis of pancreatic malignancy, Sci. Transl. Med. 9 (2017).
[430] A. Thakur, G. Qiu, S.-P. Ng, J. Guan, J. Yue, Y. Lee, C.-M.L. Wu, Direct detection of two different tumor-derived extracellular vesicles by SAM-AuNIs LSPR biosensor, Biosens. Bioelectron. 94 (2017) 400–407.
[431] K. Liang, F. Liu, J. Fan, D. Sun, C. Liu, C.J. Lyon, D.W. Bernard, Y. Li, K. Yokoi, M.H. Katz, E.J. Koay, Z. Zhao, Y. Hu, Nanoplasmonic quantification of tumor-derived extracellular vesicles in plasma microsamples for diagnosis and treatment monitoring, Nat. Biomed. Eng., 1 (2017) 0021.
[432] S. Zong, L. Wang, C. Chen, J. Lu, D. Zhu, Y. Zhang, Z. Wang, Y. Cui, Facile detection of tumor-derived exosomes using magnetic nanobeads and SERS nanoprobes, Anal. Methods 8 (2016) 5001–5008.
[433] S. Stremersch, M. Marro, B.-E. Pinchasik, P. Baatsen, A. Hendrix, S.C. De Smedt, P. Loza-Alvarez, A.G. Skirtach, K. Raemdonck, K. Braeckmans, Identification of individual exosome-like vesicles by surface enhanced Raman spectroscopy, Small 12 (2016) 3292–3301.
[434] J. Park, M. Hwang, B. Choi, H. Jeong, J.-h. Jung, H.K. Kim, S. Hong, J.-h. Park, Y. Choi, Exosome classification by pattern analysis of surface-enhanced Raman spectroscopy data for lung cancer diagnosis, Anal. Chem. 89 (2017) 6695–6701.
[435] M. Cristofanilli, G.T. Budd, M.J. Ellis, A. Stopeck, J. Matera, M.C. Miller, J.M. Reuben, G.V. Doyle, W.J. Allard, L.W.M.M. Terstappen, D.F. Hayes, Circulating tumor cells, disease progression, and survival in metastatic breast cancer, N. Engl. J. Med. 351 (2004) 781–791.
[436] H. Ito, N. Yamaguchi, M. Onimaru, S. Kimura, T. Ohmori, F. Ishikawa, J. Sato, S. Ito, H. Inoue, Change in number and size of circulating tumor cells with high telomerase activity during treatment of patients with gastric cancer, Oncol. Lett. 12 (2016) 4720–4726.
[437] M. Yu, S. Stott, M. Toner, S. Maheswaran, D.A. Haber, Circulating tumor cells: approaches to isolation and characterization, J. Cell Biol. 192 (2011) 373–382.
[438] L. Carter, D.G. Rothwell, B. Mesquita, C. Smowton, H.S. Leong, F. Fernandez-Gutierrez, Y. Li, D.J. Burt, J. Antonello, C.J. Morrow, C.L. Hodgkinson, K. Morris, L. Priest, M. Carter, C. Miller, A. Hughes, F. Blackhall, C. Dive, G. Brady, Molecular analysis of circulating tumor cells identifies distinct copy-number profiles in patients with chemosensitive and chemorefractory small-cell lung cancer, Nat. Med. 23 (2017) 114–119.
[439] S.H. Au, J. Edd, A.E. Stoddard, K.H.K. Wong, F. Fachin, S. Maheswaran, D.A. Haber, S.L. Stott, R. Kapur, M. Toner, Microfluidic isolation of circulating tumor cell clusters by size and asymmetry, Sci. Rep. 7 (2017) 2433.
[440] S. Park, R.R. Ang, S.P. Duffy, J. Bazov, K.N. Chi, P.C. Black, H. Ma, Morphological differences between circulating tumor cells from prostate cancer patients and cultured prostate cancer cells, PLoS One 9 (2014), e85264.
[441] M.M. Ferreira, V.C. Ramani, S.S. Jeffrey, Circulating tumor cell technologies, Mol. Oncol. 10 (2016) 374–394.
[442] E.I. Galanzha, E.V. Shashkov, T. Kelly, J.-W. Kim, L. Yang, V.P. Zharov, In vivo magnetic enrichment and multiplex photoacoustic detection of circulating tumor cells, Nat. Nanotechnol. 4 (2009) 855–860.
[443] V. Yashunsky, V. Lirtsman, M. Golosovsky, D. Davidov, B. Aroeti, Real-time monitoring of epithelial cell-cell and cell-substrate interactions by infrared surface plasmon spectroscopy, Biophys. J. 99 (2010) 4028–4036.
[444] J.-S. Maltais, J.-B. Denault, L. Gendron, M. Grandbois, Label-free monitoring of apoptosis by surface plasmon resonance detection of morphological changes, Apoptosis 17 (2012) 916–925.
[445] C. Liu, S. Alwarappan, H.A. Badr, R. Zhang, H. Liu, J.-J. Zhu, C.-Z. Li, Live cell integrated surface plasmon resonance biosensing approach to mimic the regulation of angiogenic switch upon anti-cancer drug exposure, Anal. Chem. 86 (2014) 7305–7310.
[446] T. Hiragun, Y. Yanase, K. Kose, T. Kawaguchi, K. Uchida, S. Tanaka, M. Hide, Surface plasmon resonance-biosensor detects the diversity of responses against epidermal growth factor in various carcinoma cell lines, Biosens. Bioelectron. 32 (2012) 202–207.
[447] M. Mousavi, H.-Y. Chen, H.-S. Hou, C.-Y.-Y. Chang, S. Roffler, P.-K. Wei, J.-Y. Cheng, Label-free detection of rare cell in human blood using gold nano slit surface plasmon resonance, Bios 5 (2015) 98.
[448] C.D. Medley, J.E. Smith, Z. Tang, Y. Wu, S. Bamrungsap, W. Tan, Gold nanoparticle-based colorimetric assay for the direct detection of cancerous cells, Anal. Chem. 80 (2008) 1067–1072.
[449] G. Liu, X. Mao, J.A. Phillips, H. Xu, W. Tan, L. Zeng, Aptamer–nanoparticle strip biosensor for sensitive detection of cancer cells, Anal. Chem. 81 (2009) 10013–10018.
[450] X. Zhang, K. Xiao, L. Cheng, H. Chen, B. Liu, S. Zhang, J. Kong, Visual and highly sensitive detection of cancer cells by a colorimetric aptasensor based on cell-triggered cyclic enzymatic signal amplification, Anal. Chem. 86 (2014) 5567–5572.

[451] X. Wang, X. Qian, J.J. Beitler, Z.G. Chen, F.R. Khuri, M.M. Lewis, H.J.C. Shin, S. Nie, D.M. Shin, Detection of circulating tumor cells in human peripheral blood using surface-enhanced raman scattering nanoparticles, Cancer Res. 71 (2011) 1526.
[452] W. Shi, R.J. Paproski, R. Moore, R. Zemp, Detection of circulating tumor cells using targeted surface-enhanced Raman scattering nanoparticles and magnetic enrichment, BIOMEDO 19 (2014) (056014–056014).
[453] P. Zhang, R. Zhang, M. Gao, X. Zhang, Novel nitrocellulose membrane substrate for efficient analysis of circulating tumor cells coupled with surface-enhanced Raman scattering imaging, ACS Appl. Mater. Interfaces 6 (2014) 370–376.
[454] M.R. Hoonejani, A. Pallaoro, G.B. Braun, M. Moskovits, C.D. Meinhart, Quantitative multiplexed simulated-cell identification by SERS in microfluidic devices, Nano 7 (2015) 16834–16840.
[455] A. Pallaoro, M.R. Hoonejani, G.B. Braun, C.D. Meinhart, M. Moskovits, Rapid identification by surface-enhanced raman spectroscopy of cancer cells at low concentrations flowing in a microfluidic channel, ACS Nano 9 (2015) 4328–4336.
[456] Z.A. Nima, M. Mahmood, Y. Xu, T. Mustafa, F. Watanabe, D.A. Nedosekin, M.A. Juratli, T. Fahmi, E.I. Galanzha, J.P. Nolan, A.G. Basnakian, V.P. Zharov, A.S. Biris, Circulating tumor cell identification by functionalized silver gold nanorods with multicolor, super-enhanced SERS and photothermal resonances, Sci. Rep. 4 (2014) 4752.
[457] X. Wu, L. Luo, S. Yang, X. Ma, Y. Li, C. Dong, Y. Tian, L.e. Zhang, Z. Shen, A. Wu, Improved SERS nanoparticles for direct detection of circulating tumor cells in the blood, ACS Appl. Mater. Interfaces 7 (2015) 9965–9971.
[458] X. Wu, Y. Xia, Y. Huang, J. Li, H. Ruan, T. Chen, L. Luo, Z. Shen, A. Wu, Improved SERS-active nanoparticles with various shapes for CTC detection without enrichment process with supersensitivity and high specificity, ACS Appl. Mater. Interfaces 8 (2016) 19928–19938.